JAERI-M
90-006

NEANDC(J)-146/U
INDC(JPN)-133/L

A NUCLEAR CROSS SECTION CALCULATION SYSTEM WITH SIMPLIFIED INPUT-FORMAT VERSION II (SINCROS-II)

February 1990

Nobuhiro YAMAMURO*

日本原子力研究所
Japan Atomic Energy Research Institute

JAERI-Mレポートは，日本原子力研究所が不定期に公刊している研究報告書です。
入手の問合わせは，日本原子力研究所技術情報部情報資料課（〒319-11茨城県那珂郡東海村）あて，お申しこしください。なお，このほかに財団法人原子力弘済会資料センター（〒319-11 茨城県那珂郡東海村日本原子力研究所内）で複写による実費頒布をおこなっております。

JAERI-M reports are issued irregularly.
Inquiries about availability of the reports should be addressed to Information Division Department of Technical Information, Japan Atomic Energy Research Institute, Tokai-mura, Naka-gun, Ibaraki-ken 319-11, Japan.

編集兼発行　日本原子力研究所
印　　刷　いばらき印刷㈱

JAERI-M 90-006

A Nuclear Cross Section Calculation System with Simplified Input-Format

Version II

(SINCROS-II)

Nobuhiro YAMAMURO*

Japanese Nuclear Data Committee
Tokai Research Establishment
Japan Atomic Energy Research Institute
Tokai-mura, Naka-gun, Ibaraki-ken

(Received January 6, 1990)

A Nuclear Cross Section Calculation System with Simplified Input-Format, Version-II (SINCROS-II) has been developed by improving the functions of the program in SINCROS-I, and preparing some process codes for the cross section applications. There is the option of optical-model potentials for neutron and proton, and the capture cross section normalization to the experiment and the width fluctuation correction to compound nuclear cross section become possible. The method recommended for nuclear cross section calculation is described. This system will be used to estimate the cross sections of nuclei for which the experimental data do not exist.

Keywords: Nuclear Cross Section, Calculation System, Optical-model Potential, Level Density, Preequilibrium Process, Width Fluctuation Correction

* Data Engineering, Inc.

簡易入力核断面積計算システム
第Ⅱ版
（SINCROS－Ⅱ）

日本原子力研究所東海研究所
シグマ研究委員会
山室　信弘*

（1990年1月6日受理）

簡易入力核断面積計算システム第Ⅱ版（SINCROS－Ⅱ）が完成した。第Ⅱ版では，第Ⅰ版に含まれていた諸機能が一層改善され，また，核断面積を利用するために必要ないくつかのプロセスコードが用意された。中性子と陽子の光学モデルポテンシアルが，それぞれ2種類内蔵されてその選択が可能となり，捕獲断面積の実験値による規格化，反応幅の変動幅に対する補正が取り入れられた。核断面積の計算をするとき，推奨される方法が述べられている。本システムは，実験データの無い核断面積の予測に用いられるだろう。

東海研究所：〒319－11　茨城県那珂郡東海村白方字白根2－4
＊　（株）データ工学

Contents

目　　次

1. Introduction

The SINCROS-II is a revised version of the SINCROS-I[1]. The input-format of this new version is more simplified than that of version I. The level density of nuclei is represented by defining only the Fermi-gas model parameter "a", and "a" for about 200 nuclei were stored in the code as the data initialization statement. The radiative widths Γ_γ for 200 nuclei were also stored, although some of them have tentative values.

In the version I, one neutron and one proton optical-model potentials were programmed. In contrast to this, two neutron and two proton potential parameters are accepted and the options of any combination become possible in the second version. A new proton potential was introduced for the calculations above 20 MeV. The energy point at which the cross section calculation can be carried out in a single execution increased to 30 cases, while it was 20 points in the old version.

The radiative capture cross section calculation is ordinarily difficult to agree with the experimental value. The normalization of the calculated capture cross section to the experimental data at 100 keV became available to obtain the suitable gamma-ray transition probability of the compound nucleus. The width fluctuation correction is applied, according to the Tepel et al.'s method[2], resulting in the corrected inelastic-scattering cross sections in the low energy region.

The lists of reaction, ground state production, and excited states production cross sections were given in the SINCROS-I. In the new version, the total neutron, proton, deuteron, alpha-particle, and gamma-ray production cross sections are also shown in the table. Instead of the excited state productions, the isomeric state production cross sections are directly out-putted. It is not necessary, then, to find out the isomeric cross section within the excited state production cross sections. The isomer, of which the excitation function is intended to be given, can be designated in the last row of the input data. The compound elastic scattering cross section and the inelastic scattering cross sections for 1st to 18th excited levels are also presented.

For the SINCROS-II, several process codes have been written in addition to the conversion code for the general purpose file of the ENDF/B format. Various process codes may be prepared in the near future.

2. Composition of SINCROS-II

The main codes of the SINCROS-II are the ELIESE[3]-GNASH[4] joint program (EGNASH2) and the simplified input version of DWUCK4[5] (DWUCKY). EGNASH2 calculates the nuclear cross sections over the wide mass region using the built-in optical-model potential parameters. In DWUCKY, the same accepted neutron potentials are programmed as in EGNASH2.

The discrete level data - excitation energy, spin, parity, and branching ratios of gamma-ray decay channels - are prepared from the ENSDF through the format conversion and the editorial work. It is not necessary that too many levels are quoted from the ENSDF, rather it should be assured that the number of levels approximately increases as an exponential function of the excitation energy. In the discrete level data, no transition from the isomeric state is given when the half-life is longer than about 1 sec, to calculate the isomeric state production cross section as well as the ground state production cross section.

EGNASH2 reads the discrete level data, the direct inelastic-scattering cross sections calculated with DWUCKY, and the input data for the nuclear reactions. In addition to the output lists, the results of calculation can be stored into the several files which are selected according to the object of calculation. The composition of SINCROS-II and the flow of data processing are shown in Fig. 1.

The particle and gamma-ray total production cross sections, and the production cross sections for reaction products, including isomeric states, are held in file 12. By programs "XTOB10" and XTOTHI", these cross sections can be converted to the file 10 of ENDF/B-format for the activation cross sections and the group constants for nuclear transmutation cross sections, respectively. In the case of charged particle incident reactions, the thick-target yield of the neutron can be obtained with a program "THICK". The programs, mentioned above, all are operated with a personal computer. The code CASTHY[6] can immediately be executed using file 14, if it is necessary. The file 10 includes particles and gamma-ray emission spectra for each incident energy. At this time, the file is used for the comparison of the calculated spectra with experimental ones. The GAMFIL[7] code makes the general purpose file of ENDF/B format from the output data of EGNASH2 stored in file 44.

3. Input and Output Format of EGNASH2

When we used the GNASH[4] code, the transmission coefficients for the projectile and outgoing particles were previously calculated with the ELIESE3[3] and these data were inputted in the GNASH. In order to keep the procedure as simple as possible, the subroutines in the ELIESE3, which are necessary to calculate the transmission coefficients, are picked up and combined with the GNASH. The code is improved in many routines and has a fairly simple input-format.

The input parameters required for the EGNASH2 code are described in Table 1. The following sequence of input cards is used.

A. (2 cards)	FORMAT 20A4	TITLE
B. (1 card)	FORMAT 16I5	NI, IPR, IOM, ITC, IANG, LPEQ, NLDIR, ICAPT, ISO
C. (1 card)	FORMAT 8E10.3	ZAP, ZAT, DE, F2, F3, F4, FSIGCN
D. (1 card)	FORMAT 8E10.3	SIGNRN, ANG1, ANG2, ANG3, EGS, SPINGS, PARGS
E. (1 card)	FORMAT 16I5	NELAB
F. (1-4 cards)	FORMAT 8E10.3	ELABS(I), I=1,NELAB
G. (1-20 cards)	FORMAT 8E10.3	ZACN(I), XNIP(I), AI(I), GWD(I), I=1,NI
H. (1 card)	FORMAT 8E10.3	RE1(I), I=1,NMP
I. (1 card)	FORMAT 8E10.3	EG1, GG1, PG1, EG2, GG2, PG2, RGG
J. (1 card)	FORMAT 8E10.3	EG3, GG3, PG3, EGCON, EGCNM1
K. (0-1 card)	(1) ISO=0 (0 card)	
	(2) ISO>0 (1 card)	
	FORMAT 8(I6,I4)	IZASO(I), NLV(I), I=1,ISO

Since many of the parameters shown above were predetermined and stored in the program, the parameters which should be inputted are a small number. A sample input is given in Table 2.

In addition to the output of the original GNASH, the present code has a table of reaction cross sections to examine the results of calculation as soon as possible. The table includes the compound, direct, rate of preequilibrium processes, and particles and gamma-ray total production cross sections. The ground and isomeric states production cross sections of isotopes, and level inelastic scattering cross sections are also shown. The output lists are described in Table 3 and a sample output data of reaction cross sections is shown in Table 4.

4. Optical-Model Potential Parameters

In the statistical nuclear model, the angular momentum dependent particle transmission coefficients are calculated by optical-model potential parameters. In the SINCROS, as a general rule, the global optical-model potentials are employed to calculate the transmission coefficients.

For the neutron, a modified Walter-Guss potential[8] and the Wilmore-Hodgson[9] potential parameters are built into the EGNASH2. Walter-Guss recommend their potential to be applied above 53 in mass-number and 10 to 80 MeV in energy range. To apply the potential below 10 MeV neutron energy, the following surface absorption term W_S (in MeV) is assumed between 0 and 20 MeV,

$$W_S = 7.71 - 14.94(N-Z)/A. \quad (1)$$

This was determined so that the calculated nonelastic cross sections agree with the experimental ones within about 10 percent uncertainty, as shown in Figs. 2 through 4. However, the neutron total cross section was not used in the procedure. The SINCROS can accept the more refined potential, if a user wants to use it[1].

For the proton, Perey[10], and Perey and Walter-Guss[8] combined potentials are defaulted. The Perey potential reproduces the data well for medium weight nuclei up to 50 MeV as shown in Fig. 5. However, Fig. 6 shows that it underestimates the proton reaction cross sections above 20 MeV for heavy nuclei. The Perey and Walter-Guss combined potential is recommended to use in the cross section calculation for medium and heavy nuclei. For some nuclei, there is about 5 percent gap at most between the reaction cross sections calculated with Perey and Walter-Guss potentials at 10 MeV, which is the connection energy between both potentials. However, this gap probably has no effect on the cross section calculation.

The Lemos set modified by Arthur and Young[11], and the Lohr-Haeberli[12] potentials are cited for alpha-particle and deuteron, respectively. The Becchetti, Jr. - Greenlees potential parameters[13] are programmed for triton and ^{3}He-particles. According to the control flag, the transmission coefficients for these particles are calculated using the optical-model potentials before the calculation of nuclear decaying processes.

5. Parameters for Level Density and Gamma-Ray Transitions

In the continuum level region, the Fermi-gas and the constant temperature model are used to represent the level density of nucleus. The Fermi-gas model formula as a function of energy E and spin J is

$$\rho(E,J) = \frac{\exp\{2[a(E-\Delta)]^{1/2}\}}{C_0\ (E-\Delta)^2} R(J,E), \tag{2}$$

where $C_0 = 24\sqrt{2}\ (0.146)^{3/2} a\ A$, and the spin term is given by

$$R(J,E) = (2J+1)\exp[-(J+1/2)^2/(2\sigma^2(E))], \tag{3}$$

where $\sigma^2(E)$ is the spin cutoff factor defined by

$$\sigma^2(E) = 0.146[a(E-\Delta)]^{1/2}A^{2/3}. \tag{4}$$

The pairing correction Δ was quoted from the Gilbert and Cameron's paper[14].

In the lower excitation, the constant temperature formula expressed by

$$\rho(E,J) = \rho(E_X)\exp[(E-E_X)/T]R(J,E), \quad E<E_X, \tag{5}$$

is used, where E_X is the energy at which both densities are smoothly connected, and $\rho(E_X)$ is the energy term of level density at the energy E_X. If the spin dependent level density $\rho(E,J)$ is summed over the spin J, we get the density $\rho(E)$ of levels of all J, which has a different form from the constant temperature formula of Gilbert and Cameron[14], as the spin cutoff factor $\sigma^2(E)$ is energy dependent.

The GNASH code[4] is able to automatically determine the nuclear temperature, T, if the discrete levels in the low energy region and the Fermi-gas level density parameter "a" were suitably inputted. Then the level density of nucleus in the continuum can be described by the parameter "a" only. In some cases, however, the code is unable to match discrete levels, and thus the temperature, which connects smoothly between the Fermi-gas and discrete levels, is not determined. For those cases, the temperature is calculated with a systematic relation between level density parameter and temperature,

$$T = 7.50\ a^{-0.84}, \tag{6}$$

in the code EGNASH2. Figure 7 shows the relation of temperature and level density paremter, derived from more than 100 cases in which the temperature is successfully determined in the code. The straight line, in Fig. 7, indicates the above equation of temperature T as a function of level density parameter "a".

At the beginning of the calculation, when the experimental value of the average spacing D_0 of s-wave neutron resonances at the neutron binding energy E_B is known[15], the parameter "a" was assumed to have a value which is calculated from the spacing D_0 by inversely solving the equation[16],

$$D_0 = C_0(E_B-\Delta)/(2I+1) \exp\left[(3 + (2I+1)^2)/(8\sigma^2(E_B)) - 2\sqrt{a(E_B-\Delta)}\right], \quad (7)$$

where I is the spin of target nucleus. And a set of parameters "a" of isotopes in the nuclear decaying processes has practically been selected through the cross section calculation to agree with the various experimental data which could be considered to be reliable. The procedure of parameter determination is described in Sec. 7.

With the cross section calculations for about 50 nuclei, the level density parameters "a" of about 200 isotopes were determined, and stored into the EGNASH2 as the data initialization statement, at this time. These values are shown in the Tables 5(1) through 5(3). The relation between these "a" and the total shell correction S given by Gilbert and Cameron[14] is shown in Fig. 8. The tentative formula,

$$a/A = 0.008\ S + 0.170, \quad (8)$$

is programmed to give the initial value of "a" for the undeformed nuclei for which the cross section is not yet calculated.

In the mass region A<20, in which Gilbert and Cameron did not give Δ and S, it is assumed that Δ=0 for odd-odd nucleus, $\Delta = 11/\sqrt{A}$ for odd-mass nuclei, and $\Delta = 22/\sqrt{A}$ for even-even nuclei, and the shell correction energy $S = M_{exp} - M_{ldp}$, where M_{exp} and M_{ldp} are the experimental nuclear mass and the calculated nuclear mass using the mass formula of the liquid-drop model, respectively.

To provide gamma-ray transmission coefficients, the Brink-Axel[17] giant dipole resonance form was used. The defaulted energy and width of the giant resonance are $E_R = 40 \cdot A^{-1/5}$ MeV and Γ_R = 6 MeV, respectively. The normalization constant is obtained from the ratio of the average

radiative width Γ_γ to the observed resonance spacing D_0 for s-wave neutrons at the neutron binding energy E_B, which is derived in the code from the level density parameter "a" used in the cross section calculation by formula (7).

The radiative width Γ_γ was cited from reference 15 for about 200 nuclei, and was stored as the data initialization statement as well as the parameter "a". For the other nuclei, Γ_γ is estimated using the formula[15],

$$\Gamma_\gamma = 7.32[(E_B-\Delta)/a]^{3/2}/(22\ A)^{1/3}. \qquad (9)$$

6. Capture Cross Section Normalization and Width Fluctuation Correction

Even if the gamma-ray transmission coefficient was normalized by the ratio of radiative width to the average spacing of s-wave resonance levels at the neutron binding energy, the calculated radiative capture cross sections are usually in disagreement with the experimental ones. In the code EGNASH2, it is possible to fit the calculated cross section to the experimental average capture cross section at 100 keV.

Figure 9 shows the result of cross section calculation for the reaction $^{93}Nb(n,\gamma)^{94}Nb$. In this case, the 100 mb at neutron energy 100 keV is used as the experimental total capture cross section. The agreement between the calculation and measurements is good from 10 keV to 1 MeV. The ground and isomeric states production cross sections are also separately given in the figure.

In the lower energy region, the width fluctuation correction to the average compound nucleus cross section is important, especially for calculation of the inelastic scattering cross section of excited levels. Although the classical integration method seems to give the better description for the correction, the approximate method of Tepel et al.[2] was recommended[18] for practical applications. Tepel et al. derived the elastic enhancement factor and its functional dependence on the transmission coefficients in the incident channel. We introduced this width fluctuation correction in the EGNASH2 using Tepel et al.'s assumption with the improved relation of the enhancement factor to the transmission coefficients given by Hofmann et al.[19].

Since the Tepel et al.'s method is a good approximation when the number of open channels is larger than 10 or 20, the elastic enhancement factor was overestimated below the energy at which few inelastic

radiative width Γ_γ to the observed resonance spacing D_0 for s-wave neutrons at the neutron binding energy E_B, which is derived in the code from the level density parameter "a" used in the cross section calculation by formula (7).

The radiative width Γ_γ was cited from reference 15 for about 200 nuclei, and was stored as the data initialization statement as well as the parameter "a". For the other nuclei, Γ_γ is estimated using the formula[15],

$$\Gamma_\gamma = 7.32[(E_B-\Delta)/a]^{3/2}/(22\ A)^{1/3}. \qquad (9)$$

6. Capture Cross Section Normalization and Width Fluctuation Correction

Even if the gamma-ray transmission coefficient was normalized by the ratio of radiative width to the average spacing of s-wave resonance levels at the neutron binding energy, the calculated radiative capture cross sections are usually in disagreement with the experimental ones. In the code EGNASH2, it is possible to fit the calculated cross section to the experimental average capture cross section at 100 keV.

Figure 9 shows the result of cross section calculation for the reaction $^{93}Nb(n,\gamma)^{94}Nb$. In this case, the 100 mb at neutron energy 100 keV is used as the experimental total capture cross section. The agreement between the calculation and measurements is good from 10 keV to 1 MeV. The ground and isomeric states production cross sections are also separately given in the figure.

In the lower energy region, the width fluctuation correction to the average compound nucleus cross section is important, especially for calculation of the inelastic scattering cross section of excited levels. Although the classical integration method seems to give the better description for the correction, the approximate method of Tepel et al.[2] was recommended[18] for practical applications. Tepel et al. derived the elastic enhancement factor and its functional dependence on the transmission coefficients in the incident channel. We introduced this width fluctuation correction in the EGNASH2 using Tepel et al.'s assumption with the improved relation of the enhancement factor to the transmission coefficients given by Hofmann et al.[19].

Since the Tepel et al.'s method is a good approximation when the number of open channels is larger than 10 or 20, the elastic enhancement factor was overestimated below the energy at which few inelastic

scattering channels are open, if the mean transmission coefficient of the incident channel is low. However, the calculation of the inelastic scattering cross section for excited levels shows good result comparing with that without the width fluctuation correction, as shown in Fig. 10.

7. How to Determine the Value of Parameters

In the SINCROS, the global optical-model potential parameters are employed to calculate the transmission coefficients, as mentioned in Sec. 4. The nonelastic cross sections for neutron and the reaction cross sections for proton calculated with the built-in potentials agreed with experimental data within about 10 percent in the wide mass range. See Figs. 2 through 6. The key points of the cross section calculation, therefore, are the determination of level density parameters of daughter nuclei and of the rate of contribution of preequilibrium and direct processes to the statistical process. In the following, the method of parameter determination for the preequilibrium process and for the level density is described in detail at subsections 7.1 and 7.2 respectively, and comparisons between calculated and experimental cross sections are shown in 7.3.

7.1 Parameter determination of the preequilibrium process

In the code EGNASH2, the preequilibrium and direct processes of particle emission are treated with the code PRECO developed by Kalbach[20], which is coupled with GNASH, and with the code DWUCKY for the inelastic-scattering. In the GNASH, the single-particle state density and the normalization factor for exciton-model were free parameters. In contrast with this, the single-particle state density constant is not free, but related to the level density parameter "a" by the formula,

$$g = (6/\pi^2)\, a, \qquad (10)$$

in the EGNASH2. In addition the normalization factor F2, which is equal to the Kalbach constant divided by 100, the adjusting factors F3 and F4 are introduced for pick-up and knock-out processes, respectively.

The factor F2 and the contribution of direct inelastic-scattering are so determined that the calculated neutron emission spectrum is in agreement with the high energy part of the experimental neutron spectrum, when we have the experimental data at 14 MeV[21)-23]. Figures 11 through 13 show the cases of Co, Zr, and Ag, respectively. If there is the

scattering channels are open, if the mean transmission coefficient of the incident channel is low. However, the calculation of the inelastic scattering cross section for excited levels shows good result comparing with that without the width fluctuation correction, as shown in Fig. 10.

7. How to Determine the Value of Parameters

In the SINCROS, the global optical-model potential parameters are employed to calculate the transmission coefficients, as mentioned in Sec. 4. The nonelastic cross sections for neutron and the reaction cross sections for proton calculated with the built-in potentials agreed with experimental data within about 10 percent in the wide mass range. See Figs. 2 through 6. The key points of the cross section calculation, therefore, are the determination of level density parameters of daughter nuclei and of the rate of contribution of preequilibrium and direct processes to the statistical process. In the following, the method of parameter determination for the preequilibrium process and for the level density is described in detail at subsections 7.1 and 7.2 respectively, and comparisons between calculated and experimental cross sections are shown in 7.3.

7.1 Parameter determination of the preequilibrium process

In the code EGNASH2, the preequilibrium and direct processes of particle emission are treated with the code PRECO developed by Kalbach[20], which is coupled with GNASH, and with the code DWUCKY for the inelastic-scattering. In the GNASH, the single-particle state density and the normalization factor for exciton-model were free parameters. In contrast with this, the single-particle state density constant is not free, but related to the level density parameter "a" by the formula,

$$g = (6/\pi^2)\, a, \qquad (10)$$

in the EGNASH2. In addition the normalization factor F2, which is equal to the Kalbach constant divided by 100, the adjusting factors F3 and F4 are introduced for pick-up and knock-out processes, respectively.

The factor F2 and the contribution of direct inelastic-scattering are so determined that the calculated neutron emission spectrum is in agreement with the high energy part of the experimental neutron spectrum, when we have the experimental data at 14 MeV[21)-23]. Figures 11 through 13 show the cases of Co, Zr, and Ag, respectively. If there is the

neutron emission from the direct inelastic-scattering in the continuum level region, the pseudo-discrete-levels can be assumed and the direct inelastic-scattering cross sections of those levels are calculated with DWUCKY. The value of F2 also refers to the proton emission spectrum.

According to the experience gained from the calculation of about 50 nuclei, the normalization factor F2 does not have a systematic behavior, perhaps because the emission probability of nucleons in the exciton-model depends on not only the factor F2 but also the single-particle state density of composite and residual nuclei. Rather, the rate of the contribution from the preequilibrium process to the total compound nucleus formation is about from 20 to 30 percent at the 15 MeV neutron energy for many nuclei.

The pick-up factor F3 is determined from the alpha-particle emission spectrum. In Fig. 14, F3 is set to be 0.5. Since this value is suitable for almost all medium-weight nuclei, the value 0.5 is programmed in the code EGNASH2 as the default value. The factor F4 for the knock-out process is 1.0 in the calculation for neutron induced reactions.

7.2 Parameter determination of the level density

After the parameters for the preequilibrium and direct processes were selected, the free parameter to be determined is only the level density parameter "a" in the Fermi-gas model, because the nuclear temperature used in the constant temperature model can be determined automatically or by the equation (6). Since the total emission of various kinds of particles from the compound nucleus is controlled by a set of level density parameters for daughter nuclei, it is better that the level density parameter of each daughter nucleus is so practically determined that the calculated cross sections for reactions, (n,2n), (n,p), and (n,α), agree with the experimental data of respective reactions.

The first step to fix the level density parameters is the calculation of them using the experimental value of mean level spacing for S-wave neutron resonances at the neutron binding energy. The calculation was made by solving inversely equation (7), with the spin cutoff-factor defined by equation (4) and the pairing correction quoted from Gilbert and Cameron[14]. Figure 15 shows, for example, the result in the mass region from 85 to 102.

The second step to determine the level density parameters is the cross section calculation in the mass region where the reliable experimental data exist. For Zr, Nb, and Mo, as well as the structural materials from Cr to Cu, there are relatively many experimental measurements of reaction cross sections and total emission cross sections. Then, the cross section calculations for Zr, Nb, and Mo, and a set of the level density parameters in this mass region obtained as the result of the cross section calculation are described below.

Since there are seven stable isotopes of Mo and, thus, we have a few level density parameters derived from the experimental average level spacing, as shown in Fig. 15, the cross section calculations for Mo isotopes are selected as the start of this job. The cross section of the (n,p) reaction depends on the level density parameters of Nb isotopes and of Mo isotopes as the target nucleus of the reaction, and that of (n,α) reaction depends on the level density parameters of Zr isotopes and of Mo isotopes as the target nucleus. The lower energy part of the neutron emission spectrum, as shown in Figs. 11 through 13, although they are for natural elements, suggests that the level density parameters of the target nucleus are proper or not. The (n,2n) reaction cross section depends also on the radiative width of the target nucleus.

Several test calculations of cross sections around 14 MeV were carried out, referring to the experimental data for the (n,2n), (n,p), and (n,α) reactions. In this stage, the measurements of cross sections of Mo isotopes, performed by Ikeda et al.[24] and Katoh et al.[25], are very useful for the determination of level density parameters. Finally, a set of level density parameters of Mo, Nb, and Zr isotopes, used in the cross section calculations of Mo isotopes, is settled. Almost the same procedure is executed for the Nb cross section calculations, referring to the experimental data and adjusting the level density parameters. After fixing the parameters, the calculation continues for the Zr isotopes.

At the goal of all procecures, mentioned above, we can get a set of the level density parameters from Sr to Mo, as shown in Fig. 16 and Table 5(2). Probably, the level density parameters for Sr and Y are modified when the cross section calculations for Sr and Y are made. There are the same conditions for the level density parameters for Mn and Fe in Table 5(1).

7.3 Comparison between calculated and experimental corss sections for Zr, Nb and Mo isotopes

The cross section calculations for the stable isotopes, $^{90,91,92,94,96}Zr$, ^{93}Nb, $^{92,94,95,96,97,98,100}Mo$, were performed using the level density parameters, which were stored into the EGNASH2 code as the data initialization statement. The results of calculations were compared with the experimental data and shown in the following. To fit well with the experimental cross section for the reaction $^{90}Zr(n,2n)^{89}Zr$, the radiative width of ^{90}Zr was adjusted. If a reaction produces the isomeric states, the ground and isomeric state productions and sum of them are separately shown. Table 6 shows the excitation energy and half life of isomeric states.

(1)	$^{90}Zr(n,2n)^{89}Zr$ production	Figure 17
(2)	$^{90}Zr(n,p)^{90}Y$ production	Figure 18
(3)	$^{90}Zr(n,\alpha)^{87}Sr$ production	Figure 19
(4)	$^{91}Zr(n,p)^{91}Y$ production	Figure 20
(5)	$^{91}Zr(n,n'p)^{90}Y$ production	Figure 21
(6)	$^{92}Zr(n,p)^{92}Y$ production	Figure 22
(7)	$^{92}Zr(n,n'p)^{91}Y$ production	Figure 23
(8)	$^{94}Zr(n,p)^{94}Y$ production	Figure 24
(9)	$^{94}Zr(n,\alpha)^{91}Sr$ production	Figure 25
(10)	$^{93}Nb(n,2n)^{92}Nb$ production	Figure 26
(11)	$^{93}Nb(n,\alpha)^{90}Y$ production	Figure 27
(12)	$^{92}Mo(n,2n)^{91}Mo$ production	Figure 28
(13)	$^{92}Mo(n,p)^{92}Nb$ production	Figure 29
(14)	$^{92}Mo(n,\alpha)^{89}Zr$ production	Figure 30
(15)	$^{95}Mo(n,p)^{95}Nb$ production	Figure 31
(16)	$^{96}Mo(n,p)^{96}Nb$ production	Figure 32
(17)	$^{96}Mo(n,n'p)^{95}Nb$ production	Figure 33
(18)	$^{97}Mo(n,p)^{97}Nb$ production	Figure 34
(19)	$^{97}Mo(n,n'p)^{96}Nb$ production	Figure 35
(20)	$^{98}Mo(n,p)^{98}Nb$ production	Figure 36
(21)	$^{98}Mo(n,n'p)^{97}Nb$ production	Figure 37
(22)	$^{98}Mo(n,\alpha)^{95}Zr$ production	Figure 38
(23)	$^{100}Mo(n,2n)^{99}Mo$ production	Figure 39
(24)	$^{100}Mo(n,\alpha)^{97}Zr$ production	Figure 40

One of the merits of the EGNASH2 code is that the isomeric state productions are directly calculated and represented in the output table.

Then, the experimental measurements for isomeric states are applicable to the examination and the determination of level density parameters. Comparing Fig. 15 with Fig. 16, it can been seen that the level density parameters for some of Zr, Nb, and Mo isotopes, which are derived from average resonance level spacing, fairly keep the values in the final set of level density parameters. About the production cross sections through the (n,n'p) process, which are sum of (n,n'p), (n,pn'), and (n,d) reaction cross sections, we get agreement between the calculations and experiments for ^{91}Zr, ^{96}Mo, and ^{97}Mo, but disagreement for ^{92}Zr and ^{98}Mo. The reason for the disagreement is not clear at present.

In order to inspect the results of cross section calculations, total production cross sections of proton and alpha-particle are compared with the experimental data by 15 MeV incident neutron in Table 7. The excellent agreement between the Kneff et al.[26] helium productions and the calculated values, except for natural zirconium, is obtained. For proton productions, the calculations agree well with Grimes et al. experiments[27,28] for Ni, Cu, and Nb isotopes, but the calculations for Mo show systematically lower cross sections than the experimental data[29]. Although these discrepancies ought to be investigated, it seems that the results of cross section calculation, described in this section, can generally be accepted.

8. Summary

To aim the efficient execution of nuclear cross section calculations, both codes, ELIESE[3] and GNASH[4] were joined and the global optical-potentials were built into the new code, EGNASH, whose input-format became simpler than that of GNASH. This joint program was used for the cross section calculations for 25 nuclei at the time of the Mito international conference[30]. The manual of SINCROS-I[1] was published at July 1988, and more than 25 nuclei's cross sections were calculated with this system. From the experience of calculations, we have attempted to improve the program and to add the new functions in the EGNASH code, and to equip the process codes for the cross section applications.

The code EGNASH2 has a few free parameters for the preequilibrium process, level density, and radiative width. The method of the determination of these parameters is described in Sec. 7 for Zr, Nb, and Mo isotopes. A set of the level density parameters, thus derived, is cross-checked by many experimental measurements, so that it may be

Then, the experimental measurements for isomeric states are applicable to the examination and the determination of level density parameters. Comparing Fig. 15 with Fig. 16, it can been seen that the level density parameters for some of Zr, Nb, and Mo isotopes, which are derived from average resonance level spacing, fairly keep the values in the final set of level density parameters. About the production cross sections through the (n,n'p) process, which are sum of (n,n'p), (n,pn'), and (n,d) reaction cross sections, we get agreement between the calculations and experiments for ^{91}Zr, ^{96}Mo, and ^{97}Mo, but disagreement for ^{92}Zr and ^{98}Mo. The reason for the disagreement is not clear at present.

In order to inspect the results of cross section calculations, total production cross sections of proton and alpha-particle are compared with the experimental data by 15 MeV incident neutron in Table 7. The excellent agreement between the Kneff et al.[26] helium productions and the calculated values, except for natural zirconium, is obtained. For proton productions, the calculations agree well with Grimes et al. experiments[27,28] for Ni, Cu, and Nb isotopes, but the calculations for Mo show systematically lower cross sections than the experimental data[29]. Although these discrepancies ought to be investigated, it seems that the results of cross section calculation, described in this section, can generally be accepted.

8. Summary

To aim the efficient execution of nuclear cross section calculations, both codes, ELIESE[3] and GNASH[4] were joined and the global optical-potentials were built into the new code, EGNASH, whose input-format became simpler than that of GNASH. This joint program was used for the cross section calculations for 25 nuclei at the time of the Mito international conference[30]. The manual of SINCROS-I[1] was published at July 1988, and more than 25 nuclei's cross sections were calculated with this system. From the experience of calculations, we have attempted to improve the program and to add the new functions in the EGNASH code, and to equip the process codes for the cross section applications.

The code EGNASH2 has a few free parameters for the preequilibrium process, level density, and radiative width. The method of the determination of these parameters is described in Sec. 7 for Zr, Nb, and Mo isotopes. A set of the level density parameters, thus derived, is cross-checked by many experimental measurements, so that it may be

employed for the cross section calculations for the non-experimental nuclei, such as the long-lived radioactive isotopes, and for the calculations of radioactive production in the materials induced by neutrons or protons incident up to about 40 MeV.

There are, now, limited data process codes. Probably, other process codes will continually be developed. For example, the neutron or charged particle spectra in the thick target, and the kerma-factor in the materials can be obtained from files 10 and 12 of SINCROS-II. The extension of energy range in which the calculation system is applicable will be planned at the next stage of development.

Acknowledgement

The author withes to thank Mr. T. Nakagawa and members of the nuclear data center of JAERI for help to use the FACOM M780 computer.

employed for the cross section calculations for the non-experimental nuclei, such as the long-lived radioactive isotopes, and for the calculations of radioactive production in the materials induced by neutrons or protons incident up to about 40 MeV.

There are, now, limited data process codes. Probably, other process codes will continually be developed. For example, the neutron or charged particle spectra in the thick target, and the kerma-factor in the materials can be obtained from files 10 and 12 of SINCROS-II. The extension of energy range in which the calculation system is applicable will be planned at the next stage of development.

Acknowledgement

The author withes to thank Mr. T. Nakagawa and members of the nuclear data center of JAERI for help to use the FACOM M780 computer.

References

1) N. Yamamuro, "A Nuclear Cross Section Calculation System with Simplified Input-Format Version I", (SINCROS-I), JAERI-M 88-140 (1988) (in Japanese).
2) J.W. Tepel, H.M. Hofmann, and H.A. Weidenmueller, Physics Letters, 49B, 1 (1974).
3) S. Igarashi, "Program ELIESE-3; Program for Calculation of the Nuclear Cross Section by Using Local and Non-Local Optical Models and Statistical Model", JAERI 1224 (1972).
4) P.G. Young and E.D. Arthur, "GNASH: A Preequilibrium, Statistical Nuclear-Model Code for Calculation of Cross Sections and Emission Spectra", LA-6947 (1977).
5) P.D. Kunz, "Distorted Wave Code DWUCK4", University of Colorado (1974).
6) S. Igarashi, J. Nucl. Sci. Technol., 12, 67 (1975).
7) K. Hida, "GAMFIL: "A Computer Program for Generating Photon Production Nuclear Data File", JAERI-M 86-150 (1986) (in Japanese).
8) R.L. Walter and P.P. Guss, "A Global Optical Potential Model for Neutron Scattering for A>53 and 10 MeV<E<80 MeV", Proc. Int. Conf. Nuclear Data for Basic and Applied Science, Santa Fe, New Mexico, p.1079 (1985).
9) D. Wilmore and P.E. Hodgson, Nucl. Phys., 55, 673 (1964).
10) F.G. Perey, Phys. Rev., 131, 745 (1963).
11) E.D. Arthur and P.G. Young, "Evaluated Neutron-Induced Cross Sections for ^{54,56}Fe to 40 MeV", LA-8626-MS (1980).
12) J.M. Lohr and W. Haeberli, Nucl. Phys., A232, 381 (1974).
13) F.D. Becchetti, Jr. and G.W. Greenlees, "Polarization Phenomena in Nuclear Reactions", The University of Wisconsin Press, p.682 (1971).
14) A. Gilbert and A.G.W. Cameron, Can. J. Phys., 43, 1446 (1965).
15) S.F. Mughabghab, M. Divadeenam, and N.E. Holden, "Neutron Cross Sections vol.1, Neutron Resonance Parameters and Thermal Cross Sections Part A, Z=1-60" (1981).
16) S. Iijima, T. Yoshida, T. Aoki, T. Watanabe, and M. Sasaki, J. Nucl. Sci. Technol., 21, 10 (1984).
17) P. Axel, Phys. Rev., 126, 671 (1962).
18) H. Gruppelaar and G. Reffo, Nucl. Sci. Eng., 62, 756 (1977).
19) H.M. Hofmann, J. Richert, J.W. Tepel and H.A. Weidenmueller, Annals Phys., 90, 403 (1975).

20) C. Kalbach, Z. Physik, A283, 401 (1977).
21) A. Takahashi, E. Ichimura, Y. Sasaki, and H. Sugimoto, J. Nucl. Sci. Technol. 25, 215 (1988).
22) M. Baba, M. Ishikawa, N. Yabuta, T. Kikuchi, H. Wakabayashi, and N. Hirakawa, "Double-Differential Neutron Emission Spectra for Al, Ti, V, Cr, Mn, Fe, Ni, Cu, and Zr", Proc. Int. Conf. on Nuclear Data for Science and Technology, Mito, Japan, p.291 (1988).
23) Y. Watanabe, I. Kumabe, M. Hyakutake, A. Takahashi, H. Sugimoto, E E. Ichimura, and Y. Sasaki, Phys. Rev. C37, 963 (1988).
24) Y. Ikeda, C. Konno, K. Oishi, T. Nakamura, H. Miyade, K. Kawade, H. Yamamoto, and T. Katoh, "Activation Cross Section Measurements for Fusion Reactor Structural Materials at Neutron Energy from 13.3 to 15.0 MeV Using FNS Facility", JAERI 1312 (1988).
25) T. Katoh, K. Kawade, and H. Yamamoto, "Measurement of Activation Cross Sections", JAERI-M 89-083 (1989) (in Japanese).
26) D.W. Kneff, B.W. Oliver, H. Farrar IV, and L.R. Greenwood, Nucl. Sci. Eng., 92, 491 (1986).
27) S.M. Grimes, R.C. Haight, K.R. Alvar, H.H. Barschall, and R.R. Barchers, Phys. Rev. C19, 2127 (1979).
28) S.M. Grimes, R.C. Haight, and J.D. Anderson, Phys. Rev. C17, 508 (1978).
29) R.C. Haight, S.M. Grimes, and R.G. Johnson, Phys. Rev. C23, 700 (1981).
30) N. Yamamuro, "Nuclear Cross Section Calculations with A Simplified-Input Version of ELIESE-GNASH Joint Program", Proc. Int. Conf. on Nuclear Data for Science and Technology, Mito, Japan, p.489 (1988).
31) N.I. Molla and S.M. Qaim, Nucl. Phys., A283, 269 (1977).
32) D.L. Allan, Nucl. Phys., 24, 274 (1961).
33) M. Ahmad, C.E. Brient, P.M. Egun, S.M. Grimes, S. Saraf, and H. Satyanarayana, Nucl. Sci. Eng., 95, 296 (1987).
34) L.R. Greenwood and D.L. Bowers, J. Nucl. Mater., 155-157, 585 (1988).
35) M. Hille, P. Hille, M. Uhl, and W. Weitz, Nucl. Phys., A198, 625 (1972).
36) R. Colle, R. Kishore, and J.B. Cumming, Phys. Rev., C9, 1819 (1974).
37) M.W. Greene and E. Lebowitz, Int. J. Appl. Radiat. Isot., 23, 342 (1972).
38) A. Gruetter, Nucl. Phys., A383, 98 (1982).
39) P. Kopecky, Int. J. Appl. Radiat. Isot., 36, 657 (1985).

Table 1 Description of Input - Parameters

Parameter	Description
TITLE	Two cards of Hollerrith field information to describe the problem being calculated.
NI	Number of decaying nuclei in the reaction chain, including the nuclei which decay only through gamma-ray emission. Maximum of 20.
IPR	Print control for all data.
0	Input and default parameters, composite spectra of particles and gamma-ray, level density parameters, and reaction cross sections are printed.
1	Preequilibrium cross sections, multi-step neutron emission spectra, and spectra from individual reactions are printed, in addition to IPR=0.
2	Gamma-ray strength function, preequilibrium spectra, and discrete level information are printed, in addition to IPR=1.
≧3	All data, including the transmission coefficients and level densities at the mesh point of integration, are printed.
IOM	Control for transmission coefficient. IOM consists of three numbers. The number of hundreds controls the neutron potential, the number of tens the proton potential, and the number of units the calculation of transmission coefficient.
the number of units	
0	The transmission coefficients are not calculated in the EGNASH2. In this case, the energy mesh and the transmission coefficient are ought to be previously calculated with the optical-model potential which a user wants to use, and stored in the files 27 and 28, respectively.
1	The transmission coefficients are calculated with the built-in optical potentials. The options for the neutron and proton potentials are determined by the numbers of hundreds and tens, respectively.

Table 1 Description of Input Parameters (continued)

Parameters	Description
2	The transmission coefficients are calculated with the built-in optical potentials and the total (for neutron) and reaction cross sections at the mesh energy points are printed out.
the number of tens	
0	Perey potential is used to calculate proton transmission coefficients.
1	Perey and Walter-Guss combined potential is used.
the number of hundreds	
0	A modified Walter-Guss potential is used to calculate neutron transmission coefficients.
1	Wilmore-Hodgson potential is used. If IOM=11, the transmission coefficients are calculated using a modified Walter-Guss potential for neutron, Perey and Walter-Guss combined potential for proton, and the built-in potentials for other particles in the EGNASH2. This option is recommended for the cross section calculation of medium and heavy nuclei.
ITC	Control for exchange of the transmission coefficients
0	The transmission coefficients for the first compound nucleus are used in all decaying processes in the cross section calculation. This approximation is ordinarily applied.
1	In the multi-step nuclear reaction, the transmission coefficients for each decaying nucleus are calculated and used in processes from parent to daughter nuclei. This option is recommended in the calculations for cross sections of lighter nuclei, for process in which the charged particles emit successively such as (n,2p) or (n,pα), and for charged particle induced reactions.
IANG	Control for the calculation of double differential cross section for the scattering of incident particle.
0	Double differential cross section is not calculated.
1	Double differential cross section is calculated in accordance with parameters ANG1, ANG2, and ANG3. The result is printed at every 10 degrees.

Table 1 Description of Input Parameters (continued)

Parameter	Description
LPEQ	Control for preequilibrium process
0	The preequilibrium process is not included in the calculation.
1	By solving the master equation, the preequilibrium cross sections are calculated.
2	The solution of closed form approximation is applied. When the solution of master equation does not converge, this option is used.
NLDIR	Control for direct inelastic scattering.
0	No direct inelastic scattering is treated.
n	Number of levels including direct reaction cross section. In this case, file 33 supplies the information of direct process, in which the energy of discrete levels ought to be equal to the energy stored in the discrete level data file 8. If it is necessary, the pseudo-levels in the continuum energy region can be given.
ICAPT	Control for width fluctuation correction, for input-data production for the CASTHY code, and for the gamma-ray cascade transition in the initial compound nucleus.
-2	Equivalent to ICAPT=0, except that the width fluctuation correction is not applied. In the other option the correction is included.
-1	The input-data for the CASTHY code is prepared and stored in file 14, but gamma-ray cascade calculation is omitted.
0	Gamma-ray cascade calculation is omitted in the initial compound nucleus. This option is recommended unless the spectrum of capture gamma-ray is specifically required.
1	Full gamma-ray cascade calculation is made for all decaying nuclei, and input-data for CASTHY is prepared. In the calculation for the isomeric state production through the (n,γ) reaction, ICAPT=1 run is necessary. It would take more CPU time than that for ICAPT=0.
2	Full gamma-ray cascade calculation is performed, but input-data for CASTHY is not produced.

Table 1 Description of Input Parameters (continued)

Parameter	Description
ISO	Control for isomeric state production.
0	No isomeric state is included.
n	Number of isomeric states whose production cross sections are printed and stored in file 12. Maximum of 8. In the last line of input-data, the nucleus and the level number are indicated.
ZAP	1000*Z+A for the incident particle, where Z is atomic number and A is the mass number.
ZAT	1000*Z+A for the target nucleus.
DE	Energy increment for the basic integration energy mesh (in millions of electron volts). A maximum of 100 energy step is permitted.
F2	The normalization factor used with the Kalbach pre-equilibrium model (divided by 100).
F3	The normalization factor for pick-up process. Default value is 0.5.
F4	The normalization factor for knock-out process. Default value is 1.0.
FSIGCN	Constant multiplier applied to all calculated quantities. Default value is 1.0.
SIGNRN	The experimental average capture cross section at 100 keV (in barn) used to normalize the calculated capture cross section. If left blank, the capture cross section is calculated using ratio of radiative width to level spacing at neutron binding energy.
ANG1	Number of angular points for calculation of double differential cross section. Default value is 37 and maximum of 50.
ANG2	Minimum angle for calculation and default value is 0 deg.
ANG3	Angular increment for calculation and default value is 5 deg. ANG1, ANG2 and ANG3 ought to be equal to those used in the DWUCKY code.

Table 1 Description of Input Parameters (continued)

Parameter	Description
EGS	Excitation energy of the target nucleus. If left blank, target is in its ground state.
SPINGS	Spin of the target nucleus. If left blank, the spin is taken from the value in the mass table.
PARGS	Parity of the target nucleus. If left blank, the parity is taken from the value in the mass table.
NELAB	Number of incident particle energy included in the calculation, and maximum of 30.
ELABS(I)	Incident particle energies (in millions of the electron volts) in the laboratory system for the calculation.
ZACN(I)	1000*Z+A for each nucleus that is permitted to decay.
XNIP(I)	Number of decay channels permitted for decaying nucleus ZACN(I). The order of decay channel is fixed as follows;

XNIP	1	2	3	4	5	6	7
Gamma-ray	○	○	○	○	○	○	○
Neutron		○	○	○	○	○	○
Proton			○	○	○	○	○
Alpha				○	○	○	○
Deuteron					○	○	○
Triton						○	○
^{3}He							○

If XNIP(I)=5., the nucleus decay through gamma-ray, neutron, proton, alpha particle, and deuteron emissions.

AI(I)	Level density parameter "a", in the Fermi-gas model formula for the residual nucleus. Set AI(I)=0. to use the value in the data initialization statement or the equation (8) in Sec. 5.
GWD(I)	Radiative width for the decaying nucleus (in electron volts). Set GWD(I)=0. to use the value in the data initialization statement or the equation (9) in Sec. 5.

Table 1 Description of Input Parameters (continued)

Parameter	Description
RE1(I)	Relative strength of the Ith type gamma-ray transition. Set RE1(I)=0. to use a built-in value. The number of type, NMP is normally set to be 4 (E1, M1, E2, and M2), except for heavy nuclei, for which NMP=6 (E3 and M3 are added).
EG1,GG1,PG1	The position (MeV), width (MeV), and peak cross section (barn) of the giant dipole resonance. Set EG1=0. to use the default values.
EG2,GG2,PG2	The position, width, and peak cross section of the second giant dipole resonance, if it exists for the deformed nuclei. Otherwise set EG2=0..
RGG	Exponential reduction factor for Brink-Axel form gamma-ray strength function.
EG3,GG3,PG3	The position, width, and peak cross section of pygmy resonance. When it does not exist, set EG3=0..
EGCON,EGCNM1	Below these energies, E1 giant dipole resonance strength function or M1 giant dipole resonance strength function is assumed to be constant, respectively.
IZASO(I)	1000*Z+A for nucleus having isomeric state.
NLV(I)	Level number of isomeric state. Count ground state as 1, then number of (n-1)th excited level is n. If the isomeric state production cross section, whose half-life is very shorter so that the isomeric transition is allowed in the discrete level data, is wanted to be printed-out, input negative number -n as NLV(I). Table 6 gives the level number, excitation energy, half-life, and spin of isomeric state, and half-life and spin of ground state of nuclei, for which the cross section calculations were performed. The data of isomeric state of other nucleus will be added in Table 6.

Table 2 Sample of Input Data

```
  AG-109+ NEUTRON REACTION  (ELIESE-GNASH JOINT PROGRAM EGNASH2)
                                        1989 07 12  N. YAMAMURO
   9    0   11    0    0    1    5    0    7
1.       47109      0.5       0.4
0.42
  25
0.01     0.03      0.1       0.2       0.5       1.0       2.0       3.0
4.0      5.0       6.0       7.0       8.0       9.0       10.0      11.0
12.0     13.0      14.0      15.0      16.0      17.0      18.0      19.0
20.0
47110.   5.
47109.   4.
47108.   3.
47107.   1.
46109.   2.
46108.   2.
46107.   1.
45106.   2.
45105.   1.
0.
0.
0.
47110   3 47109   2 47108   3 47107   2 46109   3 45106   2 45105   2
```

Table 3 Description of Output Lists

	Description
REACTION CROSS SECTIONS (in mill-barn)	
COMPOUND	Compound formation cross section.
PRODUCTSUM	Sum of ground state and isomeric state production cross sections. PRODUCTSUM equals COMPOUND means that the isomeric states were perfectly included in the calculation and gamma-ray cascade calculations have been correctly performed. In the calculation for higher energy projectile, there is a few percent difference between COMPOUND and PRODUCTSUM, which are probably due to the imperfect gamma-ray cascade calculations. The calculation in the high energy region with ICAPT=1 or 2 shows the overestimation of PRODUCTSUM, which is caused by the lack of logic in the program. In that case, however, the (n,γ) cross section result is correct.
DIRECT	Sum of direct inelastic scattering cross sections.
PREEQRATE	Percentage of sum of preequilibrium cross sections to compound formation cross section.
NEUTRON	Total neutron production cross section.
PROTON	Total proton production cross section.
DEUTERON	Total deuteron production cross section.
ALPHA	Total alpha-particle production cross section.
GAMMA	Total gamma-ray production cross section.
G-ABOVETHRE	Gamma-ray production cross section above the detector threshold energy. Threshold energy is equal to 1.5 times energy bin width of calculation.
GROUND STATE PRODUCTION CROSS SECTIONS (in mill-barn)	Excitation functions of ground state of nuclei, which are indicated by 1000*Z+A, are shown in each column.
ISOMERIC STATE PRODUCTION CROSS SECTIONS (in mill-barn)	Excitation functions of isomeric state of nuclei inputted as IZASO(I) in the input-format are shown in each column.

Table 3 Description of Output Lists (continued)

	Description
LEVEL INELASTIC CROSS SECTIONS (in mill-barn)	The first column shows the nonelastic cross section, the second column the compound elastic scattering cross section. The following shows the inelastic scattering cross sections of from first excited level to 18th excited level.

Table 4 Sample of Output Data

AG-109+ NEUTRON REACTION (ELIESE-GNASH JOINT PROGRAM EGNASH2) 00000100
1989 07 12 N. YAMAMURO 00000200

REACTION CROSS SECTIONS

ENERGY(MEV)	COMPOUND	PRODUCTSUM	DIRECT	PREEQRATE	NEUTRON	PROTON	DEUTERON	ALPHA	GAMMA	G-ABOVTHRE
1.000-02	5.397D+03	5.397D+03	0.0	0.0	3.808D+03	0.0	0.0	0.0	1.610D+03	1.579D+03
3.000-02	5.004D+03	5.004D+03	0.0	0.0	4.064D+03	0.0	0.0	0.0	9.507D+02	9.341D+02
1.000-01	5.082D+03	5.082D+03	0.0	0.0	4.661D+03	0.0	0.0	0.0	4.248D+02	4.179D+02
2.000-01	4.705D+03	4.705D+03	0.0	0.0	4.445D+03	0.0	0.0	0.0	2.676D+02	2.583D+02
5.000-01	3.258D+03	3.258D+03	0.0	0.0	3.156D+03	0.0	0.0	1.106D-11	9.449D+02	1.015D+02
1.000+00	2.413D+03	2.413D+03	1.251D+01	3.098D-01	2.360D+03	0.0	0.0	8.551D-09	1.935D+03	1.621D+02
2.000+00	2.151D+03	2.151D+03	2.328D+01	9.565D-01	2.088D+03	1.796D-05	0.0	7.220D-07	2.812D+03	9.997D+02
3.000+00	1.973D+03	1.973D+03	5.517D+01	1.806D+00	1.915D+03	3.814D-03	0.0	2.698D-05	3.473D+03	1.788D+03
4.000+00	1.943D+03	1.943D+03	8.237D+01	2.939D+00	1.894D+03	5.128D-02	0.0	3.767D-04	4.059D+03	2.393D+03
5.000+00	1.987D+03	1.987D+03	1.007D+02	4.295D+00	1.944D+03	1.940D-01	0.0	2.214D-03	4.750D+03	3.015D+03
6.000+00	1.970D+03	1.970D+03	1.132D+02	5.772D+00	1.935D+03	3.985D-01	2.304D-09	2.018D-02	5.296D+03	3.521D+03
7.000+00	1.924D+03	1.924D+03	1.184D+02	7.310D+00	1.897D+03	6.744D-01	5.161D-06	5.527D-02	5.743D+03	3.966D+03
8.000+00	1.875D+03	1.875D+03	1.156D+02	8.885D+00	1.854D+03	1.335D+00	7.527D-04	1.205D-01	6.156D+03	4.380D+03
9.000+00	1.853D+03	1.853D+03	1.065D+02	1.044D+01	1.835D+03	2.290D+00	1.623D-02	2.612D-01	6.647D+03	4.840D+03
1.000+01	1.852D+03	1.852D+03	9.714D+01	1.198D+01	2.104D+03	3.801D+00	1.160D-01	5.555D-01	6.261D+03	4.431D+03
1.100+01	1.865D+03	1.865D+03	8.936D+01	1.349D+01	2.638D+03	5.975D+00	4.204D-01	1.081D+00	5.328D+03	3.123D+03
1.200+01	1.898D+03	1.898D+03	8.182D+01	1.500D+01	3.029D+03	9.030D+00	1.003D+00	1.868D+00	5.084D+03	2.592D+03
1.300+01	1.922D+03	1.922D+03	7.465D+01	1.649D+01	3.261D+03	1.293D+01	1.856D+00	2.901D+00	5.242D+03	2.587D+03
1.400+01	1.926D+03	1.926D+03	6.795D+01	1.794D+01	3.376D+03	1.747D+01	2.919D+00	4.118D+00	5.517D+03	2.936D+03
1.500+01	1.920D+03	1.920D+03	6.184D+01	1.953D+01	3.432D+03	2.281D+01	4.128D+00	5.464D+00	5.855D+03	3.282D+03
1.600+01	1.916D+03	1.916D+03	5.621D+01	2.117D+01	3.462D+03	2.906D+01	5.427D+00	6.923D+00	6.264D+03	3.683D+03
1.700+01	1.913D+03	1.913D+03	5.102D+01	2.278D+01	3.479D+03	3.612D+01	6.758D+00	8.476D+00	6.687D+03	4.083D+03
1.800+01	1.911D+03	1.911D+03	4.649D+01	2.433D+01	3.565D+03	4.403D+01	8.093D+00	1.012D+01	6.841D+03	4.259D+03
1.900+01	1.907D+03	1.907D+03	4.281D+01	2.581D+01	3.757D+03	5.265D+01	9.406D+00	1.184D+01	6.577D+03	4.061D+03
2.000+01	1.896D+03	1.895D+03	4.020D+01	2.726D+01	3.940D+03	6.181D+01	1.067D+01	1.364D+01	6.280D+03	3.801D+03

GROUND STATE PRODUCTION CROSS SECTIONS (MB)

ENERGY(MEV)	47110	47109	47108	47107	46109	46108	46107	45106	45105
1.000-02	1.589D+03	3.808D+03	0.0	0.0	0.0	0.0	0.0	0.0	0.0
3.000-02	9.400D+02	4.064D+03	0.0	0.0	0.0	0.0	0.0	0.0	0.0
1.000-01	4.205D+02	4.656D+03	0.0	0.0	0.0	0.0	0.0	0.0	0.0
2.000-01	2.599D+02	4.395D+03	0.0	0.0	0.0	0.0	0.0	0.0	0.0
5.000-01	1.020D+02	2.990D+03	0.0	0.0	0.0	0.0	0.0	1.106D-11	0.0
1.000+00	5.281D+01	1.944D+03	0.0	0.0	0.0	0.0	0.0	8.326D-09	0.0
2.000+00	6.343D+01	1.360D+03	0.0	0.0	1.761D-05	0.0	0.0	6.456D-07	0.0
3.000+00	5.699D+01	1.057D+03	0.0	0.0	3.568D-03	0.0	0.0	2.273D-05	0.0
4.000+00	4.796D+01	9.155D+02	0.0	0.0	4.734D-02	0.0	0.0	2.990D-04	0.0
5.000+00	4.052D+01	8.326D+02	0.0	0.0	1.783D-01	0.0	0.0	1.564D-03	0.0
6.000+00	3.240D+01	7.558D+02	0.0	0.0	3.644D-01	2.304D-09	0.0	1.378D-02	0.0
7.000+00	2.486D+01	6.927D+02	0.0	0.0	6.008D-01	5.161D-06	0.0	3.343D-02	1.776D-11
8.000+00	1.877D+01	6.385D+02	0.0	0.0	1.154D+00	7.572D-04	0.0	6.863D-02	3.946D-07
9.000+00	1.448D+01	5.924D+02	0.0	0.0	1.881D+00	2.040D-02	0.0	1.510D-01	2.823D-05
1.000+01	1.161D+01	4.534D+02	1.645D+02	0.0	2.925D+00	1.528D-01	0.0	3.034D-01	3.115D-04
1.100+01	9.625D+00	2.629D+02	5.084D+02	0.0	4.249D+00	5.794D-01	0.0	5.479D-01	1.934D-03
1.200+01	8.278D+00	1.610D+02	6.864D+02	0.0	5.701D+00	1.651D+00	0.0	8.601D-01	1.546D-02
1.300+01	7.266D+00	1.136D+02	7.414D+02	0.0	7.014D+00	3.676D+00	0.0	1.190D+00	8.813D-02
1.400+01	6.444D+00	8.724D+01	7.885D+02	0.0	7.982D+00	6.814D+00	0.0	1.519D+00	1.955D-01
1.500+01	5.771D+00	7.111D+01	7.733D+02	0.0	8.713D+00	1.108D+01	3.289D-08	1.781D+00	4.233D-01
1.600+01	5.238D+00	6.062D+01	7.507D+02	0.0	9.229D+00	1.655D+01	5.708D-05	1.932D+00	8.744D-01
1.700+01	4.809D+00	5.309D+01	7.236D+02	4.827D-01	9.444D+00	2.331D+01	2.149D-03	1.750D+00	1.577D+00
1.800+01	4.459D+00	4.743D+01	6.494D+02	1.586D+01	9.450D+00	3.128D+01	5.245D-02	1.677D+00	2.570D+00
1.900+01	4.161D+00	4.292D+01	5.143D+02	6.567D+01	9.293D+00	3.966D+01	4.289D-01	1.560D+00	3.874D+00

Table 4 Sample of Output Data (continued)

2.000+01	3.891D+00	3.930D+01	3.860D+02	1.302D+02	9.247D+00	4.742D+01	1.752D+00	1.416D+00	5.523D+00

ISOMERIC STATE PRODUCTION CROSS SECTIONS (MB)

ENERGY(MEV)	47110	47109	47108	47107	46109	45106	45105
1.000-02	3.925D-07	0.0	0.0	0.0	0.0	0.0	0.0
3.000-02	7.190D-06	0.0	0.0	0.0	0.0	0.0	0.0
1.000-01	1.626D-04	4.841D+00	0.0	0.0	0.0	0.0	0.0
2.000-01	3.992D-04	5.025D+01	0.0	0.0	0.0	0.0	0.0
5.000-01	2.262D-03	1.665D+02	0.0	0.0	0.0	3.927D-16	0.0
1.000+00	2.965D-02	4.168D+02	0.0	0.0	0.0	2.255D-10	0.0
2.000+00	5.080D-01	7.278D+02	0.0	0.0	3.520D-07	7.637D-08	0.0
3.000+00	8.753D-01	8.579D+02	0.0	0.0	2.463D-04	4.256D-06	0.0
4.000+00	1.263D+00	9.782D+02	0.0	0.0	3.946D-03	7.765D-05	0.0
5.000+00	1.581D+00	1.112D+03	0.0	0.0	1.569D-02	6.493D-04	0.0
6.000+00	1.588D+00	1.179D+03	0.0	0.0	3.413D-02	6.400D-03	0.0
7.000+00	1.395D+00	1.204D+03	0.0	0.0	7.359D-02	2.184D-02	2.267D-14
8.000+00	1.190D+00	1.215D+03	0.0	0.0	1.815D-01	5.188D-02	7.587D-08
9.000+00	1.083D+00	1.242D+03	0.0	0.0	4.043D-01	1.101D-01	5.904D-06
1.000+01	1.027D+00	1.112D+03	1.049D+02	0.0	8.398D-01	2.518D-01	5.082D-05
1.100+01	1.004D+00	7.933D+02	2.825D+02	0.0	1.567D+00	5.313D-01	2.964D-04
1.200+01	9.938D-01	5.637D+02	4.655D+02	0.0	2.681D+00	9.904D-01	2.006D-03
1.300+01	9.500D-01	4.192D+02	6.218D+02	0.0	4.094D+00	1.603D+00	1.993D-02
1.400+01	8.833D-01	3.291D+02	6.892D+02	0.0	5.595D+00	2.353D+00	4.976D-02
1.500+01	8.109D-01	2.665D+02	7.702D+02	0.0	7.149D+00	3.157D+00	1.024D-01
1.600+01	7.508D-01	2.271D+02	8.304D+02	0.0	8.708D+00	3.922D+00	1.955D-01
1.700+01	7.016D-01	2.009D+02	8.753D+02	2.361D+00	1.011D+01	4.812D+00	3.365D-01
1.800+01	6.647D-01	1.825D+02	8.837D+02	6.508D+01	1.130D+01	5.362D+00	5.085D-01
1.900+01	6.348D-01	1.689D+02	8.276D+02	2.093D+02	1.234D+01	5.723D+00	6.857D-01
2.000+01	6.072D-01	1.579D+02	7.438D+02	3.480D+02	1.283D+01	5.842D+00	8.586D-01

LEVEL INELASTIC SCATTERING CROSS SECTIONS (MB)

ENERGY(MEV)	NONELASTIC	GROUND	1ST-LEV	2ND-LEV	3RD-LEV	4TH-LEV	5TH-LEV	6TH-LEV	7TH-LEV	8TH-LEV
1.000-02	1.589D+03	3.808D+03	0.0	0.0	0.0	0.0	0.0	0.0	0.0	0.0
3.000-02	9.400D+02	4.064D+03	0.0	0.0	0.0	0.0	0.0	0.0	0.0	0.0
1.000-01	4.254D+02	4.656D+03	4.841D+00	0.0	0.0	0.0	0.0	0.0	0.0	0.0
2.000-01	3.101D+02	4.395D+03	4.493D+01	5.317D+00	0.0	0.0	0.0	0.0	0.0	0.0
5.000-01	1.063D+03	2.195D+03	1.325D+02	3.404D+01	6.101D+02	1.844D+02	0.0	0.0	0.0	0.0
1.000+00	1.800D+03	6.137D+02	1.369D+02	5.712D+01	3.207D+02	2.410D+02	1.701D+02	2.003D+02	2.028D+02	1.487D+02
2.000+00	1.994D+03	1.576D+02	8.345D+01	5.063D+01	1.054D+02	1.062D+02	1.072D+02	8.998D+01	9.904D+01	7.671D+01
3.000+00	1.937D+03	3.604D+01	2.504D+01	1.721D+01	2.671D+01	2.863D+01	4.363D+01	2.465D+01	3.581D+01	2.327D+01
4.000+00	1.935D+03	8.272D+00	7.028D+00	5.401D+00	6.559D+00	7.395D+00	2.503D+01	6.148D+00	1.813D+01	6.051D+00
5.000+00	1.984D+03	2.540D+00	2.390D+00	1.992D+00	2.466D+00	2.909D+00	2.263D+01	2.306D+00	1.517D+01	1.903D+00
6.000+00	1.969D+03	1.119D+00	1.083D+00	9.470D-01	2.302D+00	2.795D+00	2.248D+01	8.456D-01	1.512D+01	7.773D-01
7.000+00	1.923D+03	6.770D-01	6.757D-01	6.085D-01	1.740D+00	2.150D+00	2.122D+01	5.513D-01	1.424D+01	4.899D-01
8.000+00	1.875D+03	4.816D-01	5.056D-01	4.669D-01	1.388D+00	1.741D+00	1.893D+01	4.196D-01	1.268D+01	3.750D-01
9.000+00	1.852D+03	3.727D-01	4.159D-01	3.945D-01	1.154D+00	1.470D+00	1.664D+01	3.422D-01	1.114D+01	3.125D-01
1.000+01	1.852D+03	3.018D-01	3.562D-01	3.468D-01	9.951D-01	1.285D+00	1.461D+01	2.925D-01	9.779D+00	2.727D-01
1.100+01	1.865D+03	2.523D-01	3.121D-01	3.108D-01	8.732D-01	1.140D+00	1.317D+01	2.567D-01	8.813D+00	2.435D-01
1.200+01	1.898D+03	2.167D-01	2.797D-01	2.846D-01	7.883D-01	1.039D+00	1.194D+01	2.314D-01	7.989D+00	2.225D-01
1.300+01	1.922D+03	2.958D-01	3.958D-01	6.667D-01	4.254D-01	5.649D-01	1.088D+01	2.103D-01	7.279D+00	2.048D-01
1.400+01	1.926D+03	2.535D-01	3.480D-01	6.045D-01	3.735D-01	4.987D-01	9.956D+00	1.890D-01	6.658D+00	1.859D-01
1.500+01	1.920D+03	2.202D-01	3.078D-01	5.480D-01	3.306D-01	4.433D-01	9.135D+00	1.708D-01	6.108D+00	1.689D-01
1.600+01	1.916D+03	1.938D-01	2.747D-01	5.007D-01	2.966D-01	3.991D-01	8.344D+00	1.558D-01	5.578D+00	1.544D-01
1.700+01	1.912D+03	1.711D-01	2.454D-01	4.574D-01	2.669D-01	3.604D-01	7.566D+00	1.426D-01	5.058D+00	1.413D-01
1.800+01	1.911D+03	3.717D-01	2.788D-01	3.013D-01	1.735D-01	2.349D-01	6.862D+00	1.311D-01	4.587D+00	1.299D-01
1.900+01	1.907D+03	3.310D-01	2.541D-01	2.762D-01	1.571D-01	2.134D-01	6.290D+00	1.207D-01	4.204D+00	1.197D-01

Table 5(1) Level Density Parameters "a" (Z=25-32)

A	$_{25}$Mn	$_{26}$Fe	$_{27}$Co	$_{28}$Ni	$_{29}$Cu	$_{30}$Zn	$_{31}$Ga	$_{32}$Ge
50	6.8							
51	6.9							
62	7.0	6.6						
63	7.2	6.7	7.0					
54	7.3	6.8	7.2					
55	9.2	8.4	7.4	6.2				
56	9.8	8.4	7.6	6.5	6.6			
57	10.0	9.2	8.0	6.8	7.0			
58	10.4	9.2	8.6	7.0	7.2			
59		9.8	8.8	7.6	8.1	8.5		
60		10.6	9.7	8.1	8.5	8.8		
61		11.4	10.1	9.0	8.8	9.1		
62			11.5	9.1	9.2	9.5		
63			12.0	9.4	9.5	9.7		
64			12.5	9.8	10.0	9.8		
65				10.3	10.5	10.2		
66				10.7	10.7	10.3		
67				11.0	10.8	10.9		
68					11.3	10.8		
69					11.5	11.4		
70					11.8	11.7		
71						11.9		

Table 5(2) Level Density Parameters "a" (Z=36-43)

A	$_{36}Kr$	$_{37}Rb$	$_{38}Sr$	$_{39}Y$	$_{40}Zr$	$_{41}Nb$	$_{42}Mo$	$_{43}Tc$
80								
81								
82								
83								
84								
85								
86			17.0					
87			16.5					
88			12.0	12.2	13.5			
89			13.0	10.7	12.8			
90			14.0	11.0	11.3	10.7		
91			16.2	11.6	11.8	11.0	10.0	
92			16.8	14.3	11.9	11.5	10.6	
93			17.6	15.4	13.7	13.0	11.7	
94				17.3	14.0	14.4	12.5	
95				18.4	16.2	15.6	13.1	
96				19.6	16.5	16.0	14.3	
97					17.8	16.5	15.3	
98						16.7	15.8	
99						18.4	17.0	
100						19.6	17.9	
101							18.8	

Table 5(3) Level Density Parameters "a" (Z=44-51)*

A	$_{44}$Ru	$_{45}$Rh	$_{46}$Pd	$_{47}$Ag	$_{48}$Cd	$_{49}$In	$_{50}$Sn	$_{51}$Sb
100								
101								
102		16.2	16.0					
103		16.8	16.5					
104		17.5	17.0		13.6			
105		18.8	17.5	15.6	14.2			
106		20.0	18.3	16.2	15.0			
107			19.1	16.8	16.3			
108			20.0	17.5	17.2			
109			20.6	18.3	18.0			
110			22.8	20.0	18.5	18.7	18.6	
111			23.8	22.6	19.0	18.5	18.3	
112			25.0	24.1	19.4	18.5	18.0	
113			26.0	25.0	20.3	18.2	17.7	
114				26.0	21.0	18.1	17.4	
115				26.5	21.4	18.0	17.1	
116				27.0	22.1	18.1	16.7	
117					22.8	18.2	16.6	
118					23.0	19.0	16.5	
119					23.5	20.0	16.5	21.2
120					24.0	21.0	16.5	21.0
121					24.5	21.3	16.5	20.8
122						21.6	16.5	20.4
123						21.9	16.5	20.0
124						22.2	16.5	19.6
125							16.5	

* Some of level density parameter in this table are tentative, because $_{48}$Cd, $_{50}$Sn and $_{51}$Sb are calculated with SINCROS-I. The cross sections of these elements will be calculated with SINCROS-II.

Table 6 Table of Isomeric States

Nuclide	Reaction	Isomer State Level No.	E_x (MeV)	$T_{1/2}$	J	Ground State $T_{1/2}$	J
^{27}Al	(n,2n)^{26}Al	2	0.2284	6.34s	0^+	7.2E05y	5^+
	(n,α) ^{24}Na	2	0.4723	20.2ms	1^+	15.02h	4^+
^{45}Sc	(n,2n)^{44}Sc	5	0.2712	58.6h	6^+	3.93h	2^+
^{54}Fe	(n,2n)^{53}Fe	(21)	3.0407	2.58m	$19/2^-$	8.51m	$7/2^-$
	(n,t) ^{52}Mn	2	0.3777	21.1m	2^+	5.59d	6^+
^{59}Co	(n,γ) ^{60}Co	2	0.0586	10.48m	2^+	5.272y	5^+
	(n,2n)^{58}Co	2	0.0249	9.1h	5^+	70.91d	2^+
^{58}Ni	(n,p) ^{58}Co	2	(see above)				
^{60}Ni	(n,p) ^{60}Co	2	(see above)				
^{61}Ni	(n,np)^{60}Co	2	(see above)				
^{62}Ni	(n,p) ^{62}Co	2	0.022	13.9m	5^+	1.50m	2^+
^{63}Cu	(n,α) ^{60}Co	2	(see above)				
	(n,2nα)^{58}Co	2	(see above)				
^{65}Cu	(n,α) ^{62}Co	2	(see above)				
	(n,2nα)^{60}Co	2	(see above)				
^{68}Zn	(n,γ) ^{69}Zn	2	0.4387	13.8h	$9/2^+$	57m	$1/2^-$
	(n,p) ^{68}Cu	4	0.7216	3.8m	6^-	31s	1^+
^{70}Zn	(n,γ) ^{71}Zn	2	0.157	3.97h	$9/2^+$	2.4m	$1/2^-$
	(n,2n)^{69}Zn	2	(see above)				
	(n,p) ^{70}Cu	3	0.140	46s	4^-	5s	1^+

Table 6 Table of Isomeric States (continued)

Nuclide	Reaction	Isomer State Level No.	E_x (MeV)	$T_{1/2}$	J	Ground State $T_{1/2}$	J
^{90}Zr	$(n,n')^{90}Zr$	4	2.319	0.809s	5^-	sta.	0^+
	$(n,2n)^{89}Zr$	2	0.5878	4.18m	$1/2^-$	78.4h	$9/2^+$
	$(n,p)\ ^{90}Y$	3	0.6820	3.19h	7^+	64.0h	2^-
	$(n,np)^{89}Y$	2	0.9092	15.7s	$9/2^+$	sta.	$1/2^-$
	$(n,\alpha)\ ^{87}Sr$	2	0.3884	2.80h	$1/2^-$	sta.	$9/2^+$
^{91}Zr	$(n,2n)^{90}Zr$	4	(see above)				
	$(n,p)\ ^{91}Y$	2	0.5556	49.7m	$9/2^+$	58.5d	$1/2^-$
	$(n,np)^{90}Y$	3	(see above)				
^{92}Zr	$(n,3n)^{90}Zr$	4	(see avove)				
	$(n,np)^{91}Y$	2	(see above)				
^{93}Nb	$(n,\gamma)\ ^{94}Nb$	2	0.04095	6.26m	3^+	2.0E04y	6^+
	$(n,n')^{93}Nb$	2	0.03082	15.8y	$1/2^-$	sta.	$9/2^+$
	$(n,2n)^{92}Nb$	2	0.1355	10.13d	2^+	3.7E07y	7^+
	$(n,3n)^{91}Nb$	2	0.1045	62d	$1/2^-$	7.0E02y	$9/2^+$
	$(n,\alpha)\ ^{90}Y$	3	(see above)				
	$(n,n\alpha)^{89}Y$	2	(see above)				
^{94}Nb	$(n,\gamma)\ ^{95}Nb$	2	0.2357	3.61d	$1/2^-$	34.98d	$9/2^+$
^{92}Mo	$(n,\gamma)\ ^{93}Mo$	(13)	2.4252	6.9h	$21/2^+$	3.5E03y	$5/2^+$
	$(n,2n)^{91}Mo$	2	0.6530	65s	$1/2^-$	15.5m	$9/2^+$
	$(n,p)\ ^{92}Nb$	2	(see above)				
	$(n,np)^{91}Nb$	2	(see above)				
	$(n,\alpha)\ ^{89}Zr$	2	(see above)				
^{94}Mo	$(n,2n)^{93}Mo$	(13)	(see above)				
	$(n,p)\ ^{94}Nb$	2	(see above)				
	$(n,np)^{93}Nb$	2	(see above)				
	$(n,n\alpha)^{90}Zr$	4	(see above)				
^{95}Mo	$(n,p)\ ^{95}Nb$	2	(see above)				
	$(n,np)^{94}Nb$	2	(see above)				

Table 6 Table of Isomeric States (continued)

Nuclide	Reaction	Isomer State Level No.	E_x (MeV)	$T_{1/2}$	J	Ground State $T_{1/2}$	J
^{96}Mo	(n,np)^{95}Nb	2	0.2357	3.61d	$1/2^-$	34.98d	$9/2^+$
^{97}Mo	(n,p) ^{97}Nb	2	0.7434	54s	$1/2^-$	73.6m	$9/2^+$
^{98}Mo	(n,p) ^{98}Nb	2	0.084	51m	5^+	2.8s	1^+
	(n,np)^{97}Nb	2	0.7434	54s	$1/2^-$	73.6m	$9/2^+$
^{100}Mo	(n,np)^{99}Nb	2	0.3653	2.6m	$1/2^-$	15s	$9/2^+$
	(n,2np)^{98}Nb	2	(see above)				
^{107}Ag	(n,γ) ^{108}Ag	3	0.10947	127y	6^+	2.37m	1^+
	(n,n')^{107}Ag	2	0.0931	44.2s	$7/2^+$	sta.	$1/2^-$
	(n,2n)^{106}Ag	2	0.08963	8.5d	6^+	24.0m	1^+
	(n,3n)^{105}Ag	2	0.0255	7.23m	$7/2^+$	41.29d	$1/2^-$
	(n,p) ^{107}Pd	3	0.2149	20.9s	$11/2^-$	6.5E06y	$5/2^+$
	(n,α) ^{104}Rh	4	0.12896	4.36m	5^+	41.8s	1^+
	(n,nα)^{103}Rh	2	0.03975	56.12m	$7/2^+$	sta.	$1/2^-$
^{109}Ag	(n,γ) ^{110}Ag	3	0.1176	249.8d	6^+	24.6s	1^+
	(n,n')^{109}Ag	2	0.08803	39.8s	$7/2^+$	sta.	$1/2^-$
	(n,2n)^{108}Ag	3	(see above)				
	(n,3n)^{107}Ag	2	(see above)				
	(n,p) ^{109}Pd	3	0.1890	4.68m	$11/2^-$	13.43h	$5/2^+$
	(n,α) ^{106}Rh	2	0.14	2.18h	6^+	29.8s	1^+
	(n,nα)^{105}Rh	2	0.12978	45s	$1/2^-$	35.4h	$7/2^+$

Table 6 Table of Isomeric States (continued)

Nuclide	Reaction	Isomer State Level No.	E_x (MeV)	$T_{1/2}$	J	Ground State $T_{1/2}$	J
^{106}Cd	(n,p) ^{106}Ag	2	0.08963	8.5d	6^+	24.0m	1^+
	(n,np)^{105}Ag	2	0.02547	7.23m	$7/2^+$	41.3d	$1/2^-$
^{108}Cd	(n,p) ^{108}Ag	3	0.10947	1.3E02y	6^+	2.42m	1^+
	(n,np)^{107}Ag	2	0.0931	44.2s	$7/2^+$	sta.	$1/2^-$
^{110}Cd	(n,γ) ^{111}Cd	4	0.3962	48.6m	$11/2^-$	sta.	$1/2^+$
	(n,p) ^{110}Ag	3	0.1176	249.8d	6^+	24.6s	1^+
	(n,np)^{109}Ag	2	0.08803	39.8s	$7/2^+$	sta.	$1/2^-$
	(n,α) ^{107}Pd	3	0.2149	20.9s	$11/2^-$	6.5E06y	$5/2^+$
^{111}Cd	(n,n')^{111}Cd	4	(see above)				
	(n,p) ^{111}Ag	2	0.05982	64.8s	$7/2^+$	7.47d	$1/2^-$
	(n,np)^{110}Ag	3	(see above)				
	(n,nα)^{107}Pd	3	(see above)				
^{112}Cd	(n,γ) ^{113}Cd	2	0.2636	14.1y	$11/2^-$	9.0E15y	$1/2^+$
	(n,2n)^{111}Cd	4	(see above)				
	(n,np)^{111}Ag	2	(see above)				
	(n,α) ^{109}Pd	3	0.18899	4.69m	$11/2^-$	13.43y	$5/2^+$
^{113}Cd	(n,n')^{113}Cd	2	(see above)				
	(n,p) ^{113}Ag	2	0.0432	68.7s	$7/2^+$	5.3h	$1/2^-$
	(n,nα)^{109}Pd	3	(see above)				
^{114}Cd	(n,γ) ^{115}Cd	2	0.181	44.6d	$11/2^-$	53.5h	$1/2^+$
	(n,2n)^{113}Cd	2	(see above)				
	(n,np)^{113}Ag	2	(see above)				
	(n,α) ^{111}Pd	3	0.1722	5.5h	$11/2^-$	22m	$5/2^+$
^{116}Cd	(n,γ) ^{117}Cd	3	0.1364	3.36h	$11/2^-$	2.49h	$1/2^+$
	(n,2n)^{115}Cd	2	(see above)				
	(n,p) ^{116}Ag	2	0.081	10.4s	( )	2.68m	( )
	(n,np)^{115}Ag	2	( )	18.0s	$7/2^+$	20m	$1/2^-$
	(n,α) ^{113}Pd	2	( )	89.0s	( )	98s	( )

Table 6 Table of Isomeric States (continued)

Nuclide	Reaction	Level No.	Isomer State E_x (MeV)	$T_{1/2}$	J	Ground State $T_{1/2}$	J
^{113}In	$(n,\gamma)\ ^{114}In$	2	0.1903	49.51d	5^+	71.9s	1^+
	$(n,n')^{113}In$	2	0.3917	1.6851h	$1/2^-$	sta.	$9/2^+$
	$(n,2n)^{112}In$	2	0.1565	20.9m	4^+	14.4m	1^+
	$(n,3n)^{111}In$	2	0.05368	7.7m	$1/2^-$	2.83d	$9/2^+$
	$(n,p)\ ^{113}Cd$	2	0.2636	14.1y	$11/2^-$	9.0E15y	$1/2^+$
	$(n,\alpha)\ ^{110}Ag$	3	0.1176	249.8d	6^+	24.6s	1^+
	$(n,n\alpha)^{109}Ag$	2	0.08803	39.8s	$7/2^+$	sta.	$1/2^-$
^{115}In	$(n,\gamma)\ ^{116}In$	5	0.2897	2.18s	8^-	14.1s	1^+
		2	0.1273	54.15m	5^+		
	$(n,n')^{115}In$	2	0.3362	4.486h	$1/2^-$	sta.	$9/2^+$
	$(n,2n)^{114}In$	2	(see above)				
	$(n,3n)^{113}In$	2	(see avobe)				
	$(n,p)\ ^{115}Cd$	2	0.181	44.6d	$11/2^-$	53.5h	$1/2^+$
	$(n,n\alpha)^{111}Ag$	2	0.05982	64.8s	$7/2^+$	7.47d	$1/2^-$

Table 6 Table of Isomeric States (continued)

Nuclide	Reaction	Isomer State				Ground State	
		Level No.	E_x (MeV)	$T_{1/2}$	J	$T_{1/2}$	J
^{112}Sn	(n,γ) ^{113}Sn	2	0.0774	21.4m	$7/2^+$	115.1d	$1/2^+$
	(n,p) ^{112}In	2	0.1565	20.9m	4^+	14.4m	1^+
	(n,np)^{111}In	2	0.5368	7.7m	$1/2^-$	2.806d	$9/2^+$
^{114}Sn	(n,2n)^{113}Sn	2	(see above)				
	(n,p) ^{114}In	2	0.1903	49.51d	5^+	71.9s	1^+
	(n,np)^{113}In	2	0.3917	1.658h	$1/2^-$	sta.	$9/2^+$
	(n,α) ^{111}Cd	4	0.3962	48.6m	$11/2^-$	sta.	$1/2^+$
^{115}Sn	(n,p) ^{115}In	2	0.3362	4.486h	$1/2^-$	sta.	$9/2^+$
	(n,np)^{114}In	2	(see above)				
	(n,nα)^{111}Cd	4	(see above)				
^{116}Sn	(n,γ) ^{117}Sn	3	0.3146	13.6d	$11/2^-$	sta.	$1/2^+$
	(n,p) ^{116}In	5	0.2897	2.18s	8^-	14.1s	1^+
		2	0.1273	54.15m	5^+		
	(n,np)^{115}In	2	(see above)				
	(n,α) ^{113}Cd	2	0.2636	14.1y	$11/2^-$	sta.	$1/2^+$
^{117}Sn	(n,n')^{117}Sn	3	(see above)				
	(n,p) ^{117}In	2	0.3153	116.5m	$1/2^-$	43.1m	$9/2^+$
	(n,np)^{116}In	5	(see above)				
		2	(see above)				
	(n,nα)^{113}Cd	2	(see above)				
^{118}Sn	(n,γ) ^{119}Sn	3	0.0895	293d	$11/2^-$	sta.	$1/2^+$
	(n,2n)^{117}Sn	3	(see above)				
	(n,p) ^{118}In	4	0.20	8.5s	8^-	5.0s	1^+
		2	0.060	4.45m	5^+		
	(n,np)^{117}In	2	(see above)				
	(n,α) ^{115}Cd	2	0.181	44.6d	$11/2^-$	53.5h	$1/2^+$
^{119}Sn	(n,n')^{119}Sn	3	(see above)				
	(n,p) ^{119}In	2	0.3114	18.0m	$1/2^-$	2.4m	$9/2^+$
	(n,np)^{118}In	4	(see above)				
		2	(see above)				
	(n,nα)^{115}Cd	2	(see above)				

Table 6 Table of Isomeric States (continued)

Nuclide	Reaction	Isomer State Level No.	E_x (MeV)	$T_{1/2}$	J	Ground State $T_{1/2}$	J
^{120}Sn	(n,γ) ^{121}Sn	2	0.0063	55y	$11/2^-$	27.0h	$3/2^+$
	(n,2n)^{119}Sn	3	0.0895	293d	$11/2^-$	sta.	$1/2^+$
	(n,p) ^{120}In	3	( )	47.3s	8^-	3.08s	1^+
		2	( )	46.2s	5^+		
	(n,np)^{119}In	2	0.3114	18.0m	$1/2^-$	2.4m	$9/2^+$
	(n,α) ^{117}Cd	3	0.1364	3.36h	$11/2^-$	2.49h	$1/2^+$
^{122}Sn	(n,γ) ^{123}Sn	2	0.0246	40.08m	$3/2^+$	129.2d	$11/2^-$
	(n,2n)^{121}Sn	2	(see above)				
	(n,p) ^{122}In	5	0.220	10.8s	8^-	1.5s	1^+
		2	( )	10.3s	4^+		
	(n,np)^{121}In	2	0.3136	3.88m	$1/2^-$	23s	$9/2^+$
	(n,α) ^{119}Cd	3	0.1465	2.20m	$11/2^-$	2.69m	$1/2^+$
^{124}Sn	(n,γ) ^{125}Sn	2	0.0275	9.52m	$3/2^+$	9.63d	$11/2^-$
	(n,2n)^{123}Sn	2	(see above)				
	(n,p) ^{124}In	5	0.190	2.4s	8^-	3.2s	3^+
	(n,np)^{123}In	2	0.320	47.8m	$1/2^-$	6.0s	$9/2^+$
	(n,α) ^{121}Cd	2	( )	4.8s	( )	13.5s	( )
^{121}Sb	(n,γ) ^{122}Sb	6	0.16356	4.21m	8^-	2.71d	2^-
	(n,2n)^{120}Sb	2	( )	5.76d	8^-	15.9m	1^+
	(n,p) ^{121}Sn	2	0.0063	55y	$11/2^-$	27.0h	$3/2^+$
	(n,α) ^{118}In	4	0.20	8.5s	8^-	5.0s	1^+
		2	0.060	4.45m	5^+		
	(n,nα)^{117}In	2	0.3153	116.5m	$1/2^-$	43.1m	$9/2^+$
^{123}Sb	(n,γ)^{124}Sb	2	0.0109	93s	5^+	60.2d	3^-
		3	0.03685	20.2m	8^-		
	(n,2n)^{122}Sb	6	(see above)				
	(n,p) ^{123}Sn	2	0.0246	40.08m	$3/2^+$	129.2d	$11/2^-$
	(n,α) ^{120}In	3	( )	47.3s	8^-	3.08s	1^+
		2	( )	46.2s	5^+		
	(n,nα)^{119}In	2	0.3114	18.0m	$1/2^-$	2.4m	$9/2^+$

Table 6 Table of Isomeric States (continued)

Nuclide	Reaction	Level No.	Isomer State E_x (MeV)	$T_{1/2}$	J	Ground State $T_{1/2}$	J
^{180}Ta	(n,α) ^{177}Lu	( )	0.97015	160d	$23/2^-$	6.71d	$7/2^+$
^{181}Ta	(n,γ) ^{182}Ta	(25)	0.5197	15.9m	10^-	114.5d	3^-
	(n,2n) ^{180}Ta	3	0.0753	1.2E+15y	9^-	8.15h	1^+
	(n,α) ^{178}Lu	3	0.30	22.7m	9^-	28.5m	1^+
^{184}W	(n,γ) ^{185}W	7	0.1974	1.67m	$11/2^+$	75.1d	$3/2^-$
	(n,2n) ^{183}W	8	0.3095	5.2s	$11/2^+$	sta.	$1/2^-$
	(n,nα) ^{180}Hf	7	1.1416	5.5h	8^-	sta.	0^+
^{185}Re	(n,γ) ^{186}Re	5	0.1490	2.0E+05y	8^+	90.7h	1^-
	(n,2n) ^{184}Re	7	0.1880	165d	8^+	38d	3^-
	(n,p) ^{185}W	7	(see above)				
^{187}Re	(n,γ) ^{188}Re	8	0.1721	18.6m	6^-	16.98h	1^-
	(n,2n) ^{186}Re	5	(see above)				
^{209}Bi	(n,γ) ^{210}Bi	3	0.2712	3.0E+06y	9^-	5.01d	1^-
	(n,α) ^{206}Tl	( )	2.643	3.76m	12^-	4.20m	0^-

Table 7 Table Production Cross Sections of Proton and Alpha-particle by 15 MeV Neutron (mb)

Nucleus	Proton		Alpha-particle	
	Experiment	Calculation	Experiment[d]	Calculation
^{59}Co		121	40±3	39.5
^{58}Ni	1000±120[a]	1068	121±8	120
^{60}Ni	325±40[a]	340	79±5	74.9
^{63}Cu	320±45[a]	331	65±4	61.5
^{65}Cu	44±5[a]	44.4	17±1	16.0
Zr		78.6	10.1±0.7	14.8
^{93}Nb	51±8[b]	48.1	14±1	13.7
Mo	195±30[c]	154	14±1	13.4
^{92}Mo	967±116[c]	846	31±2	27.0
^{94}Mo	124±15[c]	85.8	22±2	20.1
^{95}Mo	84±10[c]	66.5	17±1	18.6
^{96}Mo	64±8[c]	31.8	12±1	9.8
^{97}Mo		20.5	10±1	10.9
^{98}Mo		9.5	6.7±3.2	6.6
^{100}Mo		3.2	3.8±0.3	3.5
Ag		44.8	7.6±0.6	7.1

a) reference 27)

b) reference 28)

c) reference 29)

d) reference 26)

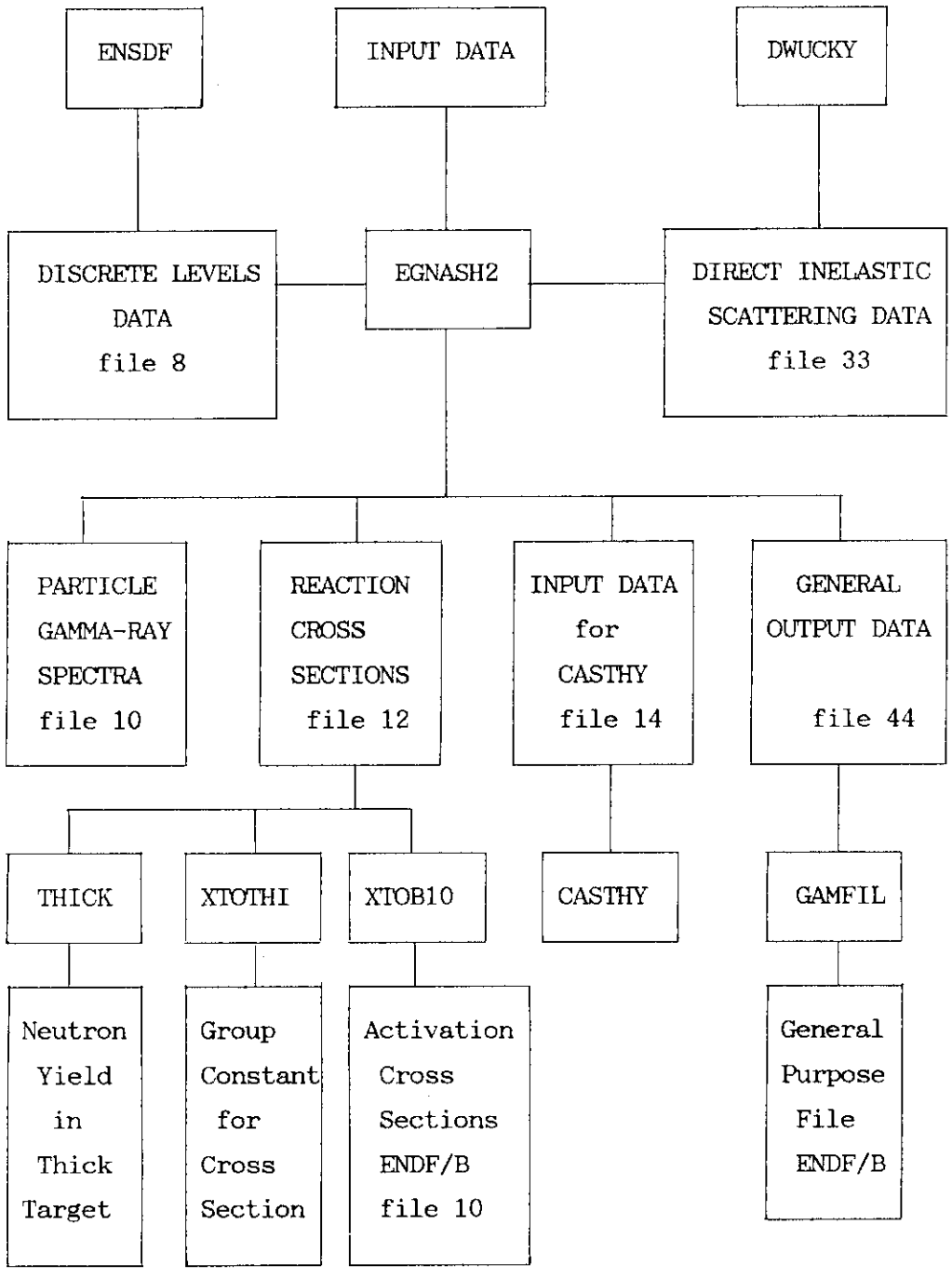

Fig. 1 Composition of SINCROS-II and the flow of dara processing.

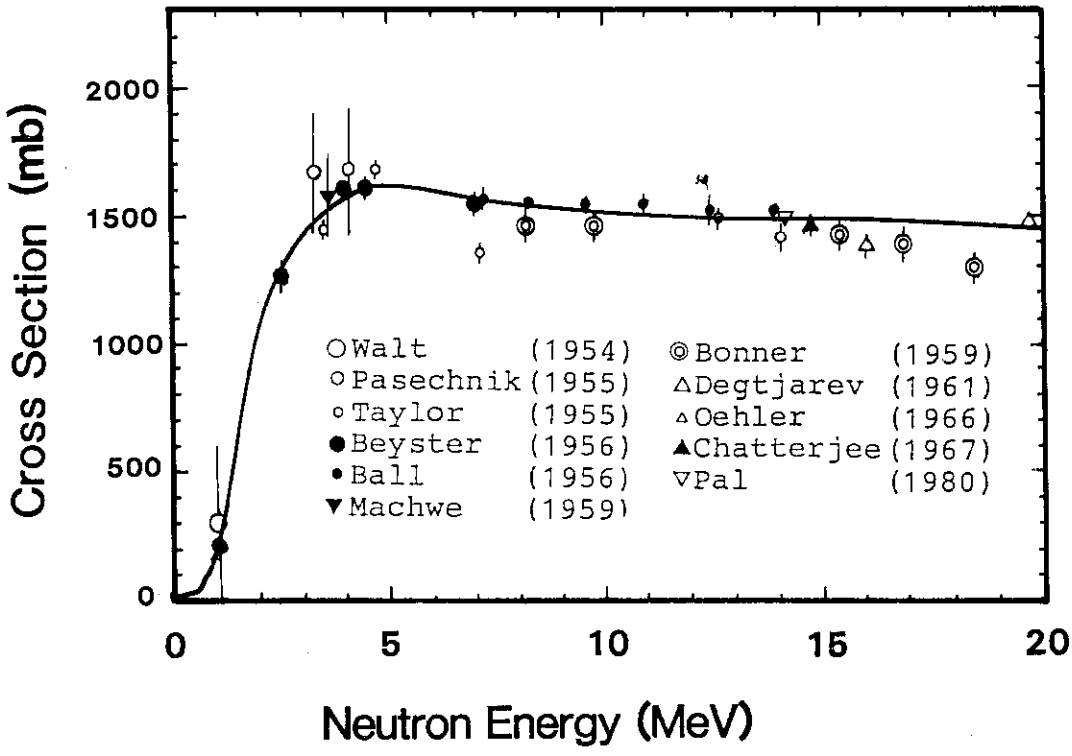

Fig. 2 Nonelastic cross sections for copper. The calculated one is obtained for ^{63}Cu using a modified Walter and Guss potential.

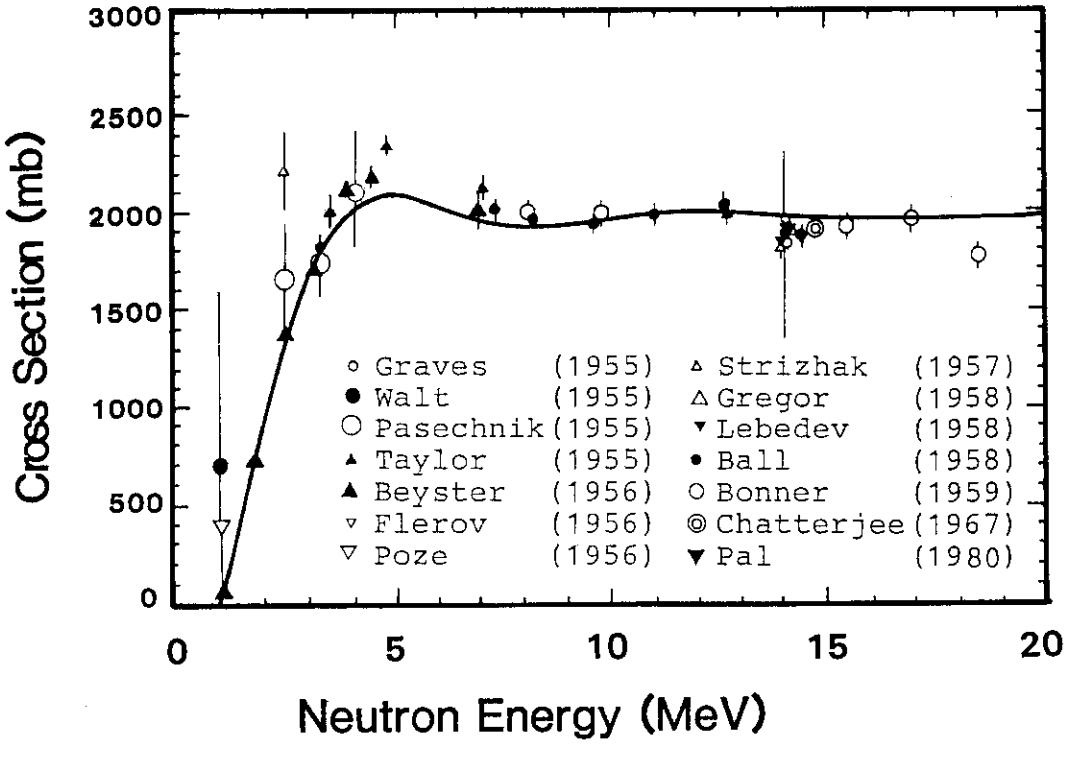

Fig. 3 Nonelastic cross sections for tin. The calculation is made for ^{120}Sn using a modified Walter and Guss potential.

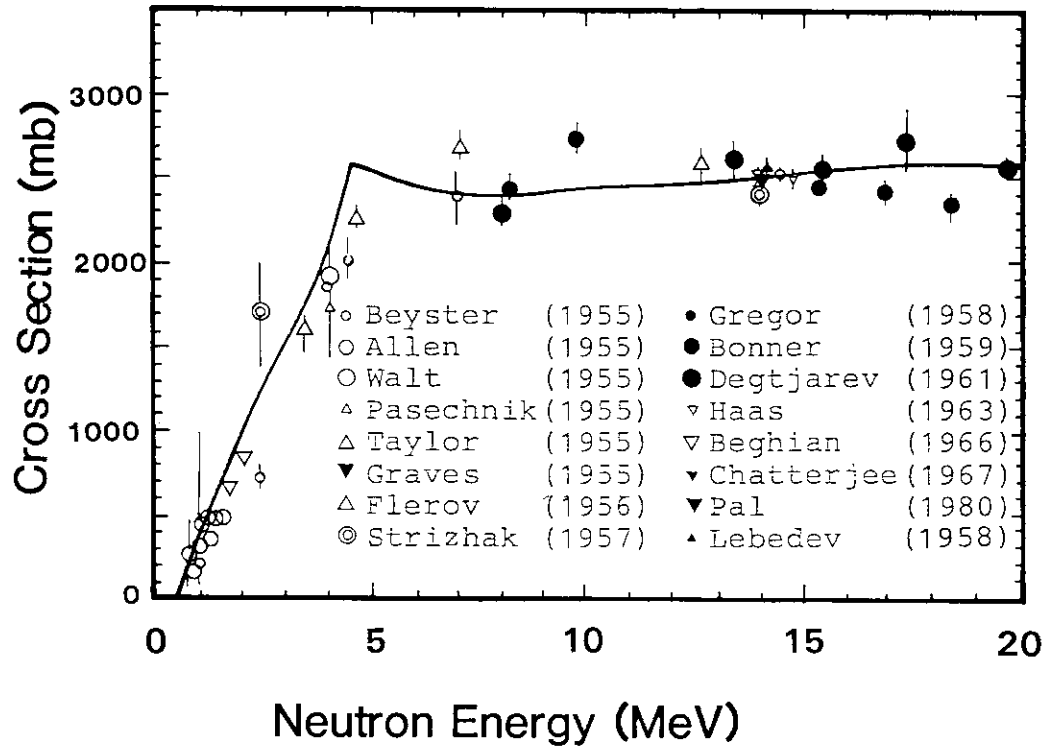

Fig. 4 Nonelastic cross sections for lead. The calculated one is obtained for natural lead using a modified Walter and Guss potential.

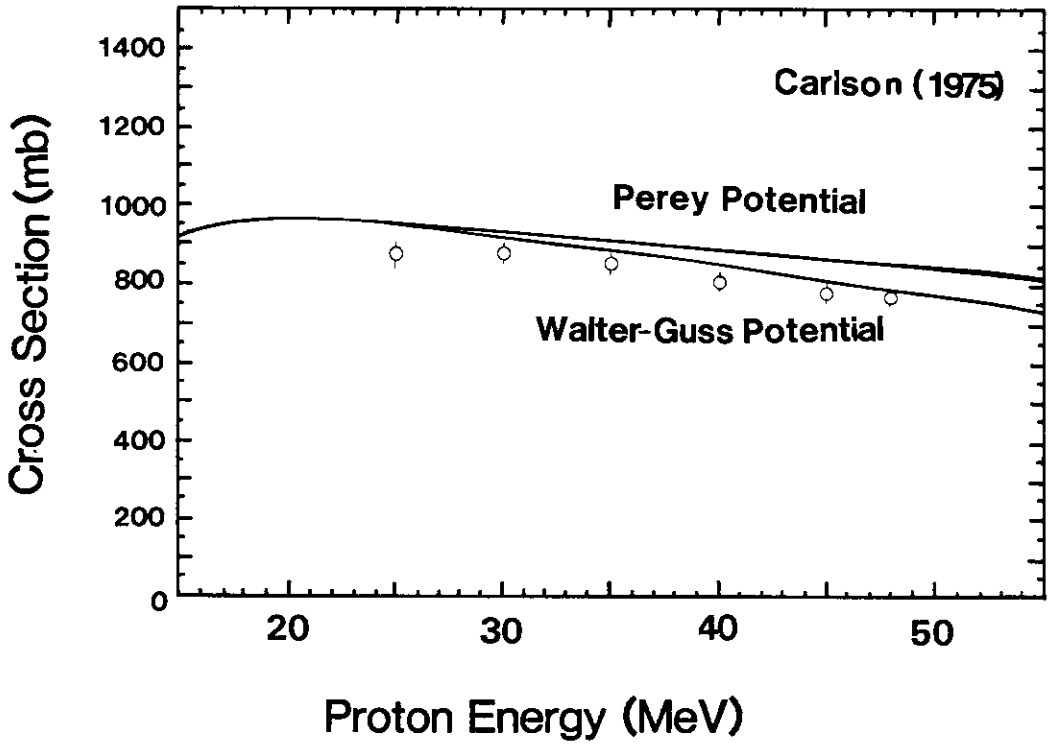

Fig. 5 Total proton reaction cross sections for ^{40}Ca. Walter and Guss potential reproduced experimental measurement better than Perey potential in higher energy region.

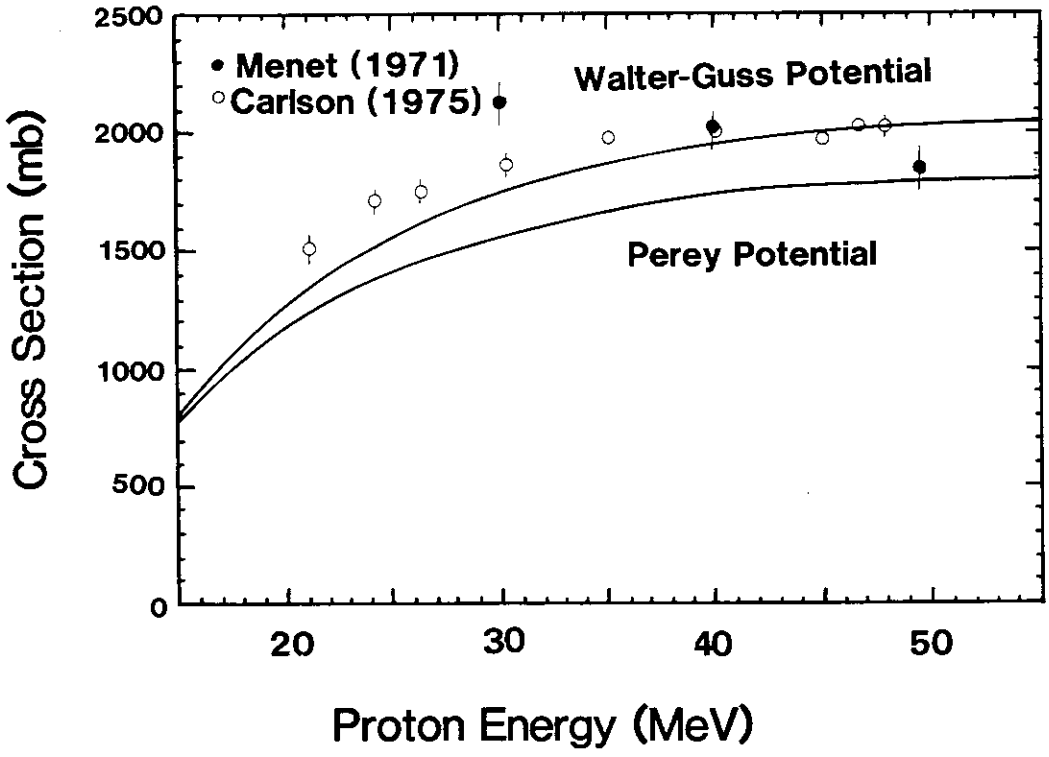

Fig. 6 Total proton reaction cross sections for ^{208}Pb. Perey potential quite underestimated the experimental data above 20 MeV.

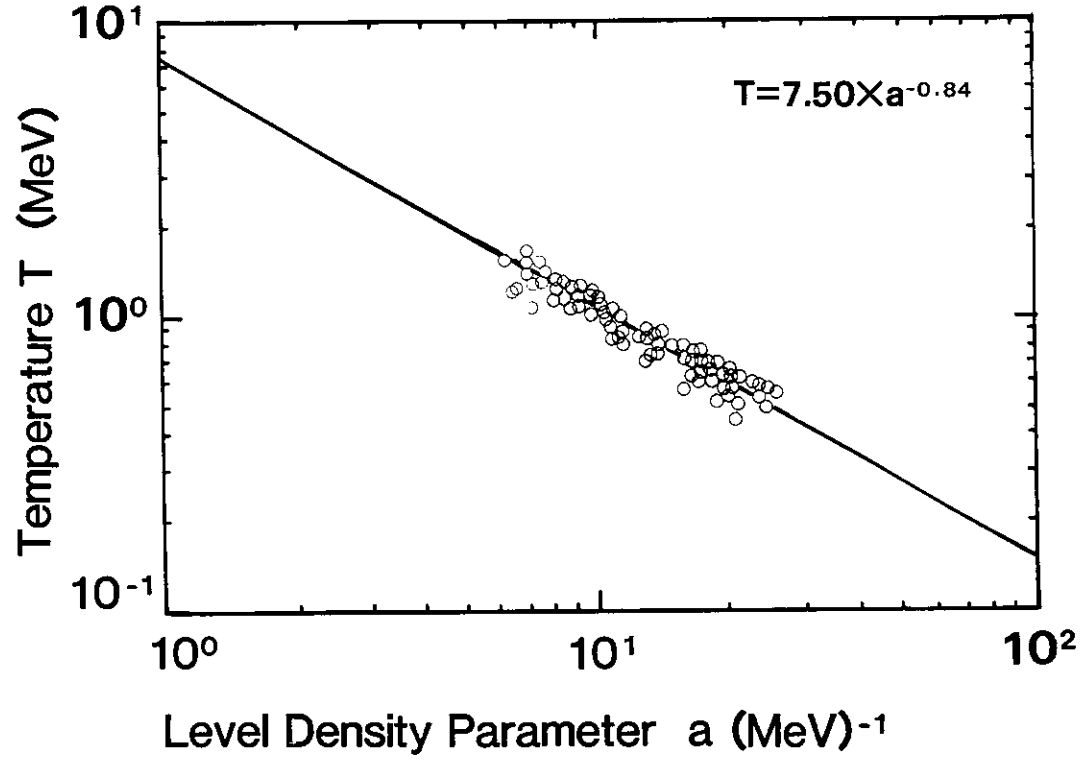

Fig. 7 The relation between the nuclear temperature and level density parameter. The straight line in the figure represents the formula $T = 7.50*a^{-0.84}$.

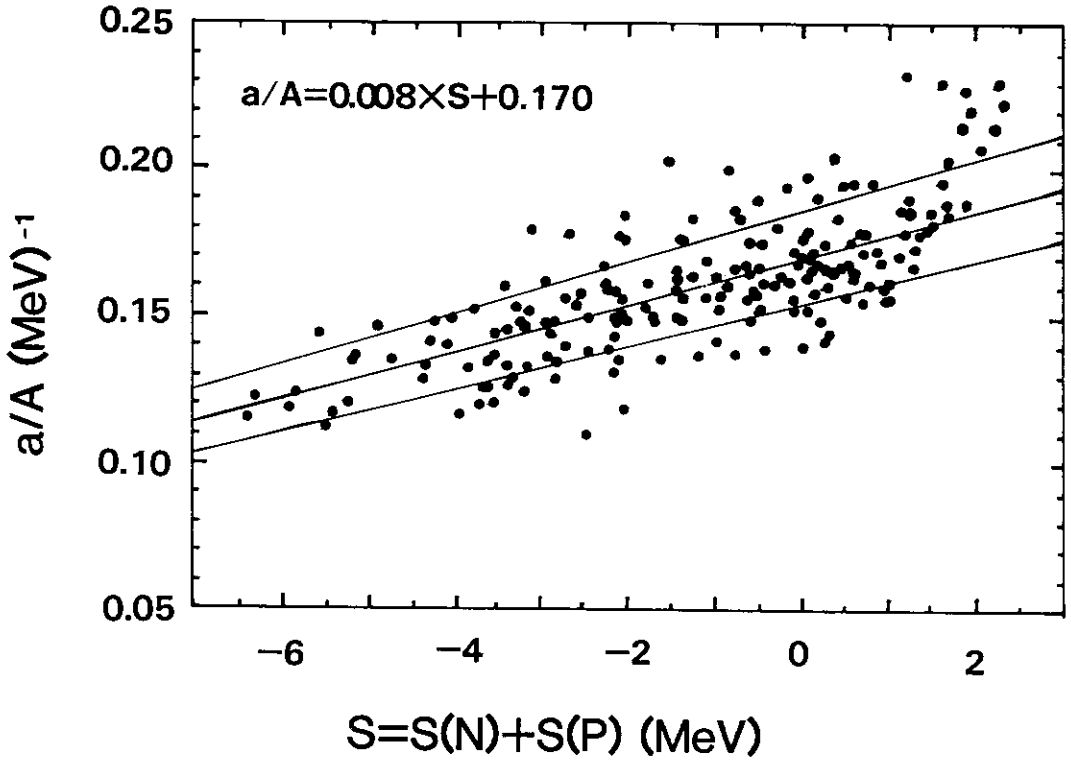

Fig. 8 The ratio of level density parameter to mass number (a/A) as a function of the shell correction energy S given by Gilbert and Cameron. The tentative relation a/A = 0.008*S + 0.170 and its ±10% lines are written in the figure.

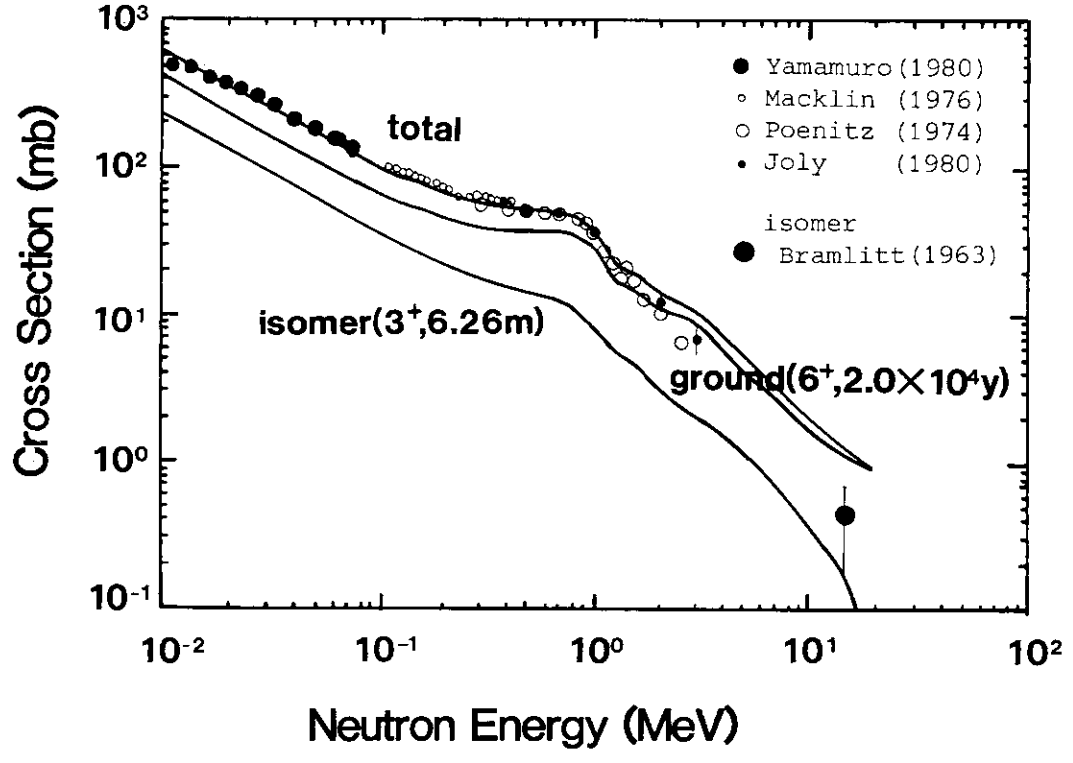

Fig. 9 Calculated and experimental $^{93}Nb(n,\gamma)^{94}Nb$ cross sections. Total capture cross section is normalized to 100 mb at 100 keV in the calculation.

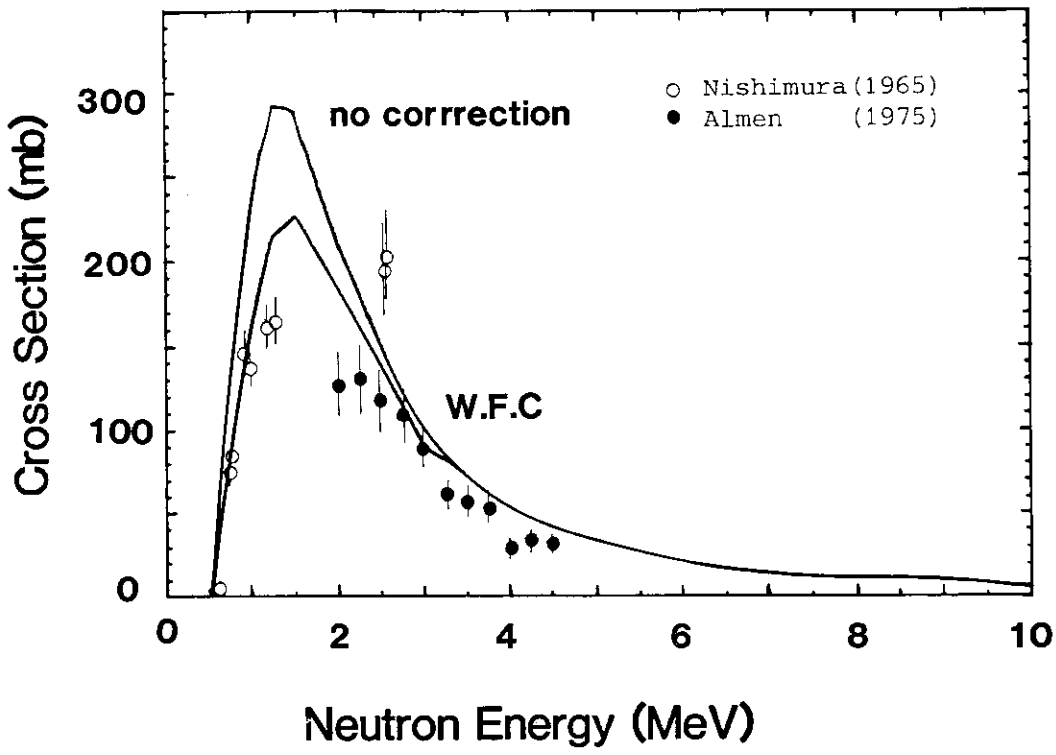

Fig. 10 Inelastic-scattering cross sections for first excited state of ^{63}Cu. Calculation was carried out with and without width fluctuation correction.

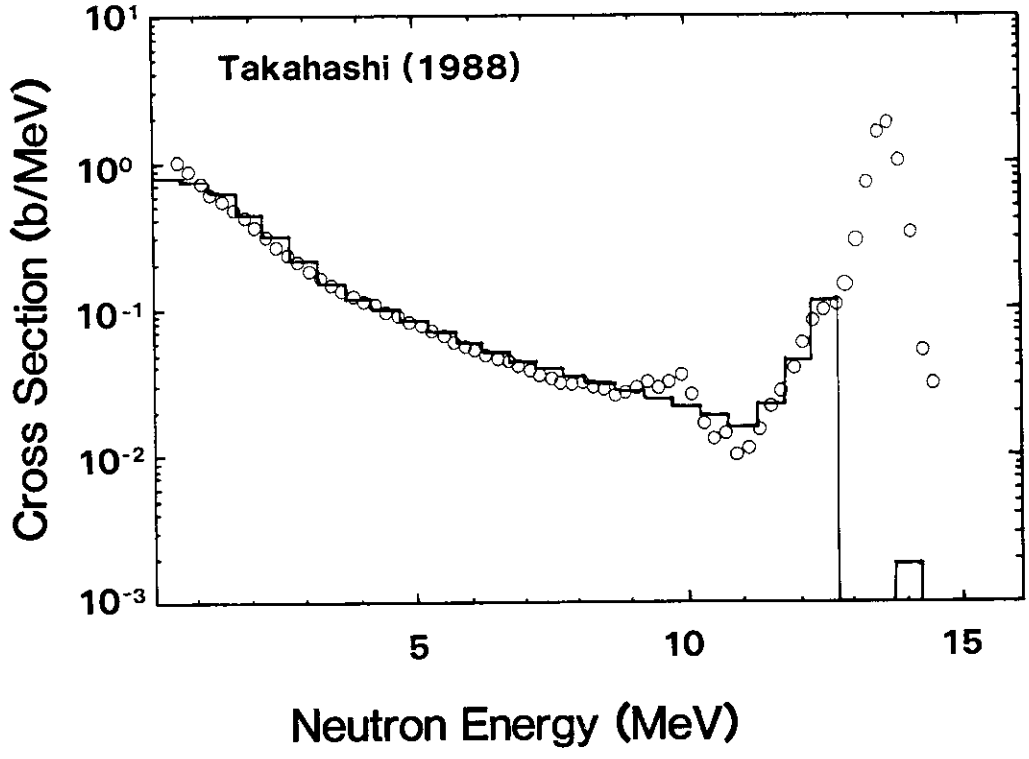

Fig. 11 Calculated and experimental neutron emission spectra for ^{59}Co at neutron energy 14.1 MeV.

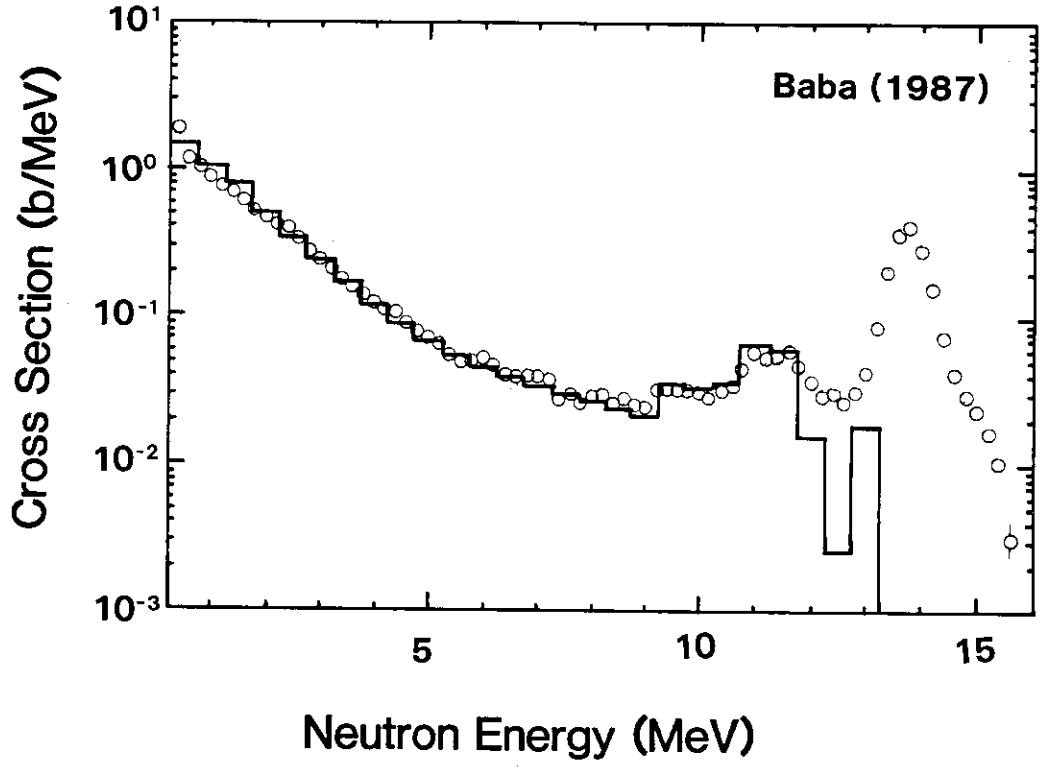

Fig. 12 Calculated and experimental neutron emission spectra for Zr at neutron energy 14.1 MeV.

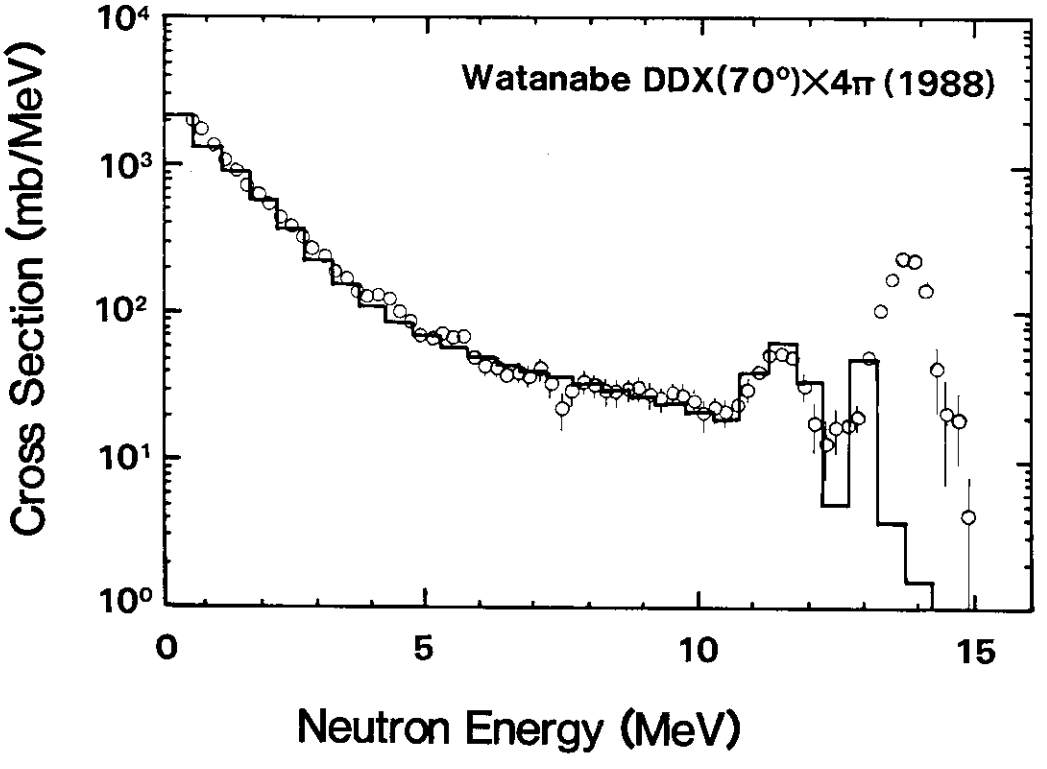

Fig. 13 4π times double differential neutron emission cross section at 70 degrees for Ag at neutron energy 14.1 MeV.

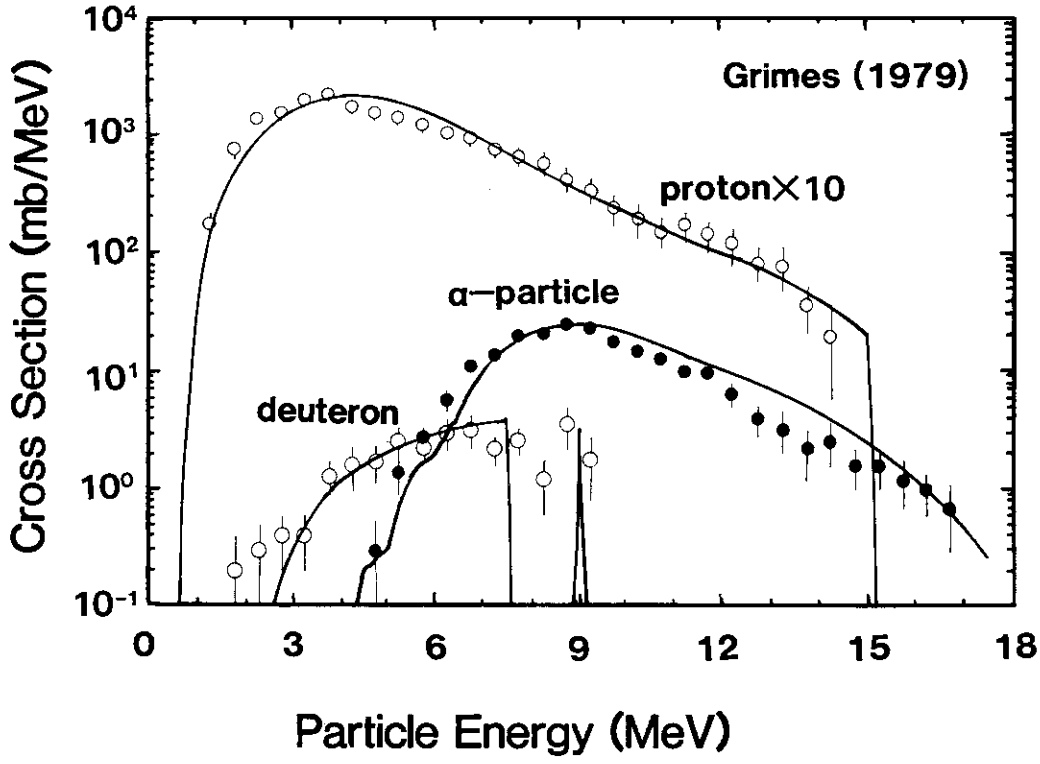

Fig. 14 Calculated and experimental proton, alpha-particle, and deuteron emission spectra for ^{58}Ni at neutron energy 15 MeV.

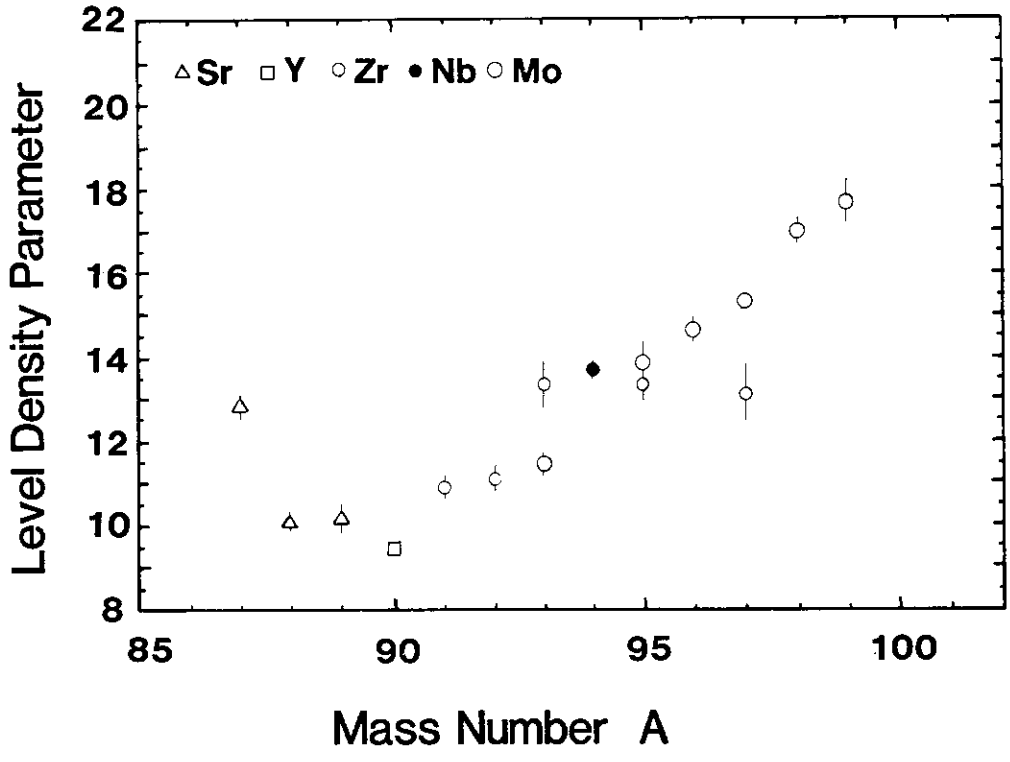

Fig. 15 Level density parameters calculated from the average s-wave neutron resonance spacing in mass range of 85 to 102.

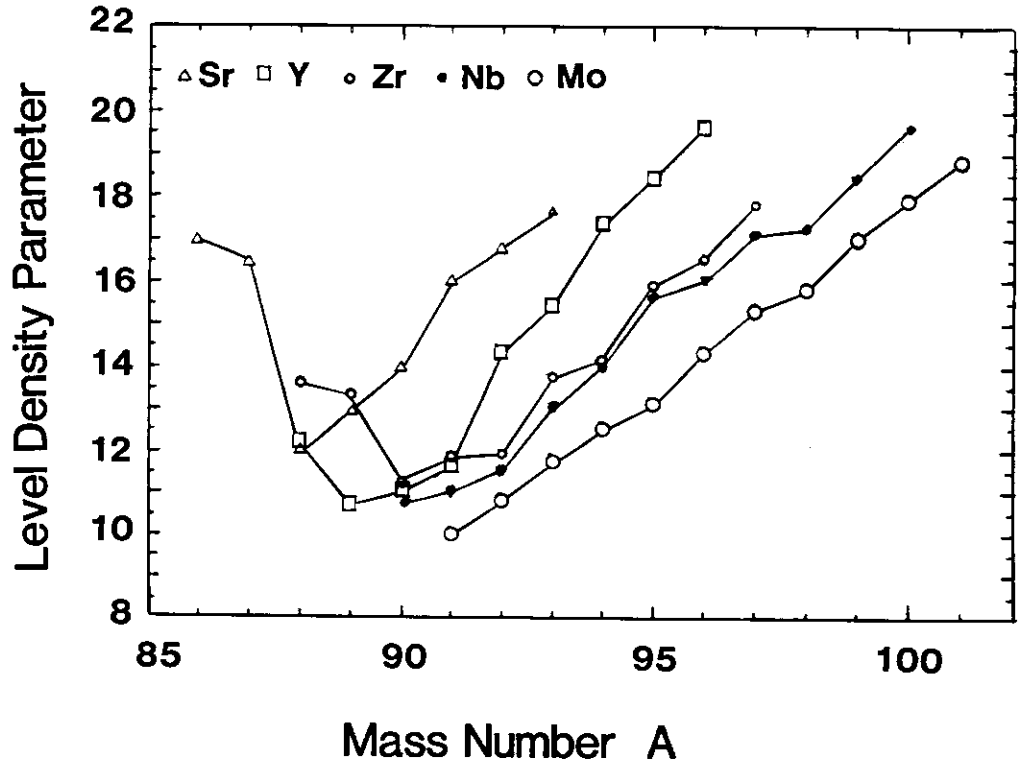

Fig. 16 A set of level density parameters determined from the cross section calculations for $_{40}Zr$, $_{41}Nb$, and $_{42}Mo$ isotopes.

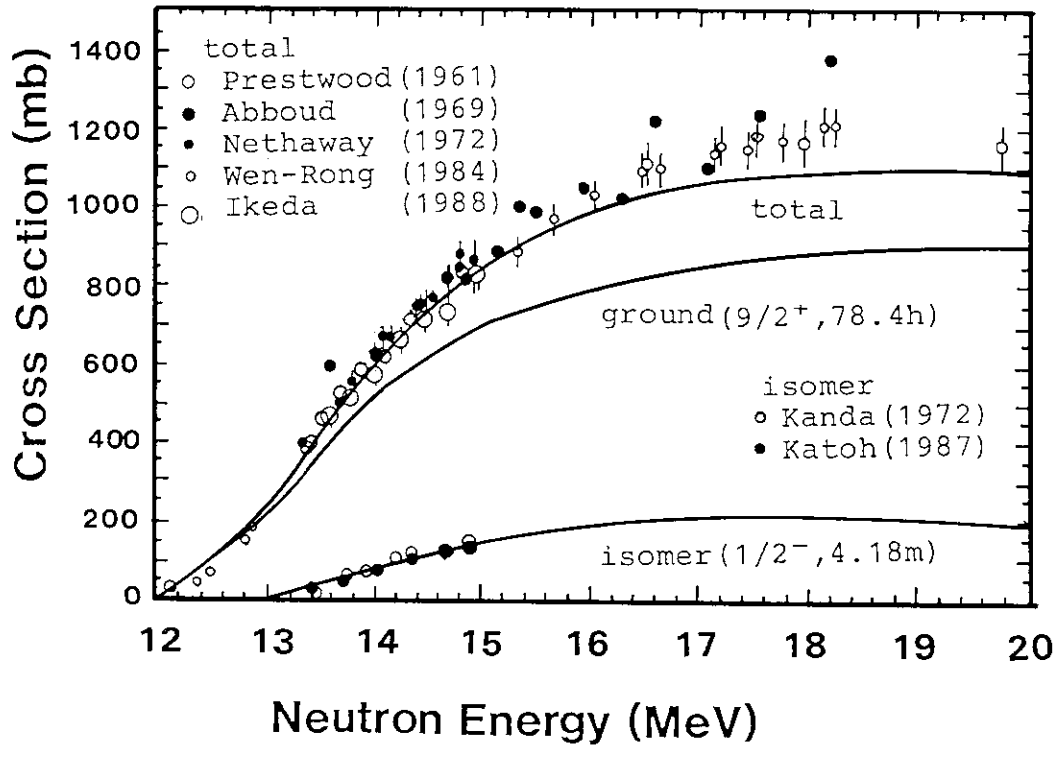

Fig. 17 Calculated and experimental production cross sections from $^{90}Zr(n,2n)^{89}Zr$ reaction.

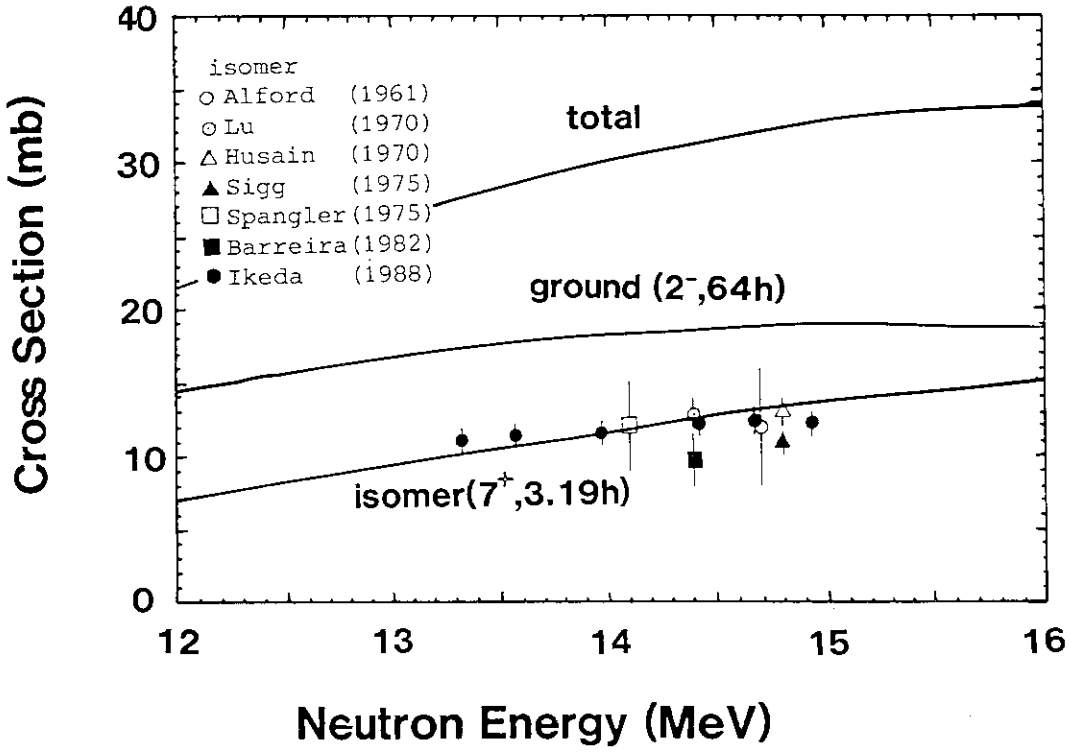

Fig. 18 Calculated and experimental production cross sections from $^{90}Zr(n,p)^{90}Y$ reaction.

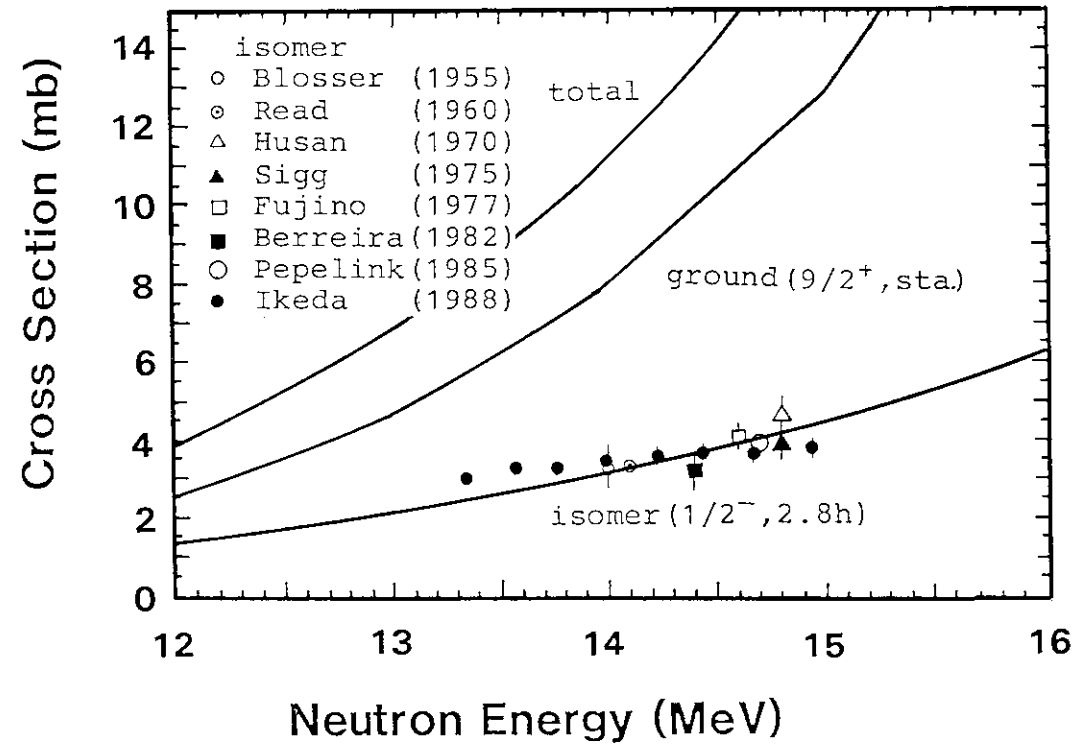

Fig. 19 Calculated and experimental production cross sections from $^{90}Zr(n,\alpha)^{87}Sr$ reaction.

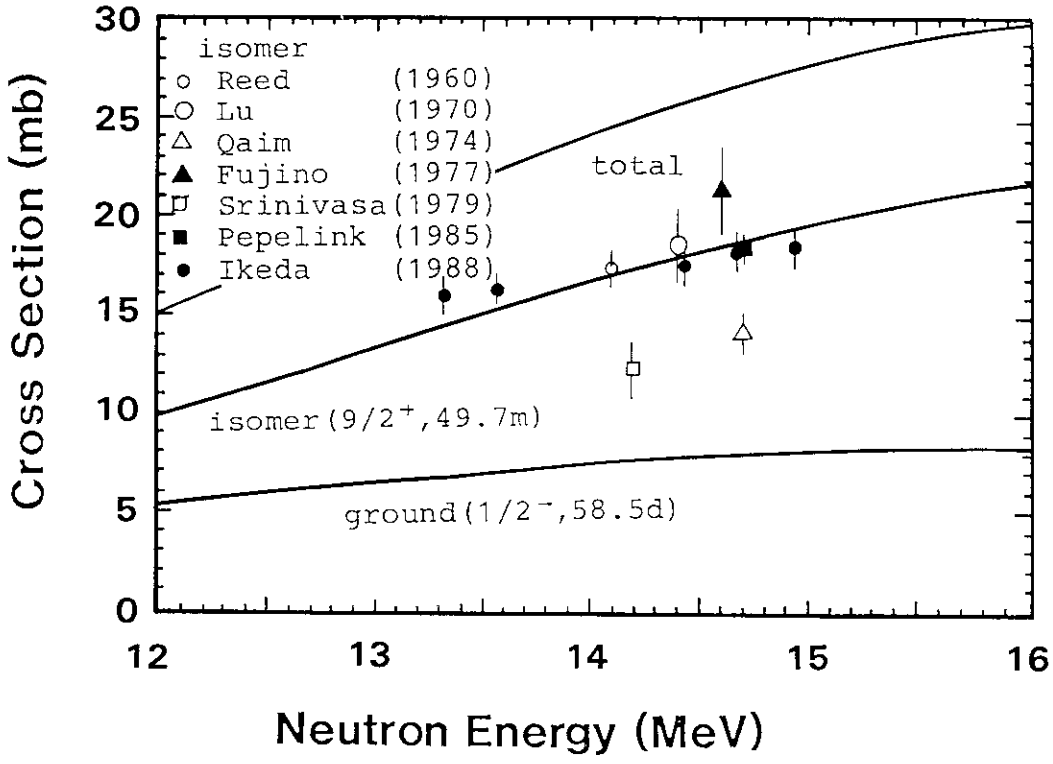

Fig. 20 Calculated and experimental production cross sections from $^{91}Zr(n,p)^{91}Y$ reaction.

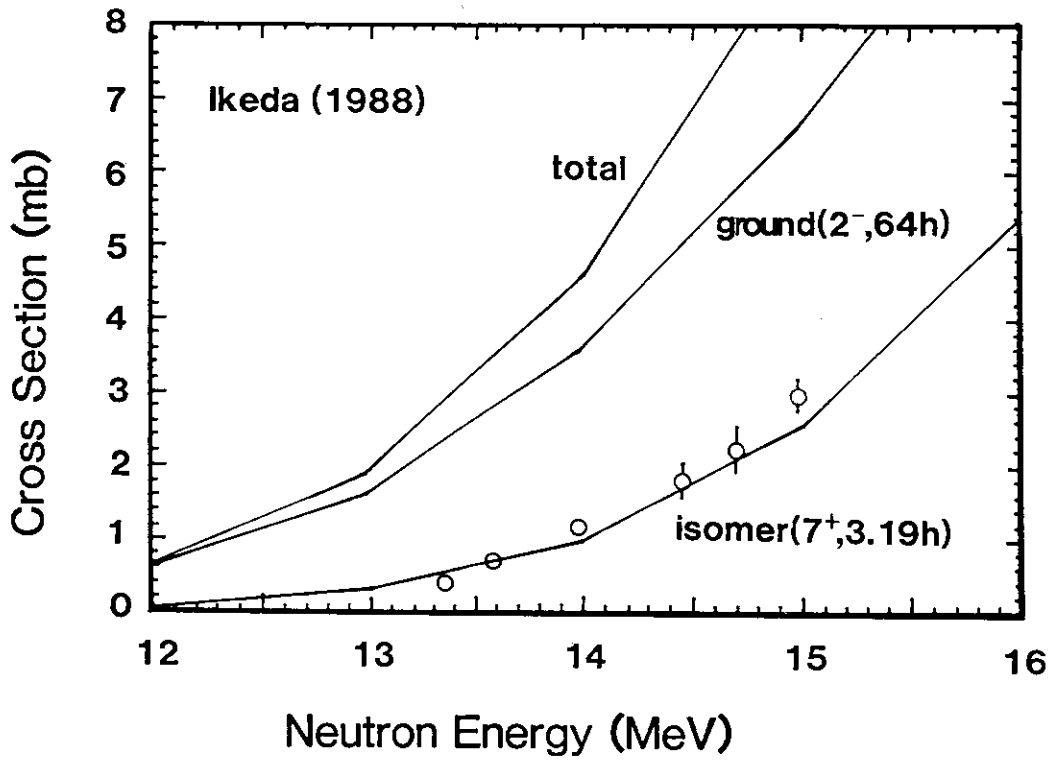

Fig. 21 Calculated and experimental production cross sections from $^{91}Zr(n,n'p)^{90}Y$ reaction.

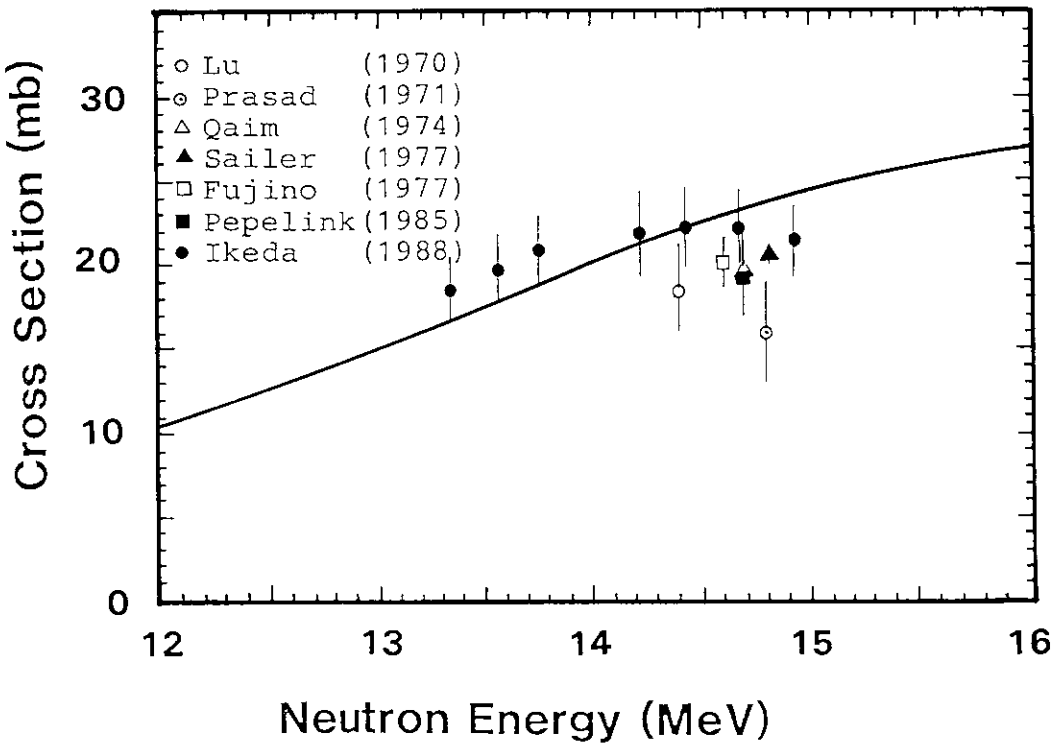

Fig. 22 Calculated and experimental production cross sections from $^{92}Zr(n,p)^{92}Y$ reaction.

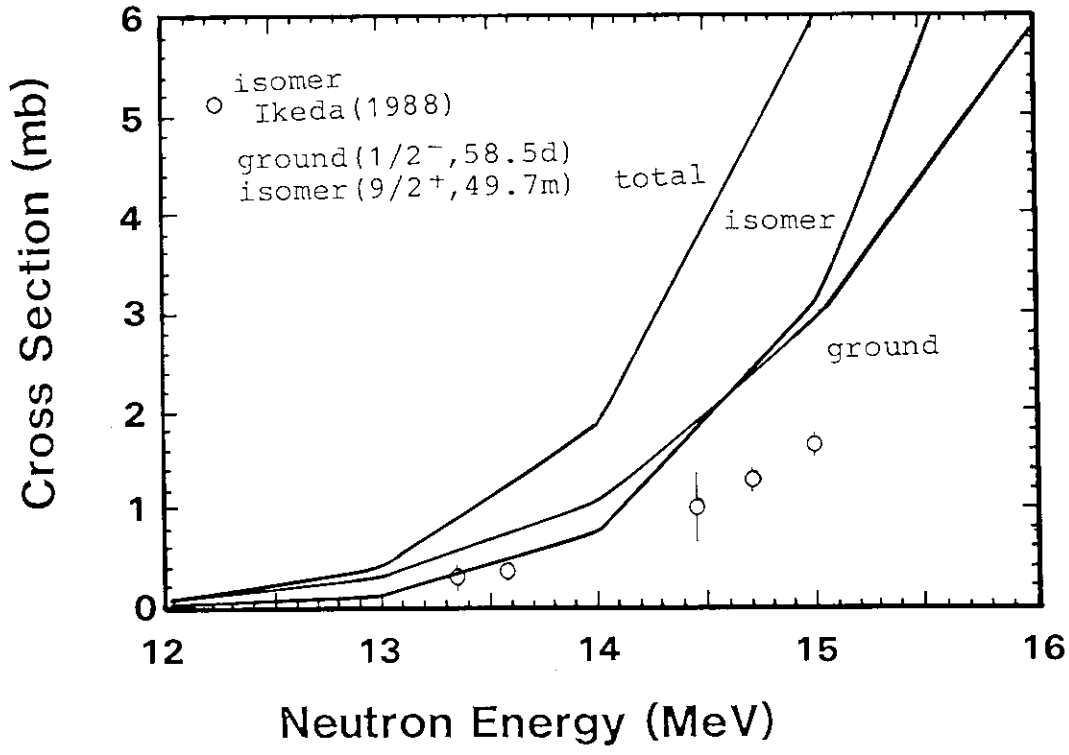

Fig. 23 Calculated and experimental production cross sections from $^{92}Zr(n,n'p)^{90}Y$ reaction.

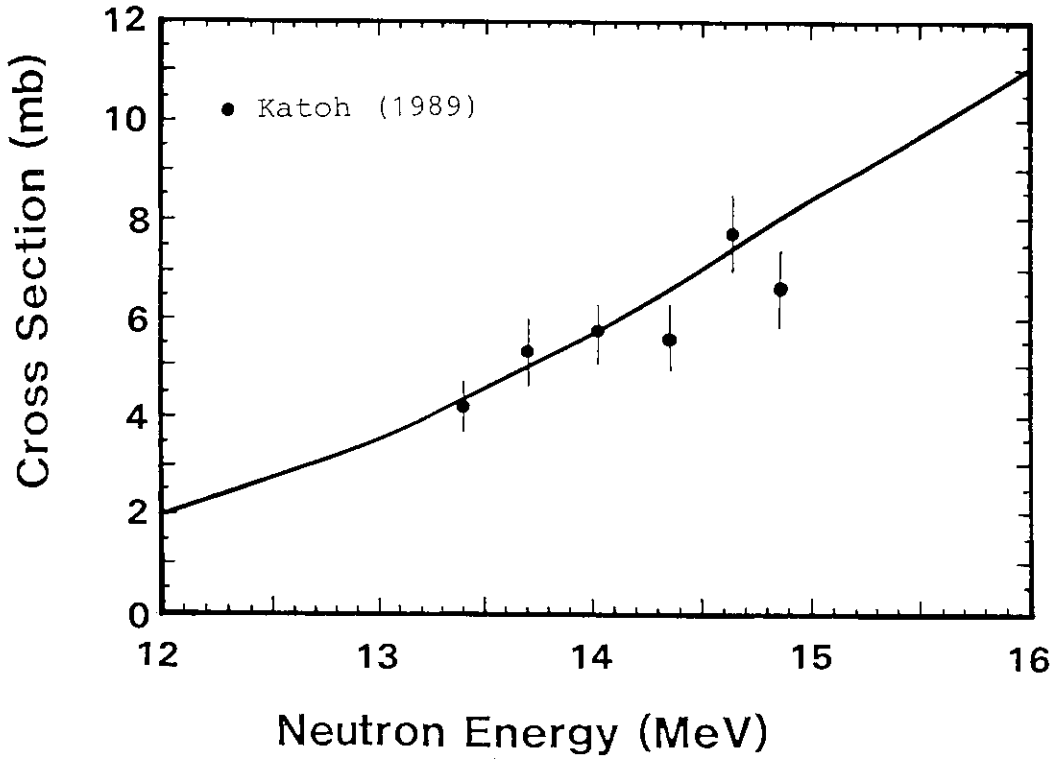

Fig. 24 Calculated and experimental production cross sections from $^{94}Zr(n,p)^{94}Y$ reaction.

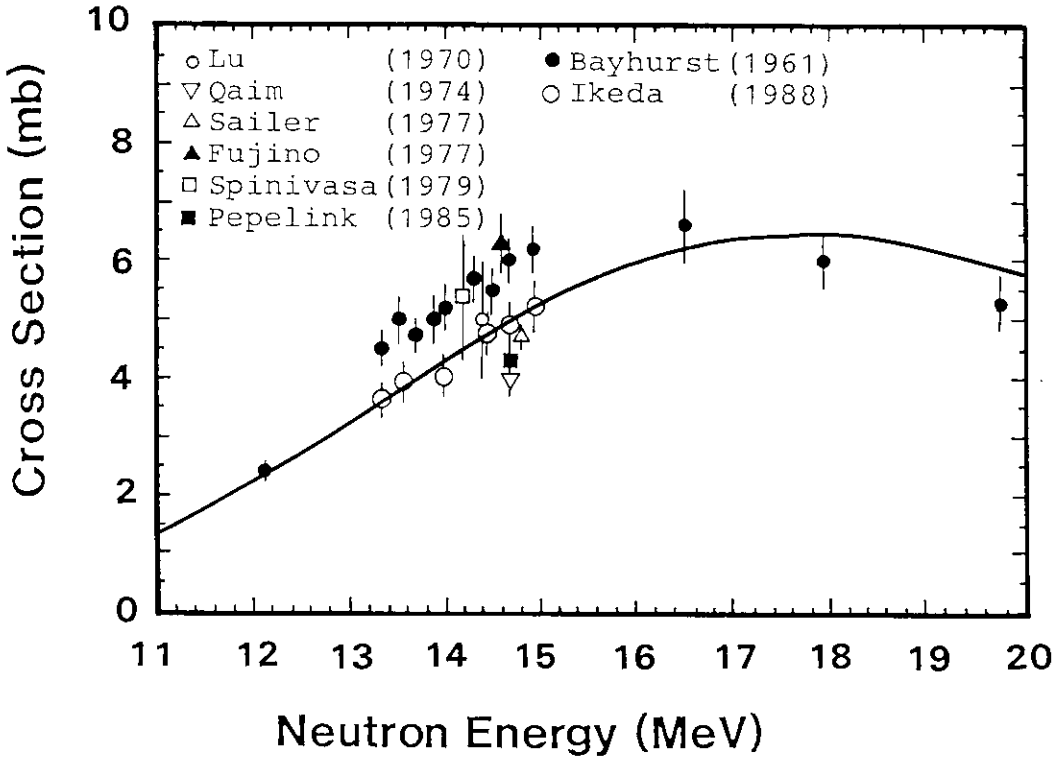

Fig. 25 Calculated and experimental production cross sections from $^{94}Zr(n,\alpha)^{91}Sr$ reaction.

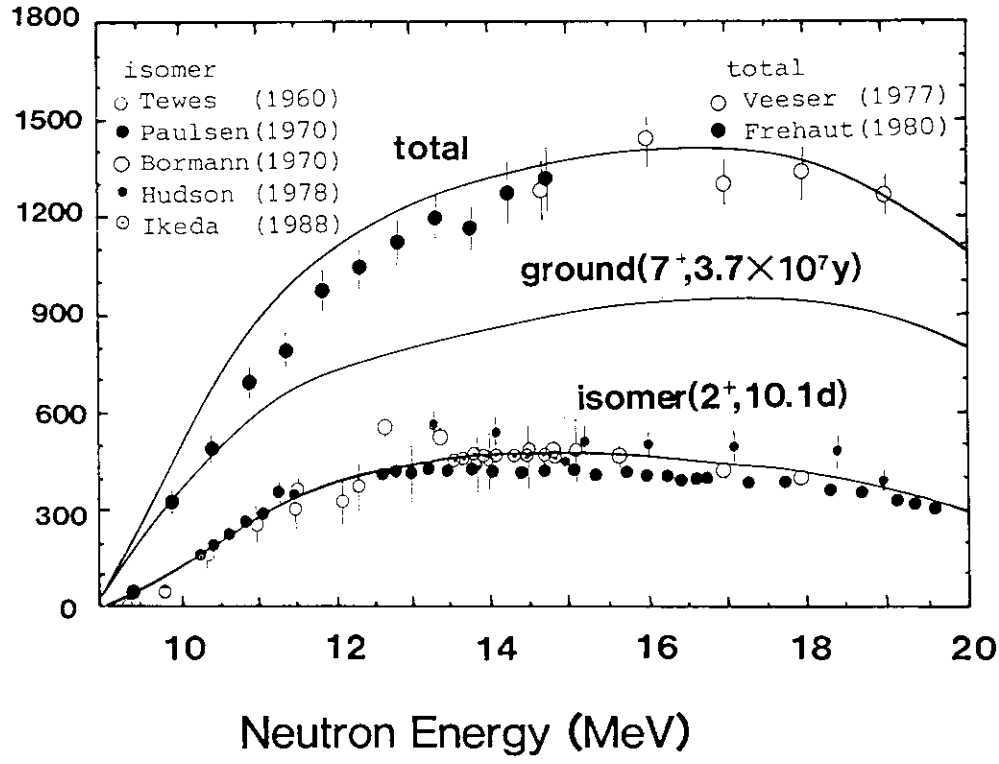

Fig. 26 Calculated and experimental production cross sections from $^{93}Nb(n,2n)^{92}Nb$ reaction.

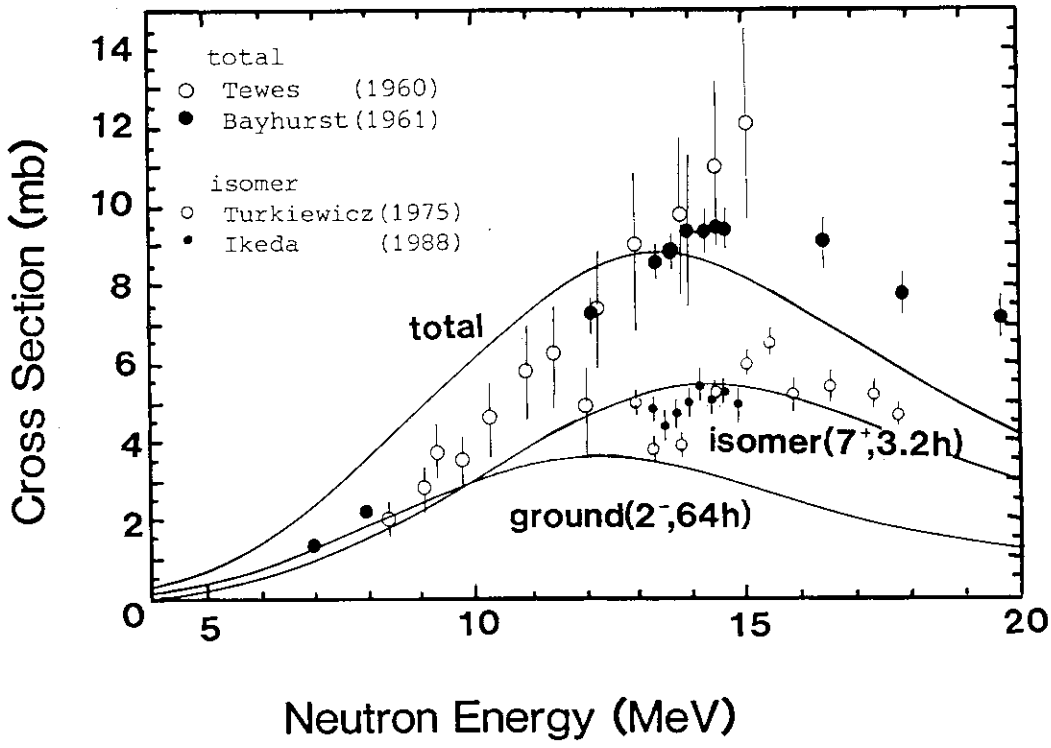

Fig. 27 Calculated and experimental production corss sections from $^{93}Nb(n,\alpha)^{90}Y$ reaction.

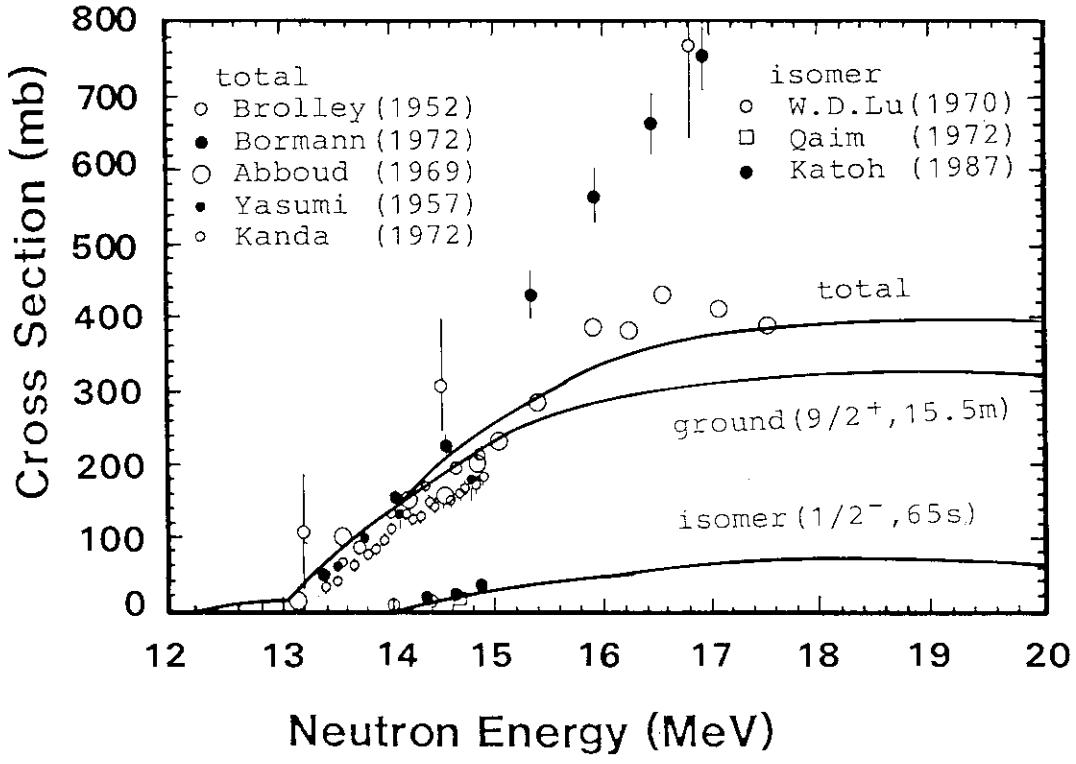

Fig. 28 Calculated and experimental production cross sections from $^{92}Mo(n,2n)^{91}Mo$ reaction.

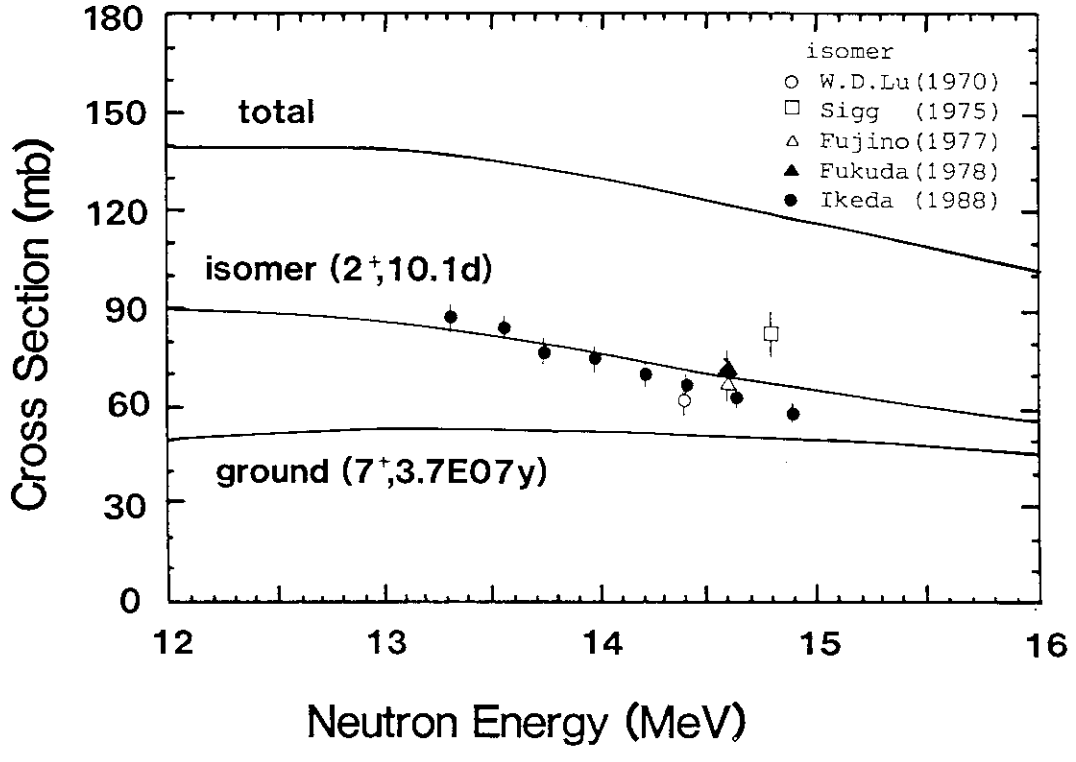

Fig. 29 Calculated and experimental production cross sections from $^{92}Mo(n,p)^{92}Nb$ reaction.

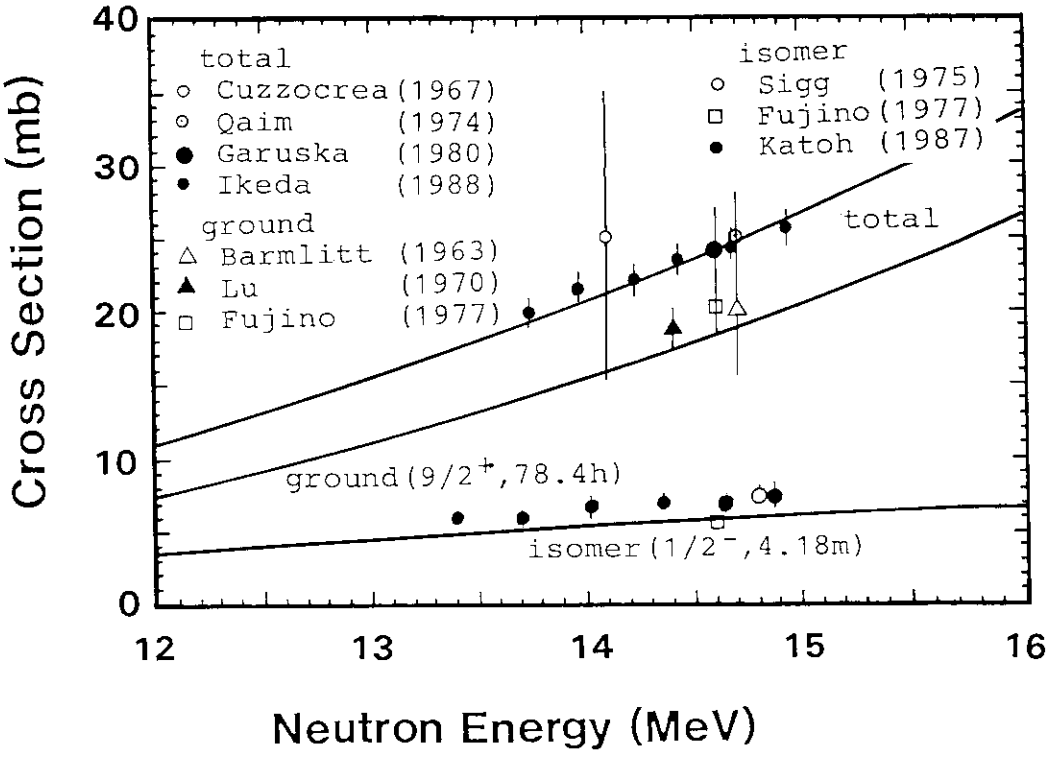

Fig. 30 Calculated and experimental production cross sections from $^{92}Mo(n,\alpha)^{89}Zr$ reaction.

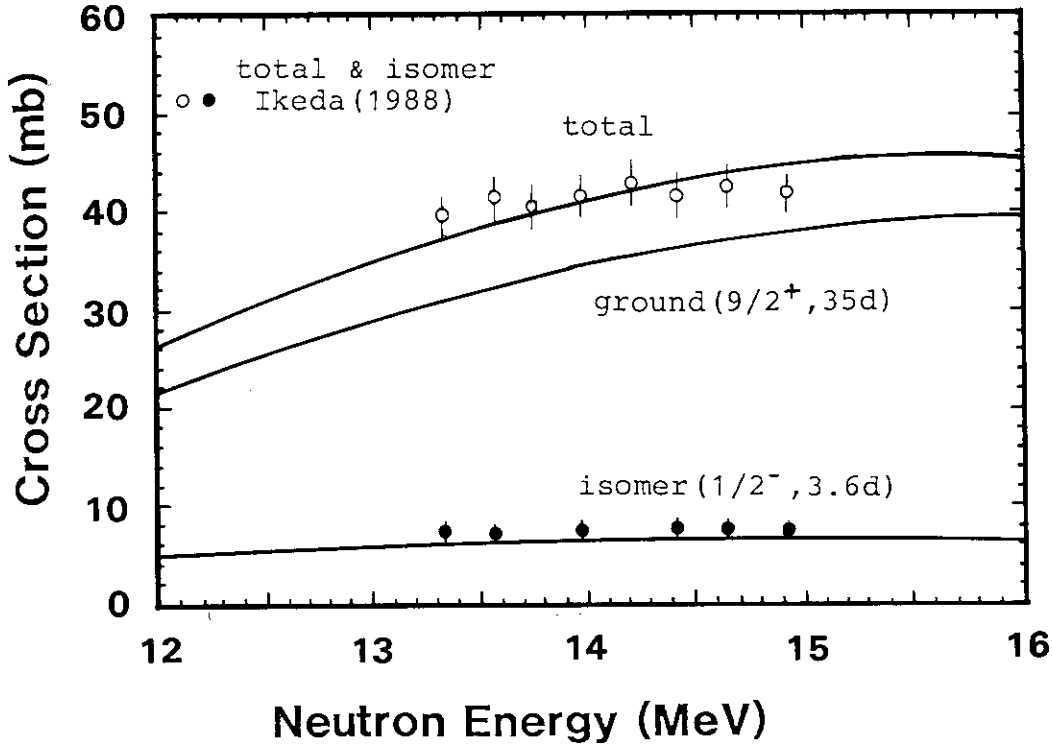

Fig. 31 Calculated and experimental production cross sections from $^{95}Mo(n,p)^{95}Nb$ reaction.

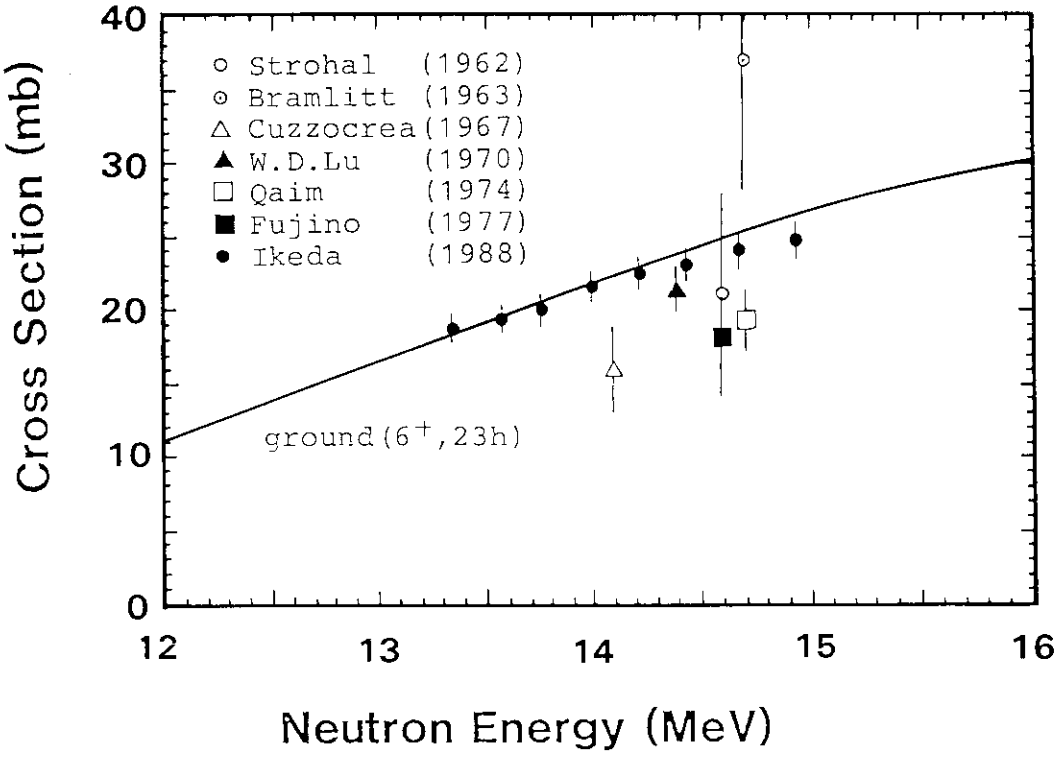

Fig. 32 Calculated and experimental production cross sections from $^{96}Mo(n,p)^{96}Nb$ reaction.

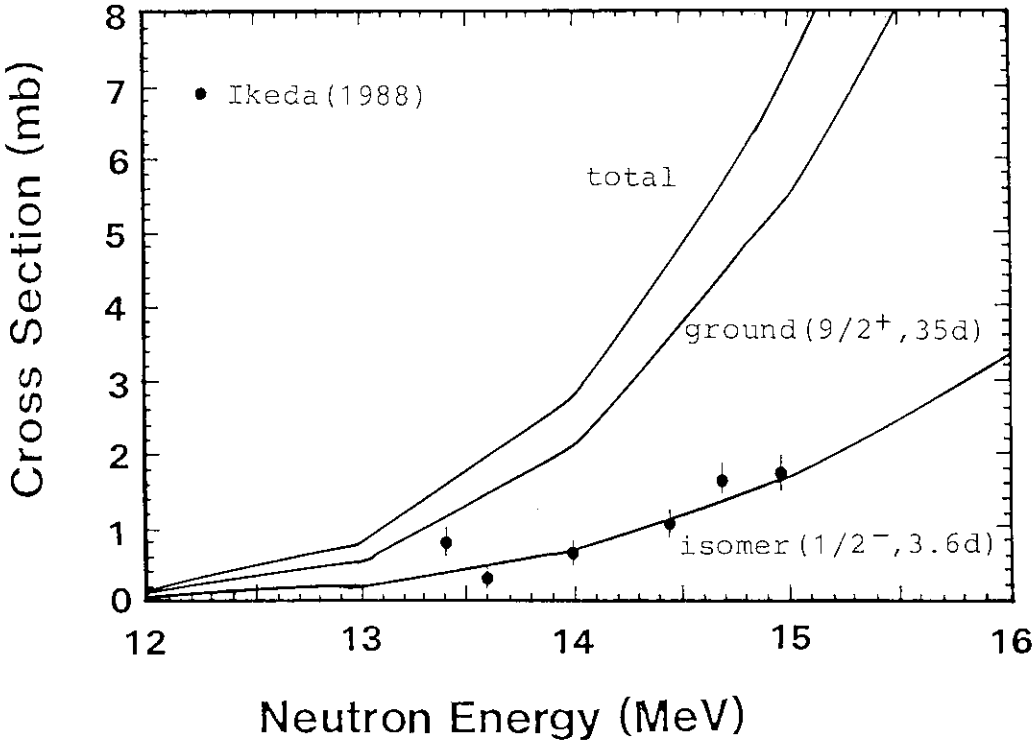

Fig. 33 Calculated and experimental production cross sections from $^{96}Mo(n,n'p)^{95}Nb$ reaction.

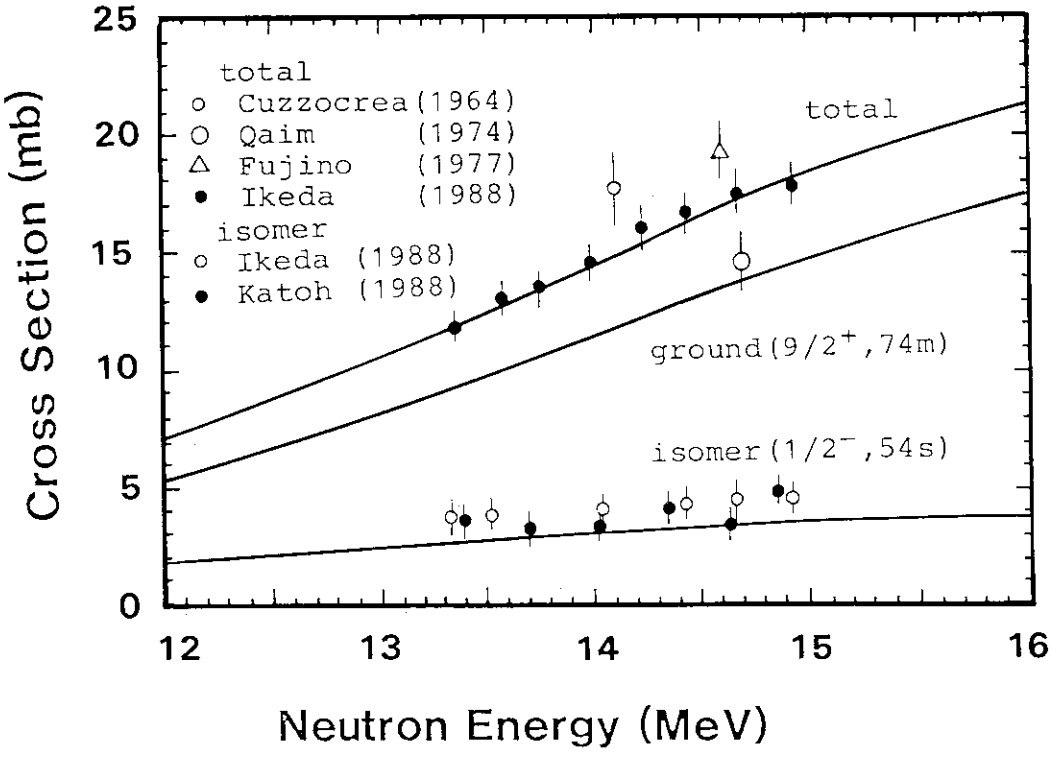

Fig. 34 Calculated and experimental production cross sections from $^{97}Mo(n,p)^{97}Nb$ reaction.

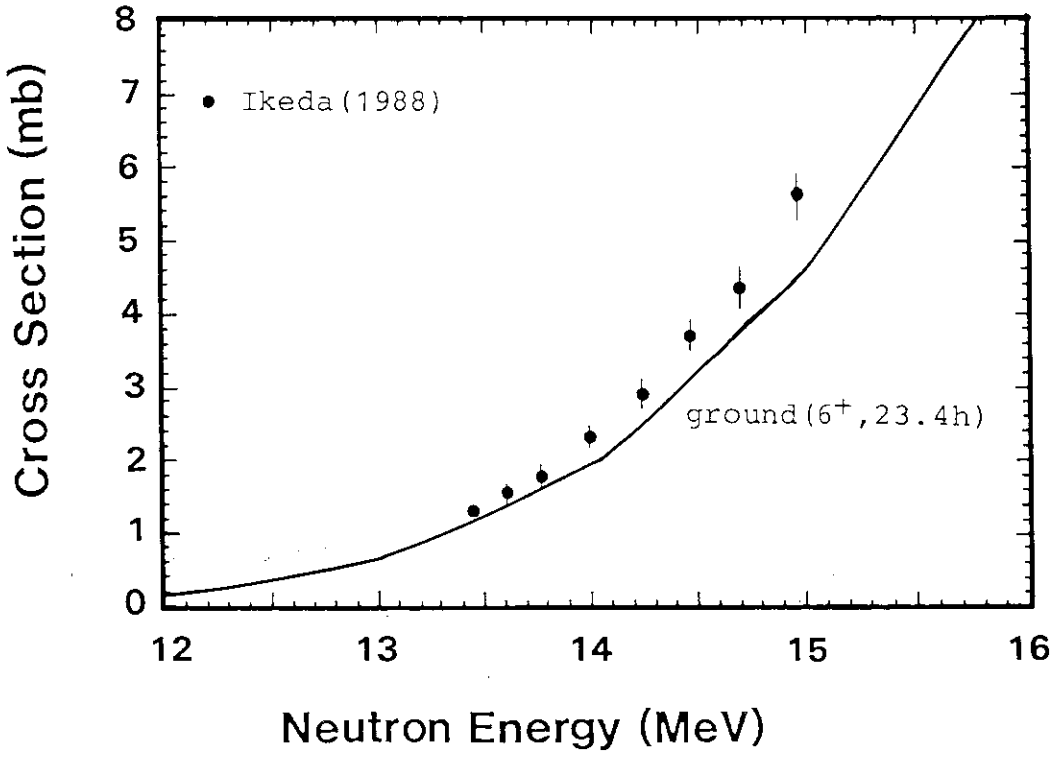

Fig. 35 Calculated and experimental production cross sections from $^{97}Mo(n,n'p)^{96}Nb$ reaction.

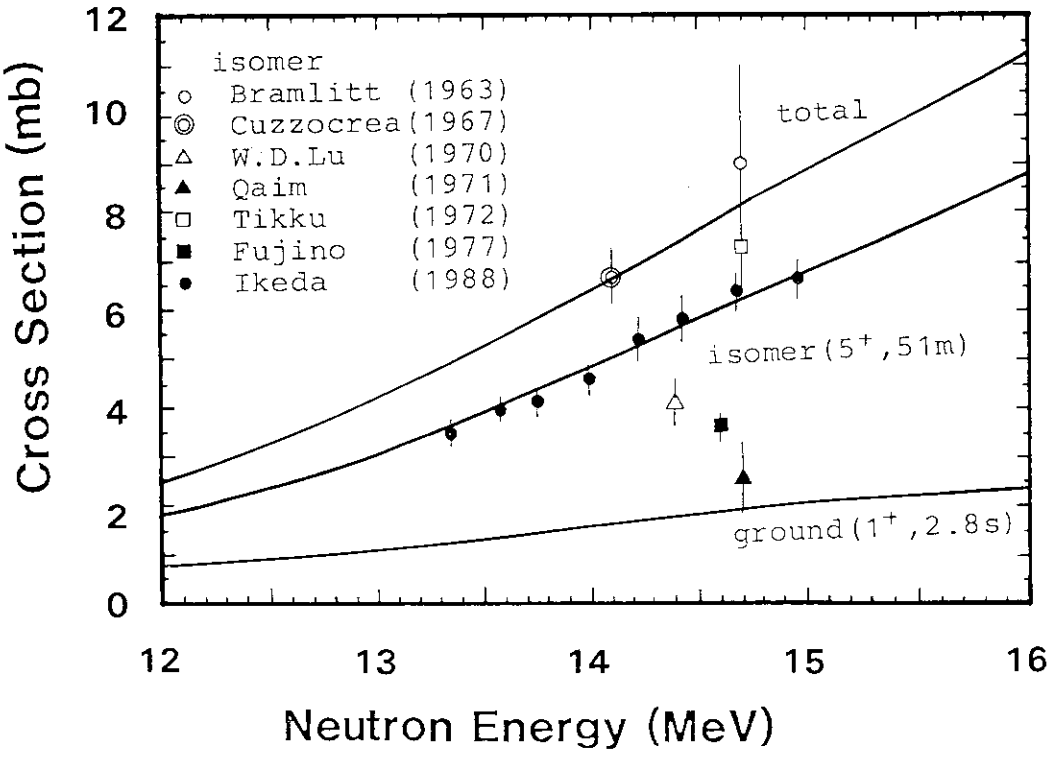

Fig. 36 Calculated and experimental production cross sections from $^{98}Mo(n,p)^{98}Nb$ reaction.

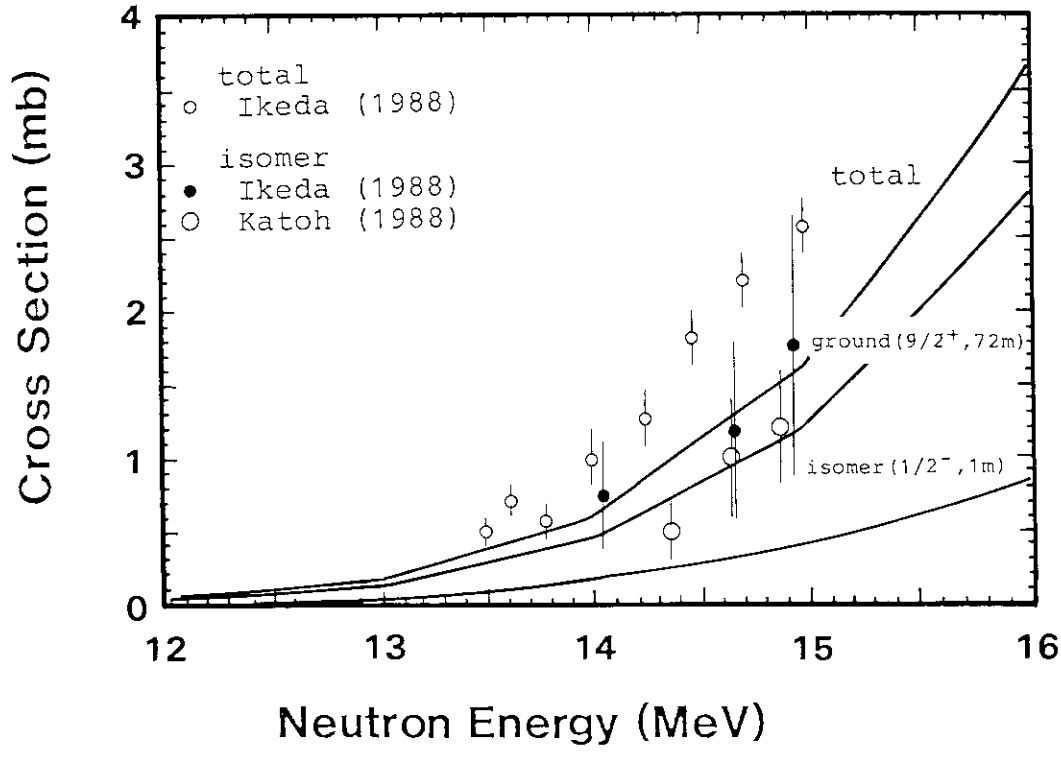

Fig. 37 Calculated and experimental production cross sections from $^{98}Mo(n,n'p)^{97}Nb$ reaction.

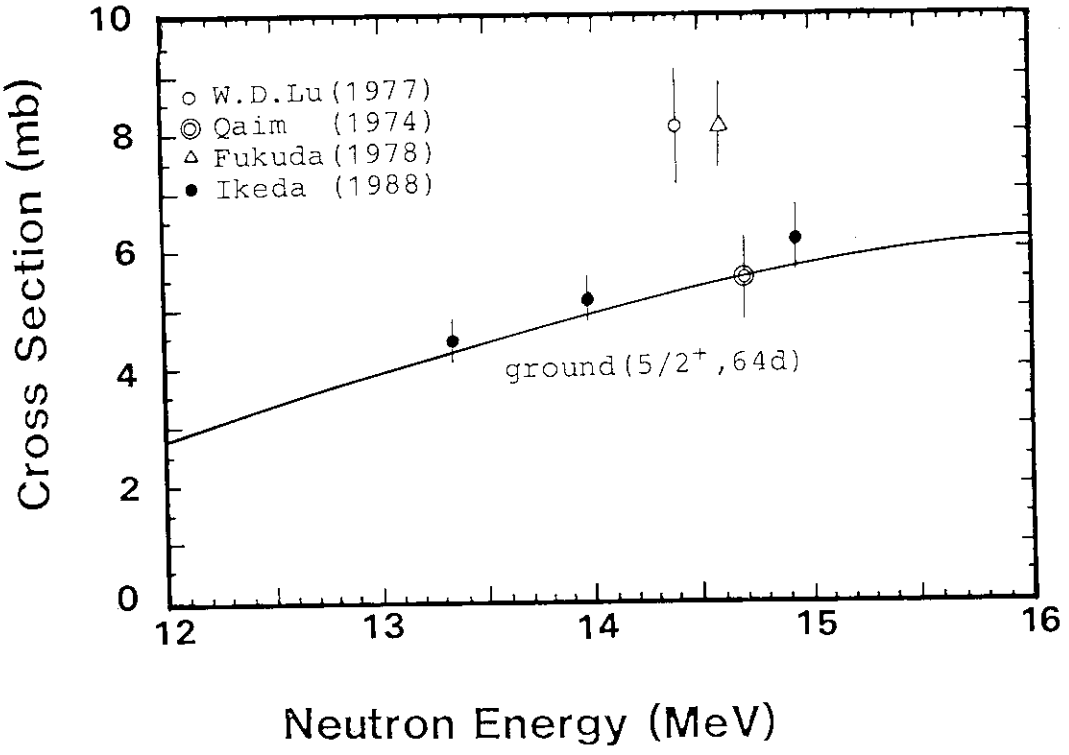

Fig. 38 Calculated and experimental production cross sections from $^{98}Mo(n,\alpha)^{95}Zr$ reaction.

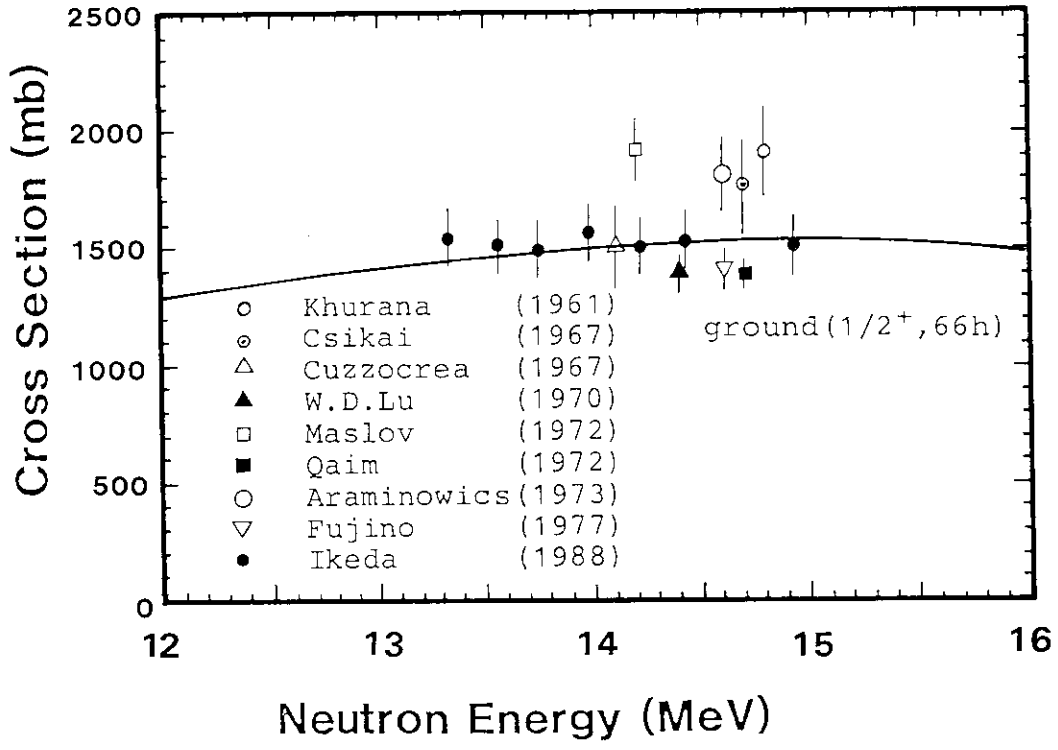

Fig. 39 Calculated and experimental production cross sections from $^{100}Mo(n,2n)^{99}Mo$ reaction.

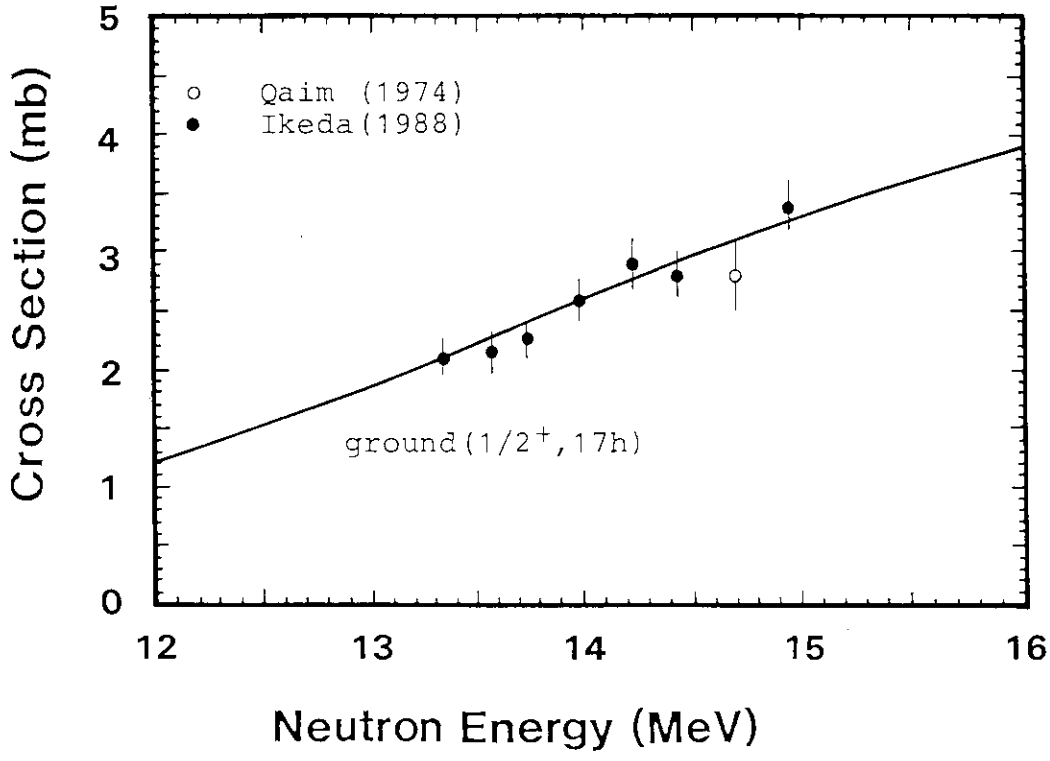

Fig. 40 Calculated and experimental production cross sections from $^{100}Mo(n,\alpha)^{97}Zr$ reaction.

Appendix Calculations of Neutron and Proton Induced Reactions up to 40 MeV

Although the built-in optical-model potentials for neutrons and protons can be employed up to 80 MeV, the maximum nucleon energy, below which the nuclear cross sections are calculated, is about 40 MeV, because the detailed statistical-model calculation is performed and the number of decaying nuclei in the multi-step nuclear reactions is 20 at maximum. To examine the availability of the SINCROS-II for the cross section calculations up to 40 MeV, the neutron induced reaction for Cu and the proton induced reaction for ^{63}Cu are calculated to obtain the excitation functions of isotope productions.

The discrete level data and the level density parameters from Mn to Zn are already prepared, and stored in the file 8 and in the EGNASH2 as the data initialization statement, respectively. Also the direct inelastic-scattering cross sections are stored in the file 33, then the cross section calculation to be done is very easily executed, if we analyze the multi-step nuclear reaction chain and give the input data in a similar manner to that shown in Table 2. The examples of calculated results are shown in Figs. A-1 and A-2.

Figure A-1 indicates the excitation functions of the long-lived radioactive cobalt isotopes ^{57}Co, ^{58}Co, and ^{60}Co productions from natural copper bombarded with neutrons up to 40 MeV. A very long-lived radioactive isotope ^{63}Ni is produced in the same reaction as above, whose excitation function is shown in Fig. A-2. Below 20 MeV, ^{63}Ni is produced by only the reaction ^{63}Cu(n,p), and above that by both reactions, ^{63}Cu(n,p) and ^{65}Cu(n,p2n). Figure A-3 shows the comparison with the experimental data for ^{63}Cu(n,p) and ^{63}Cu(n,xp) cross sections. From the figure, we see that the activation measurement[31] and the measurement using the emulsion plates[32] of ^{63}Cu(n,p) reaction around 14 MeV show higher values than that of calculation, but the total proton countings[27),33] show the agreement with the calculated total proton production. Recently a new measurement of the ^{63}Cu(n,p) cross section near 14 MeV is performed and shows good agreement with the calculation[34].

Above 20 MeV, it is rare to have the experimental data for neutron cross sections. Rather, we have data for charged-particle induced reactions. So it is useful to compare the calculated cross sections for proton induced reactions with the respective experimental measurements,

to examine the results of cross section calculation for the higher energy neutrons.

The reactions of ^{63}Cu induced by proton up to 44 MeV are calculated with the same procedure as the neutron induced reactions. As the results of this calculation, ^{63}Zn, ^{62}Zn, and ^{61}Cu production cross sections are compared with the experimental measurements and are shown in Figs. A-4 through A-6. In this case, all level density parameters are cited from the predetermined values, which are stored in the code as the data initialization statement, then they are all the same as those used in the neutron cross section calculations. But the preequilibrium process constant F2 is set to be 0.5 to get a good fit to the $^{63}Cu(p,2n)^{62}Zn$ cross section, though the value of F2 was 0.6 in the neutron reactions for Cu and Zn isotopes. Agreements between the calculation and the recently measured experimental data[35)-39)] are excellent for the (p,n) reaction, and are fairly well for (p,2n) and (p,p2n) multi-step reactions.

These results, mentioned above, suggest the following: It is expected that the cross section, for which we have no experimental measurements, can be obtained from the calculation with the SINCROS-II.

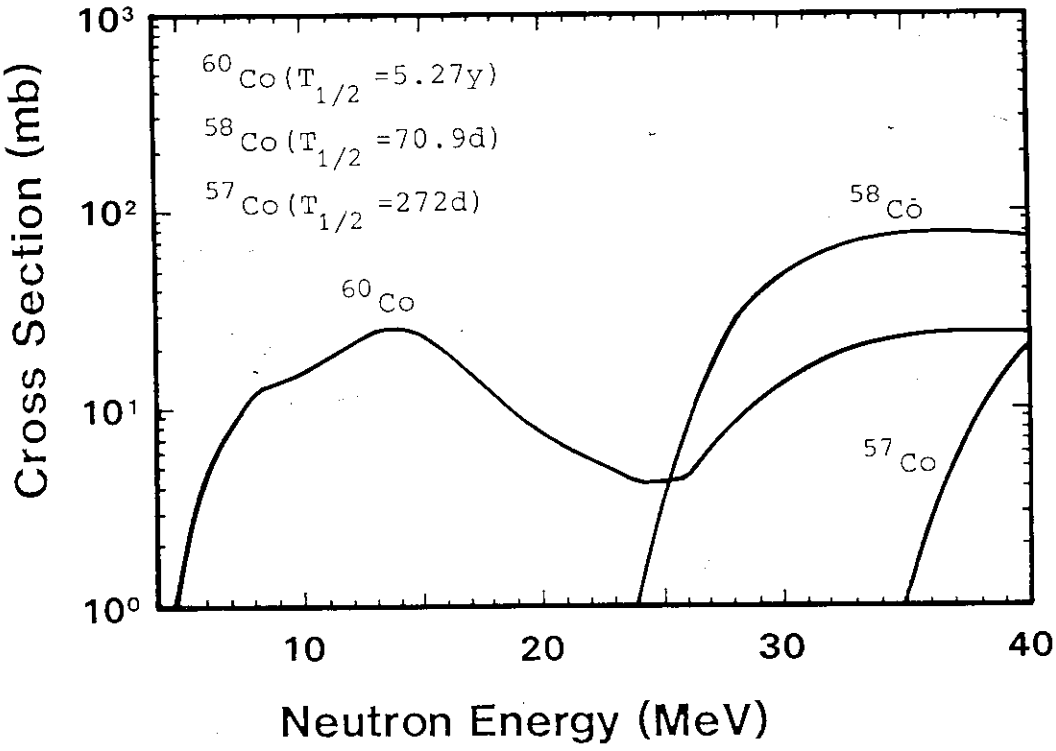

Fig. A-1 Production cross sections for the long-lived radioactive cobalt isotopes from natural copper reaction with neutron up to 40 MeV.

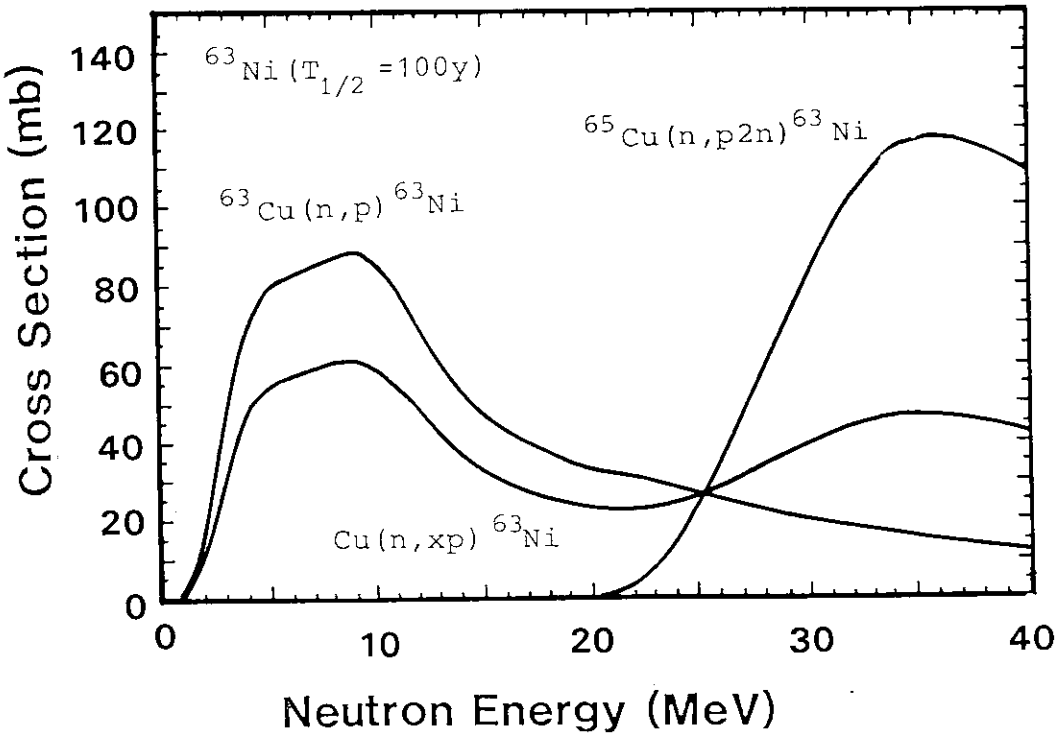

Fig. A-2 Calculation of long-lived ^{63}Ni isotope production from Cu(n,xnp) reactions up to 40 MeV neutron energy.

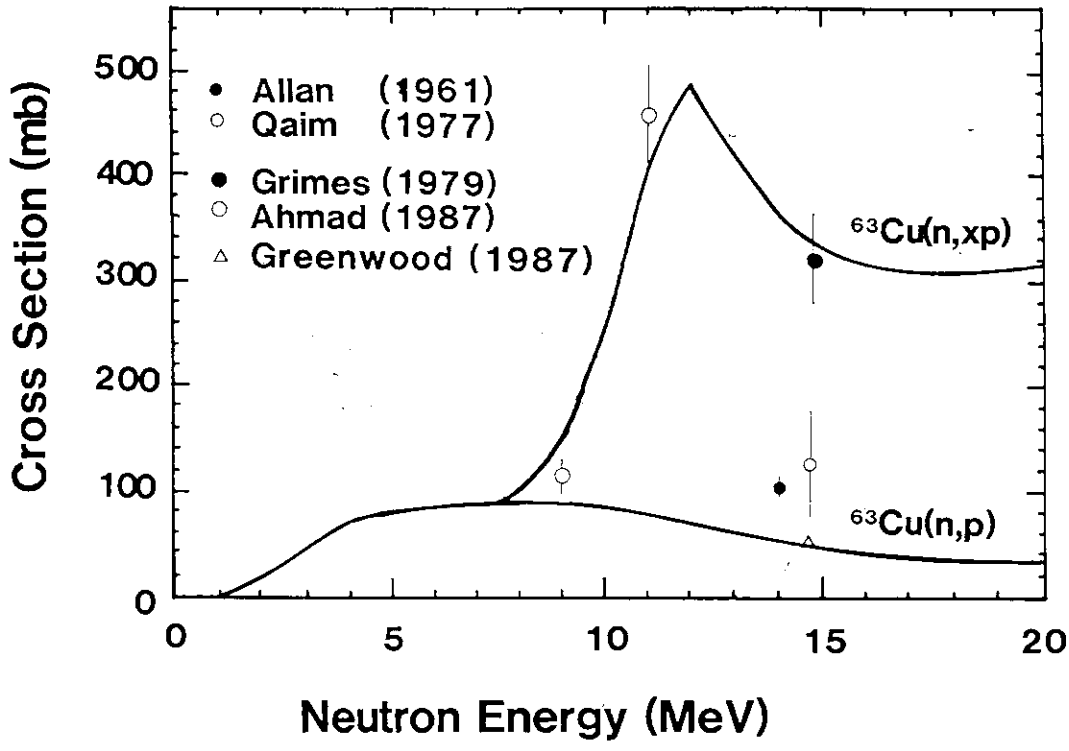

Fig. A-3 Calculated and experimental cross sections for $^{63}Cu(n,p)$ and $^{63}Cu(n,xp)$ reactions.

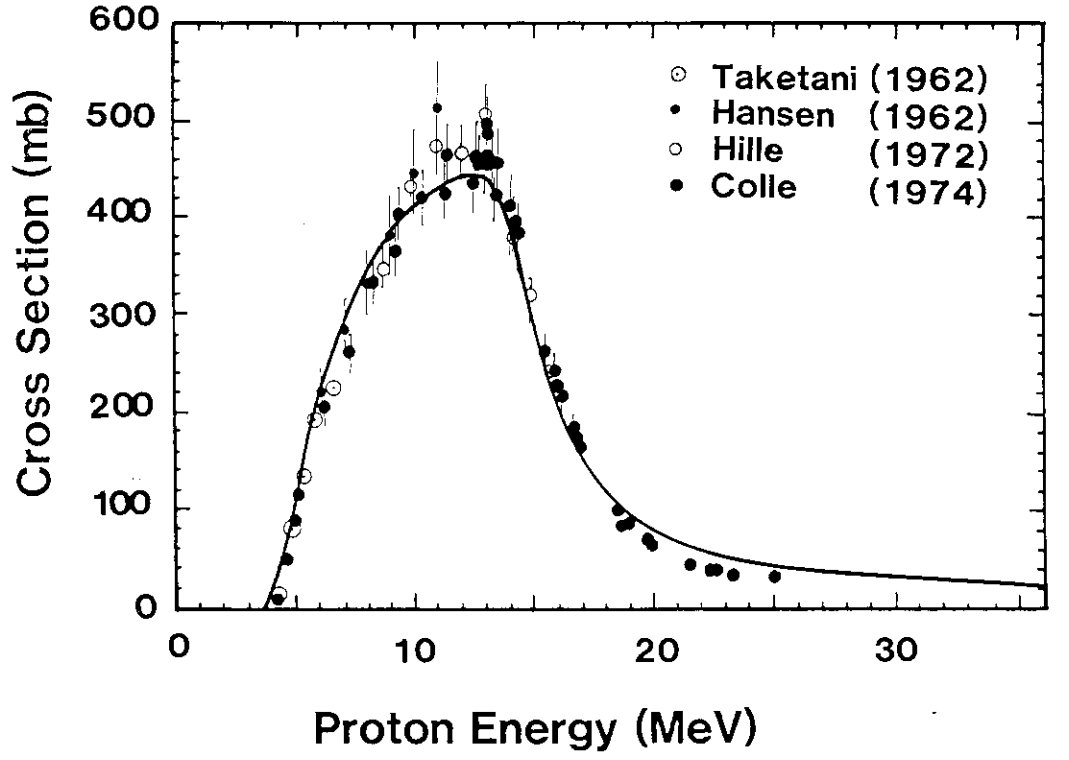

Fig. A-4 Comparison of calculated cross section with experimental measurements for $^{63}Cu(p,n)^{63}Zn$ reaction.

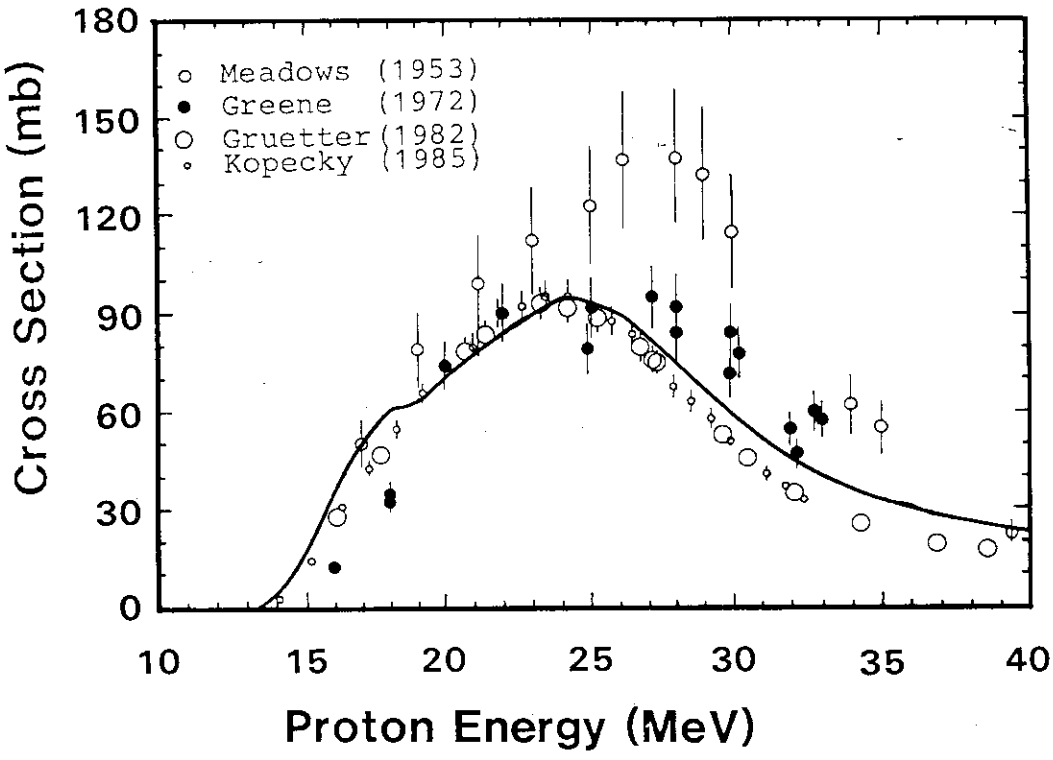

Fig. A-5 Calculated and experimental production cross sections of ^{62}Zn from $^{63}Cu(p,2n)$ reaction.

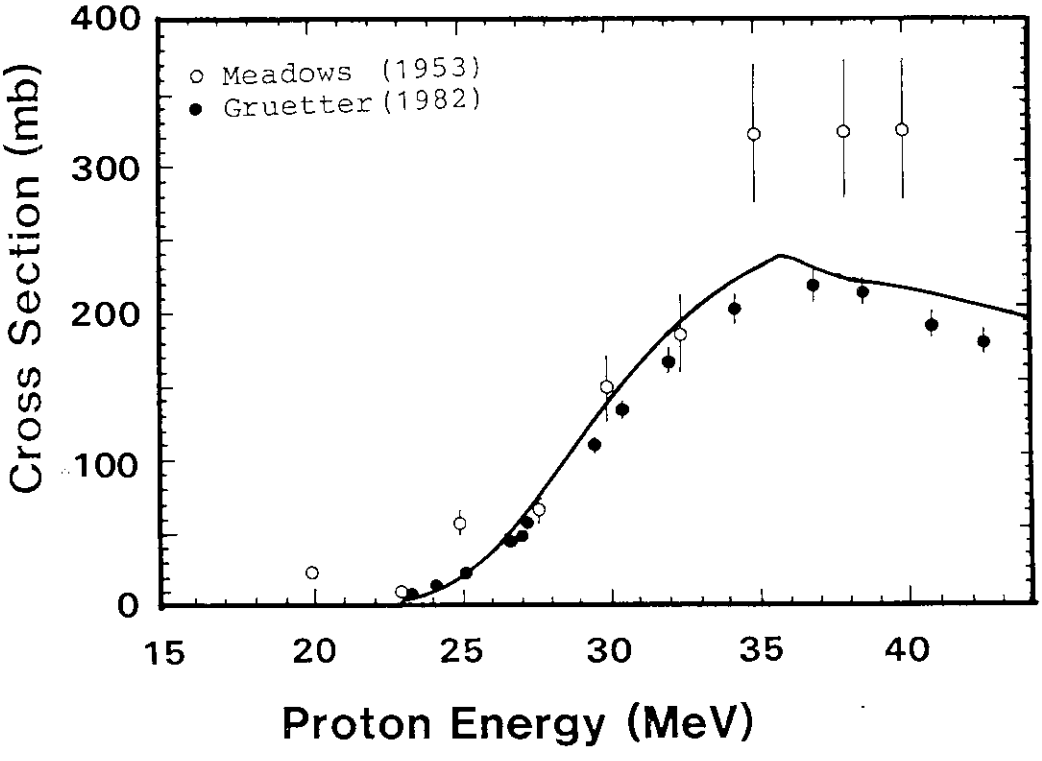

Fig. A-6 Calculated and experimental production cross sections of ^{61}Cu from $^{63}Cu(p,p2n)$ reaction.